Summer 9-1-2014

Discovery and Characterization of Novel Polyomaviruses in Humans

Erica Anne Siebrasse
Washington University in St. Louis

Follow this and additional works at: https://openscholarship.wustl.edu/etd

WASHINGTON UNIVERSITY IN ST. LOUIS

Division of Biology and Biological Sciences

Molecular Microbiology and Microbial Pathogenesis

Dissertation Examination Committee:
David Wang, Chair
Jacco Boon
Erika Crouch
Michael S. Diamond
Henry V. Huang
Thaddeus S. Stappenbeck

Discovery and Characterization of Novel Polyomaviruses in Humans

by

Erica Anne Siebrasse

A dissertation presented to the
Graduate School of Arts and Sciences
of Washington University in
partial fulfillment of the
requirements for the degree
of Doctor of Philosophy

August 2014

Saint Louis, Missouri

TABLE OF CONTENTS

LIST OF FIGURES AND TABLES

CHAPTER 5. Discussion

APPENDIX I. Human Polyomaviruses in Children Undergoing Transplantation

ABBREVIATIONS

AIDS	acquired immunodeficiency syndrome
APyV	avian polyomavirus
ARTI	acute respiratory infections
BAL	bronchoalveolar lavage
BatPyV	bat polyomavirus
BKPyV	BK polyomavirus
bp	base pair
BPyV	bovine polyomavirus
CaPyV	canary polyomavirus
CFU	colony forming units
ChPyV	chimpanzee polyomavirus
CMV	cytomegalovirus
CoV	coronavirus
CPE	cytopathic effects
CPyV	crow polyomavirus
cr1	conserved region 1
cr2	conserved region 2
CSF	cerebrospinal fluid
cWUPyV	circular WU polyomavirus
dIF	double immunofluorescence
dIHC	double immunohistochemistry
FPyV	finch polyomavirus
FSA	Fast Statistical Alignment
GHV	goose hemorrhagic polyomavirus
GVHD	graft versus host disease
HaPyV	hamster polyomavirus
HEL	human embryonic lung
HIV	human immunodeficiency virus
HLA	human leukocyte antigen
hNEC	human nasal epithelial cells
HPyV6	human polyomavirus 6
HPyV7	human polyomavirus 7
HPyV9	human polyomavirus 9
HPyV10	human polyomavirus 10
HPyV12	human polyomavirus 12
hTEC	human tracheal epithelial cells
IF	immunofluorescence
IFN	interferon
IHC	immunohistochemistry
IRB	institutional review board
JCPyV	JC polyomavirus
KIPyV	KI polyomavirus
KI-VP1	KI polyomavirus viral protein 1

LTAg	large T antigen
LPyV	B-lymphotropic polyomavirus
MCC	Merkel cell carcinoma
MCPyV	Merkel cell polyomavirus
MERS	Middle East respiratory syndrome
MOI	multiplicity of infection
MPtV	murine pneumotropic virus
MPyV	murine polyomavirus
MTAg	middle T antigen
MWPyV	MW polyomavirus
MXPyV	MX polyomavirus
NCCR	noncoding control region
NFI	nuclear factor I
ng	nanograms(s)
NJPyV	New Jersey polyomavirus
NLS	nuclear localization signal
nm	nanometer
NPA	nasopharyngeal aspirate
nr	non-redundant
OraV1	Bornean orangutan polyomavirus
OraV2	Sumatran orangutan polyomavirus
ORF	open reading frame
PICU	pediatric intensive care unit
PML	progressive multifocal leukoencephalopathy
qPCR	real-time PCR
RCA	rolling circle amplification
RS	respiratory sample
RSV	respiratory syncytial virus
SARS	severe acute respiratory syndrome
SLPyV	California sea lion polyomavirus
SqPyV	squirrel monkey polyomavirus
STAg	small T Antigen
STLPyV	STL polyomavirus
supe	supernatant
SV40	simian virus 40
TNF	tumor necrosis factor
TSPyV	Trichodysplasia spinulosa-associated polyomavirus
uL	microliter
VLP	virus-like particles
VP	viral protein
WHIM	warts, hypogammaglobulinemia, infections and myelokathexis
WUPyV	WU polyomavirus
WU-VP1	WU polyomavirus viral protein 1

ACKNOWLEDGEMENTS

I first want to thank **Dave Wang** for being a fabulous mentor. I believe Dave exemplifies many of the qualities a great graduate mentor should have, and he was instrumental in helping me develop into a better scientist and scholar. I am especially thankful that Dave was supportive of my "non-traditional" career goals and allowed me the freedom to develop professional skills outside the lab. I could not have picked a better or more supportive mentor for my graduate studies; I do not think I could have had a more positive graduate experience in any other lab.

My family and friends kept me sane and happy, even when everything in lab was failing, and I thought I would never get a job. I am incredibly thankful for the support from my mom and best friend, **Vicki Siebrasse**. There is absolutely no way I would have made it through undergrad or grad school under a normal schedule without her totally selfless help, care and willingness to drop her plans to support mine, which was only possible given the support from my dad, **Jon Siebrasse**. I am also thankful to my dad for his constant encouragement, excellent advice and his understanding of my research. My brother **Alex Siebrasse** has always given me perspective and is constantly proud of me, no matter what stupid thing I did in lab that day, for which I am very grateful. Finally, the friends I have made in graduate school have been the best of my life. I would especially like to thank **Megan Ruhland**, **Beth Selleck** and **Hugh Bender**, who have all listened to my research troubles, lifted my spirits when they were low and generally made grad school a fun and happy time. I am fortunate to have their friendship.

My graduate career and this research would not have been possible without **Dr. David Rubin**. I thank him for giving me my life back, teaching me to be an educated, empowered patient and showing me that excellent, compassionate care exists.

ABSTRACT OF THE DISSERTATION

Discovery and Characterization of Novel Polyomaviruses in Humans

by

Erica Anne Siebrasse

Doctor of Philosophy in Biology and Biomedical Sciences

Washington University in St. Louis, 2014

Professor David Wang, Chair

The family *Polyomaviridae* is comprised of small, double-stranded DNA viruses of approximately 5,000 base pairs. Two polyomaviruses are well-established human pathogens and cause significant morbidity and mortality in immunocompromised patients. These viruses were discovered in the 1970s, but the last seven years have seen an explosion of novel human polyomavirus discoveries. The work described here seeks to address two questions: "Are there additional, novel polyomaviruses infecting humans?" and "Do these polyomaviruses cause disease in their human hosts?" The discovery of an additional novel polyomavirus, MW polyomavirus (MWPyV), is described. MWPyV was discovered in the stool of a healthy child from Malawi but was subsequently detected from pediatric patients with diarrhea in St. Louis, Missouri. As a step toward determining the pathogenicity of WU polyomavirus (WUPyV) and KI polyomavirus (KIPyV) in humans, immunohistochemical studies were completed to identify their tissue and cell tropisms. Both viruses were detected in alveolar macrophages, and WUPyV was also detected in respiratory epithelial cells and in cells associated with mucin-producing cells in the trachea. In addition, KIPyV was detected in the spleen. The immunocompromised state of the patients studied raises important questions about the role of immunosuppression in

x

the pathogenesis of WUPyV and KIPyV. Finally, this work details ultimately unsuccessful attempts to establish a cell culture system for WUPyV, which would have provided a means to study viral biology and disease causality. Overall, these studies further our understanding of human polyomavirus biology and the role of WUPyV and KIPyV in human disease and provide additional avenues for future research to further address these important questions.

CHAPTER 1

Introduction

OVERVIEW

The work presented in Chapters 2-4 seeks to address two overarching questions: "Are there additional novel polyomaviruses infecting humans?" and "Do these polyomaviruses cause disease in their human hosts?" Before describing the research itself, it is important to place it in context within the field and provide background information for the relevant research topics I address. To this end, the Introduction has been broken into two sections, with the first addressing why and how we search for novel viruses and the second describing the state of the polyomavirus field, focusing on what we knew when I began my work.

SECTION I: DISCOVERY OF NOVEL VIRUSES

Why is viral discovery important? Diseases of infectious etiology represented four of the top 10 causes of death worldwide in 2011 according to the World Health Organization (Table 1) (1). These include lower respiratory infections, diarrheal diseases, HIV/AIDS and tuberculosis. While AIDS is caused by the human immunodeficiency virus (HIV) and tuberculosis by *Mycobacterium tuberculosis*, lower respiratory infections and diarrheal diseases are both caused by a number of different pathogens. There are also non-infectious causes of diarrhea. Remarkably, approximately 30% of respiratory illnesses (2) and 40% of diarrhea cases (3) are of unknown etiology. This amounts to approximately two million respiratory- or diarrhea-related deaths every year. In other words, we have no idea what causes a significant proportion of two major diseases. These deaths can likely be attributed to a number of different causes, including non-infectious, bacterial and fungal. However, we hypothesize that unrecognized viruses play a significant role in respiratory and diarrheal diseases.

Table 1.1. Top 10 causes of death worldwide in 2011. Reproduced from (1). Diseases of infectious etiology are highlighted in gray.

World	Deaths in millions	% of deaths
Ischemic heart disease	7.25	12.8%
Stroke and other cerebrovascular disease	6.15	10.8%
Lower respiratory infections	3.46	6.1%
Chronic obstructive pulmonary disease	3.28	5.8%
Diarrheal diseases	2.46	4.3%
HIV/AIDS	1.78	3.1%
Trachea, bronchus, lung cancers	1.39	2.4%
Tuberculosis	1.34	2.4%
Diabetes mellitus	1.26	2.2%
Road traffic accidents	1.21	2.1%

A number of viruses are already known to cause respiratory illness or diarrhea. The main viral causes of diarrhea include viruses in the families *Reoviridae* (especially rotavirus), *Astroviridae*, *Caliciviridae* (especially norovirus) and *Adenoviridae*. The most common illness most people experience, regardless of their demographics, is acute respiratory infections (ARTI) (4). The predominant viral causes are rhinoviruses, influenza viruses, coronaviruses, parainfluenza viruses, respiratory syncytial virus and adenoviruses (4). Several additional causes of respiratory illness have been recently identified, and these include human metapneumovirus, and the novel human coronaviruses [severe acute respiratory syndrome coronavirus (SARS-CoV) (5), Middle East respiratory syndrome coronavirus (MERS-CoV) (6), NL63 and HKU1 (7)]. Other viruses, including WU polyomavirus (WUPyV) and KI polyomavirus (KIPyV), which are discussed in depth below, may also have roles in respiratory tract infections.

In addition to respiratory and diarrheal infections, other diseases are also of unknown etiology but thought to have infectious origins. For example, post-transplant infections are a leading cause of morbidity and mortality in cardiac transplant patients. Infections are the leading cause of death in adults and account for 15-34% of deaths in children from 31 days to one year

post-transplant (8-10). Of these deaths, approximately 30-40% are of diagnosed viral etiology (9, 11). Viral infections have also been postulated to contribute to at least a fraction of other adverse events, including graft loss, acute graft rejection and cardiac allograft vasculopathy. Several groups are attempting to identify additional viral agents in this vulnerable population, but none are looking for novel viruses, which is the subject of continued research in our lab. In fact, the effects of this type of research can be seen in the recent discovery of a novel polyomavirus, Trichodysplasia spinulosa-associated polyomavirus (TSPyV), in a heart transplant recipient. This discovery led to the successful treatment of the patient's Trichodysplasia spinulosa, a disease strongly associated with transplantation and immunosuppression, with topical cidofovir and will undoubtedly influence future cases (12). This is but one example of diseases thought to be of infectious etiology where no agents have yet been identified.

Viruses are also known to contribute to human cancers. This has been reviewed extensively (Table 1.2) (13). There are also a number of other cancers that are hypothesized to have viral etiologies, including chronic lymphocytic leukemia (14), among many others. Furthermore, some viruses have already been associated with cancers, but causation has not been definitively shown. Viral discovery methods are invaluable tools to explore types of cancer where viral causation is suspected. For example, Merkel cell carcinoma polyomavirus (MCPyV) was discovered recently and found to be clonally integrated into a large proportion of Merkel cell carcinomas (MCC) (15). While the majority of the population is seropositive for MCPyV, only a small number of people develop MCC each year. Determining how the virus induces tumorigenesis and risk factors for the disease will be critical in preventing it. For all of the potential disease states discussed here—respiratory and diarrheal diseases, infectious diseases of unknown etiology and cancers with possible viral contributions—it is impossible to develop

4

treatment and prevention methods to minimize their morbidity and mortality without the

identification of a causative agent.

Table 1.2. The human cancer viruses. Reproduced from (13) with permission from the publisher

under license 3394961343186.

Virus	Notable cancers	Reference
Epstein-Barr virus (EBV)	Most Burkett's lymphoma and nasopharyngeal carcinoma, most lymphoproliferative disorders, some Hodgkin's disease, some non-Hodgkin's lymphoma and some gastrointestinal lymphoma	(16)
Hepatitis B virus (HBV)	Some hepatocellular carcinoma	(17)
Human T-lymphotropic virus-1 (HTLV-1)	Adult T cell leukemia	(18)
Human papillomavirus (HPV)	Most cervical and penile cancers and some other anogenital and head and neck cancers	(19, 20)
Hepatitis C virus (HCV)	Some hepatocellular carcinoma and some lymphomas	(21)
Kaposi's sarcoma herpesvirus (KSHV)	Kaposi's sarcoma, primary effusion lymphoma and some multicentric Castleman's disease	(22)
Merkel cell polyomavirus (MCPyV)	Most Merkel cell carcinoma	(15)

Methods of viral discovery. There are a number of methods available for discovery of

novel viruses. Many viruses were discovered using "classical methods," most of which rely on

growth of the virus in cell culture after inoculation with patient samples of interest. As many

viruses are difficult to grow, this method biases discovery toward easily cultivatable viruses.

Before the advent of molecular techniques, viruses that could be grown were classified based on

characteristic such as their size and morphology by electron microscopy, serologic profile and

the type of cells in which they grew. This created an issue, as many viruses grew or looked alike,

although they ultimately represented distinct viral species and caused different illnesses.

With the development of molecular methods such as PCR, new approaches to viral discovery based on the detection of viral nucleic acids were created. PCR increased the sensitivity, specificity and throughput of identifying a specific viral agent. As many viruses share conserved genes (i.e. RNA-dependent RNA polymerase), primers targeting these areas could be developed to search for related but new viruses. This method is termed "consensus PCR" and is still widely used to discover novel viruses. Some examples of the applications of consensus PCR are the discoveries of human polyomavirus 7 (HPyV7), human polyomavirus 9 (HPyV9) and human polyomavirus 12 (HPyV12) (23-25). As with most of the molecular methods of discovery described here, consensus PCR is dependent on having sufficient sequence to identify shared sequences. In addition, it is a candidate-dependent approach, meaning the investigator must choose a specific candidate virus or viral family in order to use this method. This represents a serious challenge if the initial hypothesis is wrong.

Microarrays have been utilized for viral discovery, although more recent technologies have eclipsed their capacity. Pan-viral microarrays use oligonucleotide probes targeting highly conserved sequences from many viral families. For example, the first report of the ViroChip had 1,600 unique probes targeting approximately 140 viral genomes (26). A more recent version had 20,000 probes. This technology facilitated high throughput screening of a particular sample for many different viruses. While this method was also limited by its reliance on sequence similarity, it was candidate-independent.

Perhaps the biggest leap forward in viral discovery technologies came with the development of high throughput sequencing. This began with high throughput Sanger sequencing where 96 clones could be sequenced in parallel. Both WUPyV and KIPyV were discovered using this approach (27, 28). With the advent of next generation sequencing

6

technologies, including the 454 (Roche) and Illumina platforms, the number of sequencing reads obtained from a single run was vastly increased. Our lab currently uses the Illumina MiSeq platform, which generates approximately 10 million paired 250 base pair reads, allowing for assembly of contigs of approximately 450 nucleotides. The sheer volume of reads produced by these systems requires sophisticated computational analysis. Our lab utilizes a computational viral discovery pipeline (Figure 1.1) that separates reads with identity to known viral sequences from reads with similarity to other hosts. This pipeline is described in detail in Chapter 2. If evidence of a novel virus is found (i.e. the read has low identity to a known virus), sequences from the candidate virus are assembled to generate a partial genome. Full genomes are then determined using a combination of molecular approaches depending on the type of virus. A number of viruses have been discovered using these methods, including MW polyomavirus (MWPyV), the subject of Chapter 2.

Figure 1.1. Virus detection & discovery pipeline.
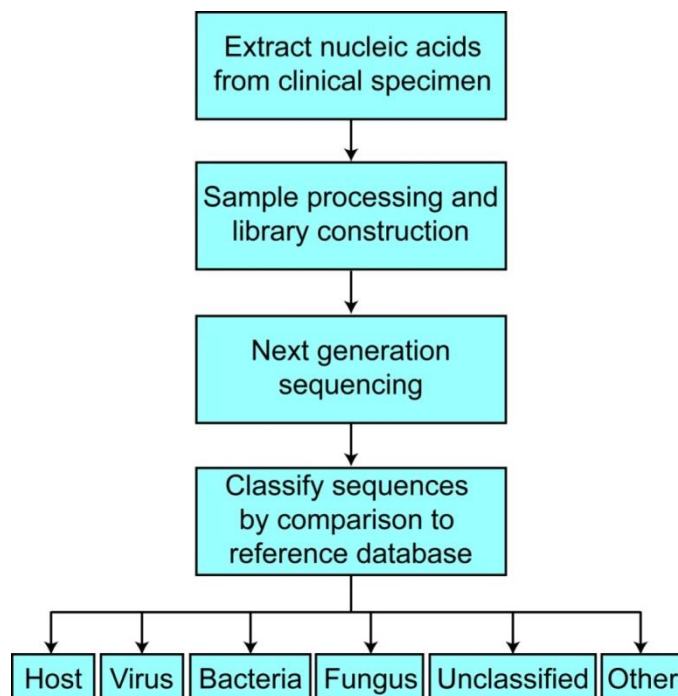
Determination of disease causality. Once a novel virus is discovered, determining if it causes a particular disease is an important, albeit often difficult, question to answer. The gold standard for establishing disease causality is to fulfill Koch's postulates, which are summarized below:

> *1. The parasite occurs in every case of the disease in question and under circumstances which can account for the pathological changes and clinical course of the disease.*
>
> *2. The parasite occurs in no other disease as a fortuitous and nonpathogenic parasite.*
>
> *3. After being fully isolated from the body and repeatedly grown in pure culture, the parasite can induce the disease anew.* (29)

As viruses cannot, by definition, be grown in pure culture, Koch's postulates must be modified to ascribe disease causality to a virus. This typically means the virus must be grown in cell culture. As previously mentioned, growing many viruses is difficult, and some viruses, such as norovirus, have yet to be cultured. Others have proposed variations of Koch's postulates which bypass the need for cell culture, including David Relman and David Fredericks:

> *1. A nucleic acid sequence belonging to a putative pathogen should be present in most cases of an infectious disease. Microbial nucleic acids should be found preferentially in those organs or gross anatomic sites known to be diseased (i.e., with anatomic, histologic, chemical, or clinical evidence of pathology) and not in those organs that lack pathology.*
>
> *2. Fewer, or no, copy numbers of pathogen-associated nucleic acid sequences should occur in hosts or tissues without disease.*

3. With resolution of disease (for example, with clinically effective treatment), the copy number of pathogen-associated nucleic acid sequences should decrease or become undetectable. With clinical relapse, the opposite should occur.

4. When sequence detection predates disease, or sequence copy number correlates with severity of disease or pathology, the sequence-disease association is more likely to be a causal relationship.

5. The nature of the microorganism inferred from the available sequence should be consistent with the known biological characteristics of that group of organisms. When phenotypes (e.g., pathology, microbial morphology, and clinical features) are predicted by sequence-based phylogenetic relationships, the meaningfulness of the sequence is enhanced.

6. Tissue-sequence correlates should be sought at the cellular level: efforts should be made to demonstrate specific in situ hybridization of microbial sequence to areas of tissue pathology and to visible microorganisms or to areas where microorganisms are presumed to be located.

7. These sequence-based forms of evidence for microbial causation should be reproducible. (29)

Despite the difficulty of determining disease causality, this research can have profound effects on morbidity and mortality of the disease. For example, identification of JC polyomavirus (JCPyV) as the etiological agent of progressive multifocal leukoencephalopathy (PML) allowed the development of screening strategies to identify affected individuals. In some cases, the patient's immunosuppression can now be modulated following detection of the virus to decrease mortality.

In conclusion, there are many suspected diseases of infectious etiology for which a candidate agent is undefined. Approximately two million worldwide deaths from respiratory and diarrheal diseases fall into this category as do a number of other diseases and cancers. While various viral discovery techniques have been utilized for decades, the past ten years have seen the emergence of increasingly high throughput, candidate-independent technologies, which have been used to discover a plethora of new viruses. Even newer methods are currently in development to identify viruses with no sequence homology to known viruses. Pandemics such as SARS and emerging viruses such as MERS teach us that new viruses are constantly emerging and can have severe impacts on both human health and global economics, making viral discovery a necessity.

SECTION II: THE *POLYOMAVIRIDAE*

General characteristics. Polyomaviruses are small circular, double-stranded DNA viruses that form non-enveloped virions of approximately 40-45 nm in diameter. Mature viral particles have a density of approximately 1.34 g/mL in cesium chloride, while empty capsids have a density of 1.29 g/mL (30). The icosahedral viral capsid is comprised of 72 pentamers in a T=7 lattice arrangement and surrounds one copy of the genome, which averages approximately 5,000 base pairs. The capsid is complexed with the cellular histones H2A, H2B, H3 and H4. The genome can be divided into three parts (Figure 1.2): the regulatory region, the early region and the late region. The regulatory region, also called the noncoding control region (NCCR), contains the origin of replication and promoters for the early and late regions. Transcription occurs bidirectionally from the regulatory region. The early region encodes the large tumor antigen (LTAg) and small tumor antigen (STAg), which are expressed prior to viral replication. The late

region is expressed after viral replication has begun and encodes the structural proteins VP1, VP2 and VP3. VP1, the major structural protein, comprises over 70% of the viral particle and is the antigenic portion of the virus to which most natural antibodies are made (31). Some polyomaviruses encode an additional one to four proteins of varying function, although the viruses described in this dissertation (MWPyV, WUPyV and KIPyV) do not.

Figure 1.2. Schematic representation of the WUPyV genome, including the early region, late region and NCCR. Reproduced from (27).
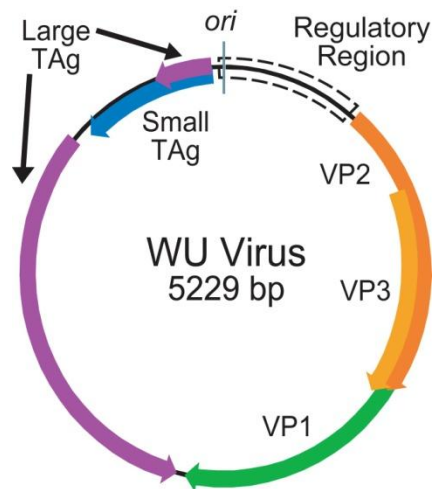
Viral life cycle. The polyomavirus life cycle (Figure 1.3) begins when the virus attaches and enters the host cell. While the receptors for most polyomaviruses, including WUPyV, KIPyV and MWPyV, are still unknown, BKPyV, JCPyV, SV40, murine polyomavirus (MPyV) and Merkel cell carcinoma polyomavirus (MCPyV) all are reported to use gangliosides. In addition, JCPyV requires the serotonin receptor 5HT-2a as a coreceptor, and some studies on SV40 have supported its use of MHC class I as a receptor (32). Following attachment, polyomaviruses enter the cell via caveolae-mediated endocytosis (SV40) or clathrin-mediated endocytosis (JCPyV)

(30). The exact mechanism of intracellular trafficking and uncoating has yet to be deciphered, but the virus is eventually delivered to the nucleus, where transcription of the early region begins. Once LTAg protein is made, it autoregulates the early promoter and drives simultaneous replication of the viral genome and transcription of the late region. After the structural proteins have accumulated in the nucleus, the virion is assembled. It is unclear how the virus exits the cell, as different studies have demonstrated both lytic release and shedding from intact cells (30). Polyomavirus genomes are relatively stable over time, with WUPyV having low nucleotide variation of 0-1.2% (33).

Figure 1.3. The polyomavirus life cycle. Figure is used with permission from Anne M. Gaynor.
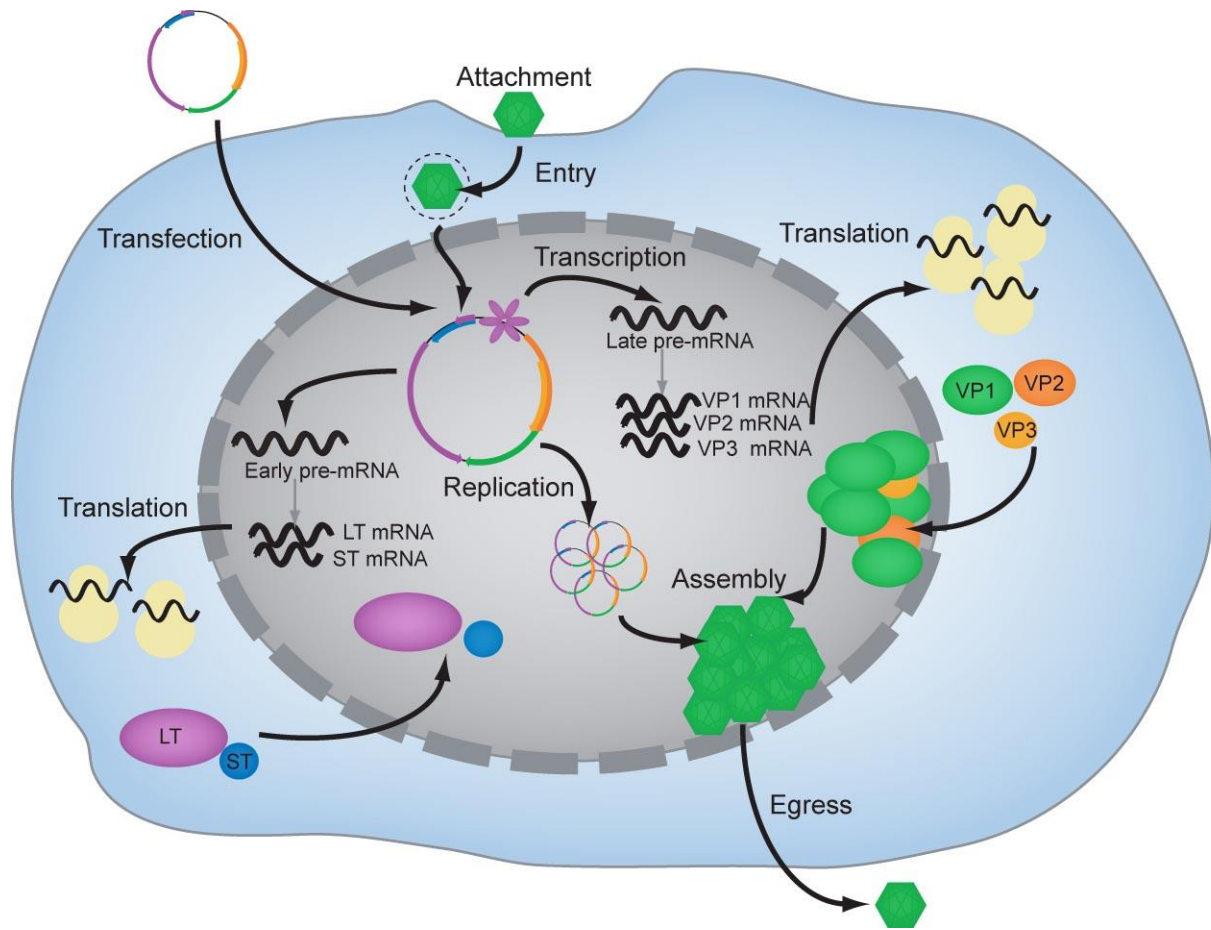
Polyomaviruses, human disease and virus tropism. Polyomaviruses infect a wide range of mammalian and avian hosts, including non-human primates, cattle, rabbits, several small rodent species, various bird species, bats, sea lions, dolphins and humans, among others. There were nine fully sequenced human polyomaviruses when this work was begun, including BKPyV, JCPyV, WUPyV, KIPyV, MCPyV, human polyomavirus 6 (HPyV6), HPyV7, TSPyV and HPyV9. BKPyV and JCPyV were both discovered in 1971. BKPyV causes BK nephropathy in kidney transplant recipients, which can lead to graft rejection, and hemorrhagic cystitis in bone marrow transplant recipients; JCPyV is the etiological agent of PML, a rare neurological condition (30).

No new human polyomaviruses were identified until the discovery of WUPyV and KIPyV in 2007 (27, 28). Both were discovered in respiratory tract secretions from patients with respiratory illness. A more thorough background on these viruses is included below. The discovery of these viruses re-invigorated the *Polyomaviridae* field and study of the family's role in human disease (34). MCPyV was discovered clonally integrated into 80% of MCCs in 2008 (15). MCC is a rare but very aggressive skin cancer. Subsequent reports have indicated the virus may play a role in all MCCs, although this is still debated (35). MCPyV was the first human polyomavirus to be definitively tied to a human cancer. There are numerous reports linking JCPyV and BKPyV to various cancers, but an abundance of conflicting data exists (36), and there is still no consensus in the field as to whether these viruses cause cancers. Following the discovery of MCPyV, HPyV6 and HPyV7 were discovered in skin swabs from healthy volunteers (23). HPyV6 was discovered using rolling circle amplification (RCA), and consensus PCR was used to find HPyV7. No diseases have been associated with either virus. TSPyV was also detected using RCA in skin spicules from a patient with Trichodysplasia spinulosa, a rare

skin condition, exclusively seen in immunocompromised patients (12). Finally, the discovery of

HPyV9 also used consensus PCR and found the virus in serum from a kidney transplant recipient

(25). Again, no diseases have been associated with HPyV9. At the time the research in this

dissertation began, these were the only known human polyomaviruses. The discovery of

MWPyV, the tenth human polyomavirus, and its role in human disease is described in Chapter 2.

Three additional human polyomaviruses have since been identified, and these are described in

the Discussion. None of the other three new viruses has been definitively associated with disease,

although some evidence exists for New Jersey polyomavirus (NJPyV) (37). A timeline of all

discoveries is depicted in Figure 1.4.

Figure 1.4. Timeline of human polyomavirus discoveries. Viruses in red are the subject of this

dissertation. STL polyomavirus (STLPyV) (38).
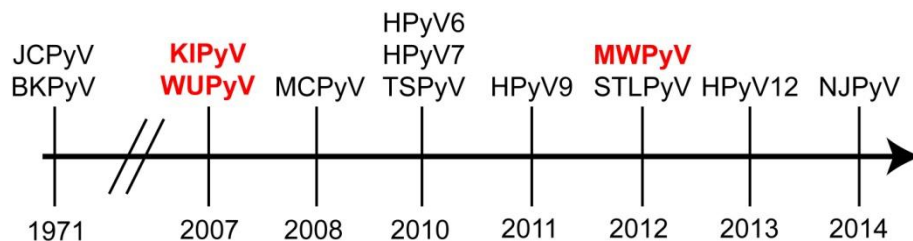
It is not currently known how any of the human polyomaviruses, including BKPyV and

JCPyV, spread among humans, but their seroprevalence is generally quite high. Antibodies

against BKPyV are detected in 82-99% of people, while the seroprevalence for JCPyV is 39-

81% (36). Several of the other human polyomaviruses also have high seroprevalences, including

KIPyV (55-90%), WUPyV (69-98%) and MCPyV (60-81%) (36). The others are somewhat

lower at 69% for HPyV6, 35% for HPyV7, 70% for TSPyV, 21-53% for HPyV9 and 17-23% for

HPyV12 (24, 36). Studies to determine the seroprevalence of MWPyV and STLPyV are

ongoing. Following primary infection in childhood, BKPyV and JCPyV establish persistent

latent infections in the kidneys but can periodically reactivate, leading to shedding of infectious

virus in the urine (30). This may be a route of virus transmission. Primary infection and periodic

reactivation are typically asymptomatic unless the host is immunocompromised, in which case

life-threatening illness can occur.

Following infection, both viruses spread efficiently within the human body and are

detected in peripheral blood leukocytes (39) and in a variety of organs, including heart, spleen,

lung, colon and liver (30). JCPyV has a well-established neurotropism and can also be identified

in human tonsil stromal cells and in other cell types of the tonsils (30). Both BKPyV and JCPyV

have been cultured in mammalian cells. JCPyV has limited cell specificity and can infect human

glial cells and tonsillar stromal cells (40). BKPyV can infect a greater variety of cells, including

African green monkey kidney cells, human embryonic kidney, human diploid lung fibroblasts,

infant urothelial cells, human fetal brain cells, monkey kidney cells and human embryonic lung

cells (41, 42). The other human polyomaviruses have been found in a variety of sample types

(see Table 4.1), but little work has been done to establish their specific cell or tissue tropisms,

although inflammatory monocytes (CD14+ CD16-) have been identified as a reservoir for

MCPyV (43). No cell culture systems for the novel polyomaviruses have been reported to date,

but a replication system similar to that described in Chapter 4 for WUPyV has been established

for MCPyV (44).

WU and KI polyomaviruses. WUPyV was discovered in a respiratory sample from a

three-year-old Australian child with pneumonia (27). KIPyV was similarly found in pooled

respiratory samples from patients with respiratory illness (28). Both viruses have since been

detected by PCR in a variety of samples, including cerebrospinal fluid (CSF), tonsillar tissue,

whole blood, plasma, stool and lymph tissue (45, 46). As noted above, the majority of the

population has generated antibodies against the viruses. Data also indicates WUPyV can

establish a persistent infection; two pediatric transplant cases from St. Louis had sequential

samples obtained over a period of several weeks that were positive for viral DNA (47). Although

this data represents important preliminary results, it is still unknown whether WUPyV and

KIPyV cause human disease. No specific cell or tissue tropisms have been identified for either

virus, and a systematic search of human tissues has not been performed. Determining the cell and

tissue tropism will help narrow down diseases potentially caused by WUPyV or KIPyV

infection. Finally, no infectious cell culture system has been established for either virus to date,

making the fulfillment of Koch's postulates impossible.

CONCLUSIONS

The study of the 11 novel polyomaviruses is in its infancy, and little is known about their

biology or ability to cause disease. In this dissertation, I took a multifaceted approach to gain a

better understanding of the biology and potential roles in disease of WUPyV, KIPyV and

MWPyV.

Using the viral discovery techniques describe above, we discovered a novel polyomavirus

in the stool of a child from Malawi, which we tentatively named MWPyV. The first aim of my

work was to sequence and characterize the complete genome of MWPyV and determine its

prevalence in humans. Obtaining a complete genome sequence is the first step in characterizing a

novel virus and allowed me to determine its phylogenetic relationship to other family members,

the size of its genome and its genomic organization. Obtaining the complete sequence was also

prerequisite to downstream studies, including generation of a genomic clone. Prevalence studies,

such as those detailed here, address questions like, "Can we detect viral persistence over time?" and "Can we identify the virus in novel sample types?" Answers to these questions give us clues as to where in the body the virus resides and are a first step in identifying the virus' cell and tissue tropism.

An important step in establishing the role of WUPyV and KIPyV in human disease is to determine the viruses' cell and tissue tropisms. The goal of this aim was to identify the kinds of tissues and the specific cell types within that are positive for WUPyV and KIPyV, which will help us better understand viral biology and possibly identify disease states associated with viral infection. I approached this step directly by using immunohistochemical methods to detect the viruses in human tissues and determine the specific cell types they infect.

Many downstream studies of WUPyV biology are dependent on having a cell culture system for the virus, including identifying the viral receptor and studying its intracellular interactions. The gold standard approach to determining disease causality is the fulfillment of Koch's postulates, which by definition requires the virus be grown in culture. As no such system currently exists for WUPyV, it is a fundamental barrier to both establishing disease causality and exploring the basic biology of this virus. The final aim of this work was to establish an infectious cell culture system for WUPyV.

While the three aims of this research were highly specific, they address the two overarching research questions presented at the beginning of this section: "Are there additional, novel polyomaviruses infecting humans?" and "Do these polyomaviruses cause disease in their human hosts?" I address the first question in Chapter 2, where I detail the discovery and characterization of the novel polyomavirus MWPyV. The second question is addressed in Chapters 2 and 3, where I report the identification of specific cell types positive for WUPyV and

17

KIPyV, describe the cases of several virus-positive patients and detail attempts to grow WUPyV in cell culture. Finally, in the Discussion, I broadly summarize these findings and return back to discuss the two questions noted above.

NOTE ON AUTHORSHIP

The candidate was the principal writer of the published article that comprises Chapter 2. The candidate was also the principal writer on the articles that comprise Chapter 3; these three manuscripts were either under review or in preparation when this dissertation was written. The candidate was not the principal writer on the published article that comprises Appendix I but was a major contributor to the writing of this paper. The remainder of this dissertation (Chapters 1, 4 and 5) will not be published, and the candidate was the principal writer of these sections. The candidate was also a major contributor to the research ideas, in concert with her advisor and relevant collaborators, and performed almost all of the research detailed in Chapters 2-4. Others who contributed to the research are noted as co-authors or in the acknowledgements sections. Permission for reprinting of articles, figures and/or tables was obtained as required by the individual journals or people and is noted.

REFERENCES

1. **World Health Organization.** June 2011. The top 10 causes of death 2011 fact sheet.
2. **Heikkinen T, and Jarvinen A.** 2003. The common cold. Lancet **361:**51-59.
3. **Klein EJ, Boster DR, Stapp JR, Wells JG, Qin X, Clausen CR, Swerdlow DL, Braden CR, and Tarr PI.** 2006. Diarrhea etiology in a Children's Hospital Emergency Department: a prospective cohort study. Clin Infect Dis **43:**807-813.
4. **Monto AS.** 2002. Epidemiology of viral respiratory infections. Am J Med **112 Suppl 6A:**4S-12S.
5. **Ksiazek TG, Erdman D, Goldsmith CS, Zaki SR, Peret T, Emery S, Tong S, Urbani C, Comer JA, Lim W, Rollin PE, Dowell SF, Ling AE, Humphrey CD, Shieh WJ, Guarner J, Paddock CD, Rota P, Fields B, DeRisi J, Yang JY, Cox N, Hughes JM,**

LeDuc JW, Bellini WJ, Anderson LJ, and Group SW. 2003. A novel coronavirus associated with severe acute respiratory syndrome. N Engl J Med **348:**1953-1966.

6. **Zaki AM, van Boheemen S, Bestebroer TM, Osterhaus AD, and Fouchier RA.** 2012. Isolation of a novel coronavirus from a man with pneumonia in Saudi Arabia. N Engl J Med **367:**1814-1820.

7. **Pyrc K, Berkhout B, and van der Hoek L.** 2007. The novel human coronaviruses NL63 and HKU1. J Virol **81:**3051-3057.

8. **Kirk R, Dipchand AI, Edwards LB, Kucheryavaya AY, Benden C, Christie JD, Dobbles F, Rahmel AO, Stehlik J, Hertz MI, International Society for H, and Lung T.** 2012. The Registry of the International Society for Heart and Lung Transplantation: fifteenth pediatric heart transplantation report--2012. J Heart Lung Transplant **31:**1065-1072.

9. **Zuppan CW, Wells LM, Kerstetter JC, Johnston JK, Bailey LL, and Chinnock RE.** 2009. Cause of death in pediatric and infant heart transplant recipients: review of a 20-year, single-institution cohort. J Heart Lung Transplant **28:**579-584.

10. **Stehlik J, Edwards LB, Kucheryavaya AY, Benden C, Christie JD, Dipchand AI, Dobbels F, Kirk R, Rahmel AO, Hertz MI, International Society of H, and Lung T.** 2012. The Registry of the International Society for Heart and Lung Transplantation: 29th official adult heart transplant report--2012. J Heart Lung Transplant **31:**1052-1064.

11. **Montoya JG, Giraldo LF, Efron B, Stinson EB, Gamberg P, Hunt S, Giannetti N, Miller J, and Remington JS.** 2001. Infectious complications among 620 consecutive heart transplant patients at Stanford University Medical Center. Clin Infect Dis **33:**629-640.

12. **van der Meijden E, Janssens RW, Lauber C, Bouwes Bavinck JN, Gorbalenya AE, and Feltkamp MC.** 2010. Discovery of a new human polyomavirus associated with trichodysplasia spinulosa in an immunocompromised patient. PLoS Pathog **6:**e1001024.

13. **Moore PS, and Chang Y.** 2010. Why do viruses cause cancer? Highlights of the first century of human tumour virology. Nat Rev Cancer **10:**878-889.

14. **Teman CJ, Tripp SR, Perkins SL, and Duncavage EJ.** 2011. Merkel cell polyomavirus (MCPyV) in chronic lymphocytic leukemia/small lymphocytic lymphoma. Leuk Res **35:**689-692.

15. **Feng H, Shuda M, Chang Y, and Moore PS.** 2008. Clonal integration of a polyomavirus in human Merkel cell carcinoma. Science **319:**1096-1100.

16. **Epstein MA, Achong BG, and Barr YM.** 1964. Virus Particles in Cultured Lymphoblasts from Burkitt's Lymphoma. Lancet **1:**702-703.

17. **Blumberg BS, Alter HJ, and Visnich S.** 1965. A "New" Antigen in Leukemia Sera. JAMA **191:**541-546.

18. **Poiesz BJ, Ruscetti FW, Gazdar AF, Bunn PA, Minna JD, and Gallo RC.** 1980. Detection and isolation of type C retrovirus particles from fresh and cultured lymphocytes of a patient with cutaneous T-cell lymphoma. Proc Natl Acad Sci U S A **77:**7415-7419.

19. **Boshart M, Gissmann L, Ikenberg H, Kleinheinz A, Scheurlen W, and zur Hausen H.** 1984. A new type of papillomavirus DNA, its presence in genital cancer biopsies and in cell lines derived from cervical cancer. EMBO J **3:**1151-1157.

20. **Durst M, Gissmann L, Ikenberg H, and zur Hausen H.** 1983. A papillomavirus DNA from a cervical carcinoma and its prevalence in cancer biopsy samples from different geographic regions. Proc Natl Acad Sci U S A **80:**3812-3815.

21. **Choo QL, Kuo G, Weiner AJ, Overby LR, Bradley DW, and Houghton M.** 1989. Isolation of a cDNA clone derived from a blood-borne non-A, non-B viral hepatitis genome. Science **244:**359-362.

22. **Chang Y, Cesarman E, Pessin MS, Lee F, Culpepper J, Knowles DM, and Moore PS.** 1994. Identification of herpesvirus-like DNA sequences in AIDS-associated Kaposi's sarcoma. Science **266:**1865-1869.

23. **Schowalter RM, Pastrana DV, Pumphrey KA, Moyer AL, and Buck CB.** 2010. Merkel cell polyomavirus and two previously unknown polyomaviruses are chronically shed from human skin. Cell Host Microbe **7:**509-515.

24. **Korup S, Rietscher J, Calvignac-Spencer S, Trusch F, Hofmann J, Moens U, Sauer I, Voigt S, Schmuck R, and Ehlers B.** 2013. Identification of a novel human polyomavirus in organs of the gastrointestinal tract. PLoS One **8:**e58021.

25. **Scuda N, Hofmann J, Calvignac-Spencer S, Ruprecht K, Liman P, Kuhn J, Hengel H, and Ehlers B.** 2011. A novel human polyomavirus closely related to the african green monkey-derived lymphotropic polyomavirus. J Virol **85:**4586-4590.

26. **Wang D, Coscoy L, Zylberberg M, Avila PC, Boushey HA, Ganem D, and DeRisi JL.** 2002. Microarray-based detection and genotyping of viral pathogens. Proc Natl Acad Sci U S A **99:**15687-15692.

27. **Gaynor AM, Nissen MD, Whiley DM, Mackay IM, Lambert SB, Wu G, Brennan DC, Storch GA, Sloots TP, and Wang D.** 2007. Identification of a novel polyomavirus from patients with acute respiratory tract infections. PLoS Pathog **3:**e64.

28. **Allander T, Andreasson K, Gupta S, Bjerkner A, Bogdanovic G, Persson MA, Dalianis T, Ramqvist T, and Andersson B.** 2007. Identification of a third human polyomavirus. J Virol **81:**4130-4136.

29. **Fredericks DN, and Relman DA.** 1996. Sequence-based identification of microbial pathogens: a reconsideration of Koch's postulates. Clin Microbiol Rev **9:**18-33.

30. **Imperiale MJ, and Major EO.** 2007. Polyomaviruses, p. 2263-2289. *In* Knipe, DM and Howley, PM (ed.), Fields Virology. Lippincott Williams & Wilkins, Philadelphia.

31. **Cole CN, and Conzen SD.** 2001. Polyomaviridae: The Viruses and Their Replication. *In* Knipe, DM and Howley, PM (ed.), Fields Virology. Lippincott Williams & Wilkins, Philadelphia.

32. **Neu U, Stehle T, and Atwood WJ.** 2009. The Polyomaviridae: Contributions of virus structure to our understanding of virus receptors and infectious entry. Virology **384:**389-399.

33. **Bialasiewicz S, Rockett R, Whiley DW, Abed Y, Allander T, Binks M, Boivin G, Cheng AC, Chung JY, Ferguson PE, Gilroy NM, Leach AJ, Lindau C, Rossen JW, Sorrell TC, Nissen MD, and Sloots TP.** 2010. Whole-genome characterization and genotyping of global WU polyomavirus strains. J Virol **84:**6229-6234.

34. **DeCaprio JA, and Garcea RL.** 2013. A cornucopia of human polyomaviruses. Nat Rev Microbiol **11:**264-276.

35. **Rodig SJ, Cheng J, Wardzala J, DoRosario A, Scanlon JJ, Laga AC, Martinez-Fernandez A, Barletta JA, Bellizzi AM, Sadasivam S, Holloway DT, Cooper DJ,**

        Kupper TS, Wang LC, and DeCaprio JA. 2012. Improved detection suggests all Merkel cell carcinomas harbor Merkel polyomavirus. J Clin Invest **122:**4645-4653.

36.   **Dalianis T, and Hirsch HH.** 2013. Human polyomaviruses in disease and cancer. Virology **437:**63-72.

37.   **Mishra N, Pereira M, Rhodes RH, An P, Pipas JM, Jain K, Kapoor A, Briese T, Faust PL, and Lipkin WI.** 2014. Identification of a Novel Polyomavirus in a Pancreatic Transplant Recipient With Retinal Blindness and Vasculitic Myopathy. J Infect Dis.

38.   **Lim ES, Reyes A, Antonio M, Saha D, Ikumapayi UN, Adeyemi M, Stine OC, Skelton R, Brennan DC, Mkakosya RS, Manary MJ, Gordon JI, and Wang D.** 2013. Discovery of STL polyomavirus, a polyomavirus of ancestral recombinant origin that encodes a unique T antigen by alternative splicing. Virology **436:**295-303.

39.   **Knowles WA.** 2006. Discovery and epidemiology of the human polyomaviruses BK virus (BKV) and JC virus (JCV). Adv Exp Med Biol **577:**19-45.

40.   **Monaco MC, Atwood WJ, Gravell M, Tornatore CS, and Major EO.** 1996. JC virus infection of hematopoietic progenitor cells, primary B lymphocytes, and tonsillar stromal cells: implications for viral latency. J Virol **70:**7004-7012.

41.   **Yoshiike K, and Takemoto KK.** 1986. Studies with BK virus and monkey lymphotropic papovavirus, p. 295-326. *In* Salzman, NP (ed.), The Papovaviridae. Plenum Press, New York.

42.   **Takemoto KK, and Mullarkey MF.** 1973. Human papovavirus, BK strain: biological studies including antigenic relationship to simian virus 40. J Virol **12:**625-631.

43.   **Mertz KD, Junt T, Schmid M, Pfaltz M, and Kempf W.** 2010. Inflammatory monocytes are a reservoir for Merkel cell polyomavirus. J Invest Dermatol **130:**1146-1151.

44.   **Feng H, Kwun HJ, Liu X, Gjoerup O, Stolz DB, Chang Y, and Moore PS.** 2011. Cellular and viral factors regulating Merkel cell polyomavirus replication. PLoS One **6:**e22468.

45.   **Babakir-Mina M, Ciccozzi M, Perno CF, and Ciotti M.** 2011. The novel KI, WU, MC polyomaviruses: possible human pathogens? New Microbiol **34:**1-8.

46.   **Sharp CP, Norja P, Anthony I, Bell JE, and Simmonds P.** 2009. Reactivation and mutation of newly discovered WU, KI, and Merkel cell carcinoma polyomaviruses in immunosuppressed individuals. J Infect Dis **199:**398-404.

47.   **Le BM, Demertzis LM, Wu G, Tibbets RJ, Buller R, Arens MQ, Gaynor AM, Storch GA, and Wang D.** 2007. Clinical and epidemiologic characterization of WU polyomavirus infection, St. Louis, Missouri. Emerg Infect Dis **13:**1936-1938.

CHAPTER 2

Identification of MW polyomavirus, a novel polyomavirus in human stool

Erica A. Siebrasse[1], Alejandro Reyes[2], Efrem S. Lim[1], Guoyan Zhao[1], Rajhab S. Mkakosya[4], Mark J. Manary[3], Jeffrey I. Gordon[2] and David Wang[1]

[1] Departments of Molecular Microbiology and Pathology & Immunology, [2] Center for Genome Sciences and Systems Biology and [3] Department of Pediatrics, Washington University School of Medicine, St. Louis, Missouri USA; [4] Department of Pathology, College of Medicine, University of Malawi, P/B 360, Chichiri, Blantyre 3, Malawi

ABSTRACT

We have discovered a novel polyomavirus present in multiple human stool samples. The virus was initially identified by shotgun pyrosequencing of DNA purified from virus-like particles isolated from a stool sample collected from a healthy child from Malawi. We subsequently sequenced the virus' 4,927 bp genome, which has been provisionally named MW polyomavirus (MWPyV). The virus has genomic features characteristic of the family *Polyomaviridae* but is highly divergent from other members of this family. It is predicted to encode the early proteins large T antigen and small T antigen and the structural proteins VP1, VP2 and VP3. A real-time PCR assay was designed and used to screen 514 stool samples from children with diarrhea in St. Louis, Missouri; 12 specimens were positive for MWPyV. Comparison of the whole genome sequences of the index Malawi case and one St. Louis case demonstrated that the two strains of MWPyV varied by 5.3% at the nucleotide level. The number of polyomaviruses found in the human body continues to grow, raising the question of how many more species have yet to be identified and what roles they play in humans with and without manifest disease.

INTRODUCTION

Over the past five years, seven novel polyomaviruses have been discovered in humans, including KI polyomavirus (KIPyV) (1), WU polyomavirus (WUPyV) (2), Merkel cell polyomavirus (MCPyV) (3), human polyomavirus 6 (HPyV6) (4), human polyomavirus 7 (HPyV7) (4), Trichodysplasia spinulosa-associated polyomavirus (TSPyV) (5) and human polyomavirus 9 (HPyV9) (6). Polyomaviruses also infect a wide variety of mammalian and avian hosts, including the recently described novel polyomaviruses of bats (*Myotis* species, (7)), sea lions (*Zalophus californianus* (8, 9)), multimammate mice (*Mastomys* species (10)), canaries (*Serinus canaria* (11)), orangutans (*Pongo* species (12)), squirrel monkeys (*Saimiri* species (13)), chimpanzees ((*Pan troglodytes verus (14)*)) and gorillas (*Gorilla gorilla* (14)).

Viruses in the *Polyomaviridae* family typically possess ~5,000 base pair (bp) circular, double-stranded DNA genomes. The genome can be divided into three parts--the regulatory region, the early region and the late region. The regulatory region, also called the noncoding control region (NCCR), contains the origin of replication and promoters for the early and late regions. Transcription occurs bidirectionally from the regulatory region. The early region is expressed from a common primary transcript and is alternatively spliced to produce the large T antigen (LTAg) and small T antigen (STAg) prior to viral replication. LTAg and STAg typically share the first ~80 amino acids. The late region is expressed after viral replication has begun and encodes the structural proteins VP1, VP2 and VP3. VP1, the major structural protein, typically comprises over 70% of the viral particle and is the antigenic portion of the virus to which most natural antibodies are made (15).

Disease associations have been established for some of the human polyomaviruses. The two well-studied human polyomaviruses BK polyomavirus (BKPyV) and JC polyomavirus

(JCPyV) are important human pathogens. BKPyV is known to cause BK nephropathy, which can lead to renal allograft failure, and hemorrhagic cystitis, while JCPyV is the etiological agent of progressive multifocal leukoencephalopathy (PML). Both viruses are ubiquitous worldwide, with seroprevalence rates of 55-85% for BKPyV and 44-77% for JCPyV (16). Following primary infection in childhood, BKPyV and JCPyV establish persistent latent infections that can periodically reactivate, leading to shedding of infectious virus in the urine (17). Primary infection and periodic reactivation are typically asymptomatic unless the host is immunocompromised, in which case life-threatening illness can occur (17). MCPyV is associated with Merkel cell carcinoma (MCC), a rare but aggressive skin cancer. MCPyV DNA is found in ~80% of MCC tumors and is clonally integrated into a subset of these (18). TSPyV has been linked to Trichodysplasia spinulosa, a very rare skin condition associated with immunosuppression following organ transplantation (19). It is unclear if the other human polyomaviruses play a role in disease.

The recently discovered human polyomaviruses have all been identified through the use of molecular methods for detection of viral nucleic acids. WUPyV and KIPyV were discovered using high-throughput Sanger sequencing (1, 2). MCPyV was identified using digital transcriptome subtraction, which entails pyrosequencing of a cDNA library followed by subtraction of human reads to identify novel viral sequences (3). HPyV6 and TSPyV were discovered using rolling circle amplification (RCA) (4, 5), and consensus PCR primers were utilized to find HPyV7 and HPyV9 (4, 6).

We used shotgun pyrosequencing of purified virus-like particles (VLPs) recovered from a fecal sample to discover a novel polyomavirus in the stool of a healthy child from Malawi. The virus was also detected in 12 additional stool samples from the United States, indicating it has a

wide geographic distribution. As stool is not a sterile site, it is currently unknown whether this polyomavirus actively infects humans. Finally, we compared the whole genome nucleotide sequences of the index Malawi case and a case from St. Louis and found these two strains to have 5.3% nucleotide variation.

MATERIALS AND METHODS

Human studies. This study was approved by the College of Medicine Research and Ethics Committee of the University of Malawi and the Human Research Protection Office of Washington University in St. Louis. The index stool specimen was obtained from a healthy, breast-fed, 15-month-old female living in Mayaka, Malawi, in September 2008 as part of a global gut microbiome survey (20).

A total of 514 stool specimens from St. Louis were tested for MWPyV. Stool samples were from children, aged birth to 18 years, with diarrhea and were submitted to the St. Louis Children's Hospital, St. Louis, Missouri, microbiology laboratory for bacterial culture from July 2009 to June 2010.

Sample preparation and 454 pyrosequencing. VLPs were purified as described earlier (21) with minor modifications. In brief, 50mg of a frozen fecal sample was resuspended in 400μL of SM buffer (100mM NaCl, 8mM MgSO$_4$, 50mM Tris (pH 7.5) and 0.002% gelatin (w/v)). Following centrifugation (2,500xg for 10 min at 4ºC) and filtration through 0.45 and 0.22μm pore-size Millex filters (Millipore) to remove bacterial cells and large particles, the sample was treated with chloroform (0.2 volumes) for 10 min and centrifuged for 5 min at 2,500xg. The aqueous phase was treated with Baseline-Zero DNase (2.5 U/ml) (Epicentre) for one hour at 37ºC to remove free DNA, followed by an incubation at 65ºC for 15 min to inactivate the

26

enzyme. To extract VLP-associated DNA, the solution was treated with 10μL 10% SDS and 3μL

Proteinase K (20mg/ml) for 20 min at 56ºC. Subsequently, 35μL of 5M NaCl and 28μL of a

solution of 10% cetyltrimethylammonium bromide/0.7M NaCl were introduced. After a 10 min

incubation at 65ºC, an equal volume of chloroform was added, and the mixture was centrifuged

for 5 min at 8,000xg at room temperature. The supernatant was transferred to a new tube, and an

equal volume of phenol/chloroform/isoamyl alcohol (25:24:1) was added, followed by

centrifugation for 5 min at 8,000xg at room temperature. The supernatant was collected, and the

DNA was purified using Qiagen MiniElute columns following manufacturer instructions, with a

final elution volume of 35μL.

Purified VLP-derived DNA (1μL) was used as input in a 20μL RCA reaction using the

illustra GenomiPhi V2 kit (GE Healthcare) as recommended by the manufacturer (n= four

independent reactions). After 90 minutes of amplification, the four reactions were pooled and

purified using the Qiagen DNeasy kit. DNA (500ng) was subjected to 454 FLX Titanium

pyrosequencing.

Analysis of pyrosequencing reads. The individual 454 reads were analyzed using a custom

bioinformatics pipeline as previously described (22). In brief, unique, high quality reads were

aligned against the reference human genome and the Genbank nt (nucleotide) database using

BLASTn. Reads with no hits or hits with an E-value greater than e-5 were then aligned using

BLASTx to the GenBank nr (non-redundant) database, and reads aligning to viral sequences with

the lowest e value were identified.

Complete genome sequencing. PCR primers were designed to span the gaps between the six

reads showing significant similarity to polyomaviruses generated by pyrosequencing to obtain an

initial whole genome sequence. The sequences for these primers are available upon request. The

complete MWPyV genome derived from the index Malawi case (designated strain MA095, Genbank JQ898291) was sequenced to greater than 3x coverage using four sets of overlapping PCR primers. They were (listed 5' to 3') (ES087) ACTTAAACCATGTTCCTGACTCTGT and (ES091) ACAGAGATTACAGCACCCATATACT, (ES088) GCATCTGCCCTGGTACAAACA and (ES092) CAGACAACTCAGAAGTTTCCACCTC, (ES089) GAAGTAGAAGGAGAGGAAAATGCCG and (ES093) TGCTGTTGAGGATACACAACAAGAC, and (ES090) AGGCTGCTTAAAGGCCTATGAATG and (ES094) CTGAAACACCAGTTGCTCCAGC. Amplicons from independent PCR reactions were cloned into pCR4 (Invitrogen) and bidirectionally sequenced. The complete genome from St. Louis sample WD976 (Strain WD976, Genbank JQ898292) was amplified and sequenced to greater than 3x coverage in the same manner, using the same primer pairs.

Genome annotation. Open reading frames (ORFs) were predicted using NCBI ORF Finder. The LTAg and STAg ORFs were manually scanned for conserved splice donor and acceptor sites. Conserved motifs in the TAgs and in the NCCR were identified using NCBI CD-Search software (23) and by manual identification. Prediction of putative binding sites for transcription factors was performed using AliBaba software, version 2.1 (24). The NCCR region was scanned for palindrome patterns using the EMBOSS palindrome software (25).

Phylogenetic analysis. Protein sequences associated with the reference genomes for 27 polyomaviruses were obtained from GenBank; these included: baboon polyomavirus (NC_007611, SA12) (26), bat polyomavirus (NC_011310, BatPyV) (7), B-lymphotropic polyomavirus (NC_004763, LPyV) (27), BKPyV (NC_001538) (28), Bornean orangutan polyomavirus (NC_013439, OraV1) (12), bovine polyomavirus (NC_001442, BPyV) (29),

California sea lion polyomavirus (NC_013796, SLPyV) (8), hamster polyomavirus (NC_001663, HaPyV) (30), JCPyV (NC_001699) (31), MCPyV (HM011557) (4), murine pneumotropic virus (NC_001505, MPtV) (32), murine polyomavirus (NC_001515, MPyV) (33), simian virus 40 (NC_001669, SV40) (34), Squirrel monkey polyomavirus (NC_009951, SqPyV) (13), Sumatran orangutan polyomavirus (FN356901, OraV2) (12), TSPyV (NC_014361) (5), HPyV6 (NC_014406) (4), HPyV7 (NC_014407) (4), KIPyV (NC_009238) (1), WUPyV (NC_009539) (2), avian polyomavirus (NC_004764, APyV) (35), canary polyomavirus (GU345044, CaPyV) (11), crow polyomavirus (NC_007922, CPyV) (36), finch polyomavirus (NC_007923, FPyV) (36), goose hemorrhagic polyomavirus (NC_004800, GHV) (37), chimpanzee polyomavirus (NC_014743, ChPyV) (38) and HPyV9 (NC_015150) (6). The predicted open reading frames for MWPyV LTAg, VP1 and VP2 were aligned with the corresponding proteins from the 27 known polyomaviruses using Fast Statistical Alignment (FSA) software, version 1.15.2 (39). For the LTAg analysis, unalignable regions were removed, and the remainder of the alignment was concatenated. Maximum likelihood trees were generated using PhyML, version 3.0 (40), with 1,000 bootstrap replicates and the best model as determined by Prot Test software, version 2.4 (41); these were RtRev for VP1 and LG for VP2 and LTAg.

Nucleic acid extraction. Stools which had been frozen at -80°C were diluted approximately 1:6 in PBS and filtered through 0.45 μm membranes prior to extraction. Total nucleic acids were extracted using an Ampliprep Cobas automated extractor (Roche) and eluted in a volume of 75μL. The samples were arrayed in a 96-well plate for storage at -80°C.

Real-time PCR screening of the St. Louis cohort. A Taqman real-time PCR assay was designed to target the MWPyV LTAg using Primer Express software (Applied Biosystems). Primers and probe used for this assay were (ES105) 5'-TGAGAAGGCCCCGGTTCT-3',

(ES106) 5'- GAGGATGGGATGAAGATTTAAGTTG-3' and (ES107) 5'-FAM-

CCTCATCACTGGGAGC-MGBNFQ-3'. The resulting amplicon was 73bp. Standard curves

were generated using serial 10-fold dilutions ranging from 5 x 10^6 to 5 copies of a positive

control plasmid (plasmid K-p31) per reaction. The 25μL PCR reactions consisted of 5μl of

extracted sample, 1x universal TaqMan® real-time PCR master mix (Applied Biosystems), 12.5

pmol of each primer and 4 pmol of the probe. Samples were tested in 96-well plate format, with

eight water negative controls (one per row) and one positive control containing 50 copies of

plasmid per plate. The cycling conditions were: 50°C for 2 min, 95°C for 10 min and 45 cycles

of 95°C for 15 sec followed by 60°C for 1 min. Reactions were run on an ABI 7500 real-time

thermocycler (Applied Biosystems). The threshold of all plates was set at a standard value, and

the data was analyzed using the ABI software. Samples were counted as positive if their Ct was

<35.

Viral genome accession numbers. The sequences reported here were deposited in GenBank

under the accession numbers JQ898291 (Index case, strain MA095) and JQ898292 (St. Louis

case, strain WD976).

RESULTS

      Discovery of a novel polyomavirus by pyrosequencing. MW polyomavirus was

discovered in a stool sample from a child from Malawi that was collected in September 2008 as

part of a global gut microbiome survey project (20). Following purification of VLPs by passage

through 0.45 and 0.22μm pore-sized filters and subsequent DNase treatment, DNA was extracted

from the VLPs and amplified using the highly processive phi29 polymerase. The resulting

material was subjected to 454 pyrosequencing. Six reads were identified with limited similarity

to known polyomaviruses. Three of the initial six reads could be assembled into one 959 bp

contig with the highest scoring BLASTx hit possessing 36% amino acid identity to LPyV STAg.

The other three reads all aligned to the VP1 protein of known polyomaviruses by BLASTx and

shared 64%, 48% and 59% amino acid identity to JCPyV VP1, TSPyV VP1 and JCPyV VP1.

Complete genome sequencing and genome analysis. A series of PCR primers were

designed based on the initial six reads. Sequencing of the resulting amplicons yielded a complete

genome of 4,927 bp (Figure 2.1). ICTV has set the demarcation criteria for proposed new

polyomaviruses at 81% nucleotide identity over the whole genome (42). Based on the limited

sequence similarity to any known polyomaviruses, we named the novel virus MW polyomavirus

(MWPyV) after its discovery in Malawi. The overall GC content of MWPyV was 37%, which is

very similar to WUPyV (39%), BKPyV (39%) and JCPyV (40%). The MWPyV genome

organization was characteristic of the known polyomaviruses and included an early region

coding on one strand for LTAg and STAg and a late region coding on the opposite strand for the

structural proteins VP1, VP2 and VP3. The sizes of the predicted ORFs were comparable to

those of known polyomaviruses (Table 2.1).

Figure 2.1. Genome organization of MWPyV. ori, origin of replication.
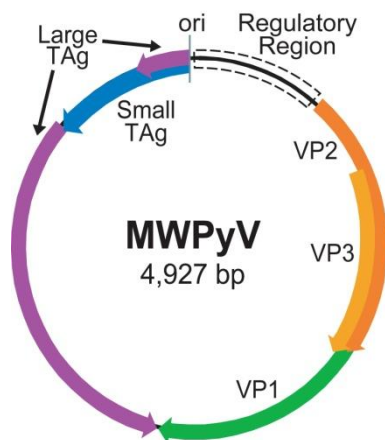
Table 2.1. Putative proteins encoded by MWPyV (strain MA095)

Protein	Putative coding region(s)	Predicted size (aa)	Calculated mass (kDa)	Range (aa) in other polyomaviruses
STAg	4927-4328	199	23.4	124-198 amino acids
LTAg	4927-4688, 4332-2566	668	77.0	599-817 amino acids
VP1	1353-2564	403	43.6	343-497 amino acids
VP2	431-1363	310	34.2	241-415 amino acids
VP3	761-1363	200	22.8	190-272 amino acids

The TAgs and VP2 were separated by a regulatory region, which had an A/T-rich tract on the late side of the putative replication origin. The core origin of replication contained three repeats of the consensus pentanucleotide LTAg binding site, G(A/G)GGC (43) (two GAGGC and one GGGGC), and one non-consensus binding site, TAGGC. Several polyomaviruses (BKPyV, JCPyV, WUPyV, KIPyV and SV40) contain an imperfect palindrome sequence followed by additional LTAg binding sites to the early side of the four binding sites. Palindrome patterns were identified in MWPyV but no additional LTAg binding sites were detected in this area. The regulatory region contained several predicted transcription factor binding sites, including multiple binding sites for four factors known to play a role in BKPyV viral transcription and regulation--Sp1, nuclear factor I (NFI), AP1 and C/EBP (44). Multiple binding sites were also identified for HNF-3, USF-2 and Oct-1. Many other transcription factors were predicted to bind to only one site.

Analysis of the MWPyV LTAg ORF revealed a conserved splice donor site immediately after amino acid 80; the position of this site was similar to that found in WUPyV, BKPyV and JCPyV, which occur after amino acids 84, 81 and 81, respectively. Two consensus splice acceptor sites were identified, which would yield introns of 355 or 463 bp and proteins of 668 or 632 amino acids, respectively. Examination of the protein sequence of the 632 amino acid form showed that it lacked the Rb-binding motif, which was contained in the excised intron. By

contrast, the predicted 668 amino acid protein included the conserved Rb-binding motif. Based on this analysis, we predicted the LTAg to be 668 amino acids.

MWPyV LTAg possessed conserved features common to other polyomavirus LTAgs, including a DNaJ domain containing the conserved region 1 (cr1) sequence and the highly conserved hexapeptide motif HPDKGG. These domains were followed by conserved region 2 (cr2), which contained the Rb-binding motif LxCxE (LSCNE in MWPyV), a putative nuclear localization signal (NLS), a canonical DNA binding domain and a zinc finger region. Closer inspection of the zinc finger region revealed a conserved C_2H_2 zinc finger motif with the sequence C324, C327, H334, H339. There are typically three highly conserved amino acids N-terminal to the first cysteine (C324) in this motif, including a tyrosine 10 amino acids away, an aspartic acid located 18 amino acids away and an alanine present 25 amino acids away (43). In MWPyV, the aspartic acid and alanine residues were conserved, while the tyrosine was not and was replaced by a leucine. A conserved leucine-rich hydrophobic region C-terminal to the aspartic acid was also present. Following the zinc finger region, the MWPyV LTAg contained the highly conserved ATPase-p53 binding domain, including the two conserved motifs GPXXXGKT and GXXXVNLE. There was no sequence corresponding to the host range domain present in SV40, BKPyV, SA12 and JCPyV (43).

In most polyomaviruses, STAg is encoded by a single unspliced ORF. In HaPyV and MPyV, the STAg transcript is spliced. Analysis of the MWPyV early region did not reveal an obvious splice donor site, so the STAg was predicted to be 199 amino acids. As LTAg and STAg share the first 80 amino acids, the STAg also contained the DNaJ domain. In the unique C-terminal part of STAg, there was a conserved cysteine-rich motif, $CX_5CX_{7-8}CXCX_2CX_{21-22}CSCX_2CX_3WFG$. This motif was conserved in MWPyV with the exception of the initial

cysteine residue and the serine residue, which were an isoleucine and a phenylalanine, respectively.

MPyV and HaPyV encode a middle T antigen (MTAg) generated by alternative splicing; the MWPyV genome was scanned for splicing motifs similar to those used by MPyV and HaPyV. No obvious splice sites that would generate an appropriately sized third T antigen protein were identified, suggesting that MWPyV likely does not encode a MTAg.

Some polyomaviruses, including JCPyV and BKPyV, also encode an agnoprotein in the late region between the NCCR and the VP2 start codon. Analysis of the MWPyV sequence in this region yielded one 45 amino acid ORF on the same strand as the structural proteins. However, because this ORF was not conserved in the other completely sequenced MWPyV strain, strain WD976 (described later in this report), we do not believe that MWPyV encodes an agnoprotein.

Phylogenetic analysis. Maximum likelihood analysis of the VP1, VP2 and LTAg proteins demonstrated MWPyV was highly divergent from all known polyomaviruses (Figure 2.2). Analysis of VP1 sequences showed that MWPyV is midway between the *Wukipolyomavirus* and *Orthopolyomavirus* genera (Figure 2.2A). By contrast, based on VP2 and LTAg sequences, MWPyV clustered with the clade containing HPyV9, LPyV, HaPyV, MPyV, TSPyV, MCV, ChPyV and the orangutan polyomaviruses (Figure 2.2B and 2.2C). The discordant phylogenetic relationships suggest that MWPyV might have been derived from an ancestral recombination event.

Figure 2.2. Phylogenetic analysis of MWPyV. Amino acid-based trees were generated using the maximum likelihood method with 1,000 bootstrap replicates. Bootstrap values less than 700 are not shown. A) VP1; B) VP2; C) LTAg.
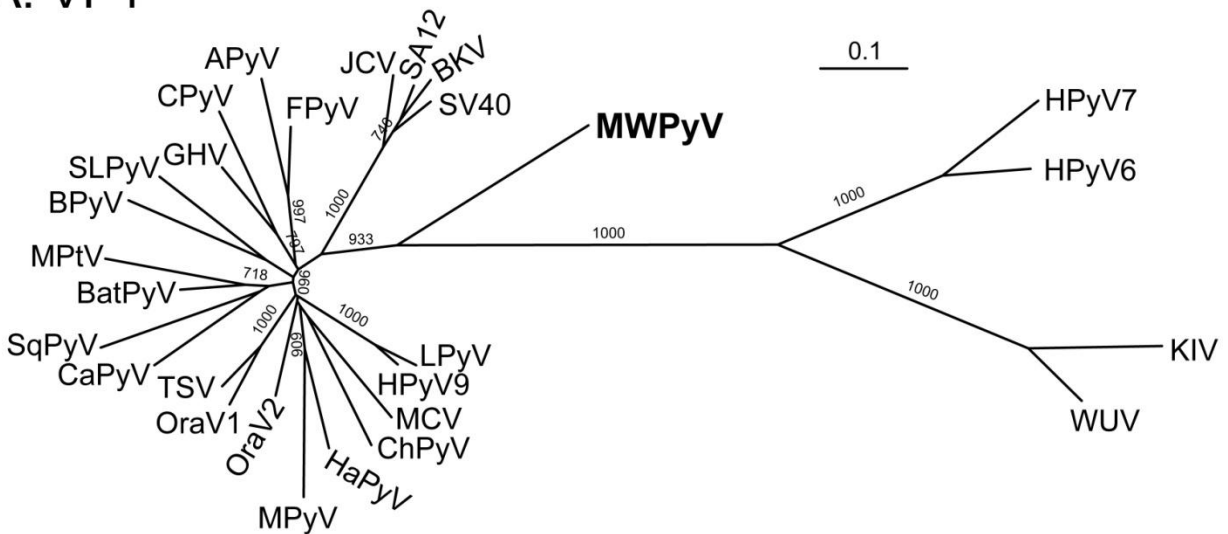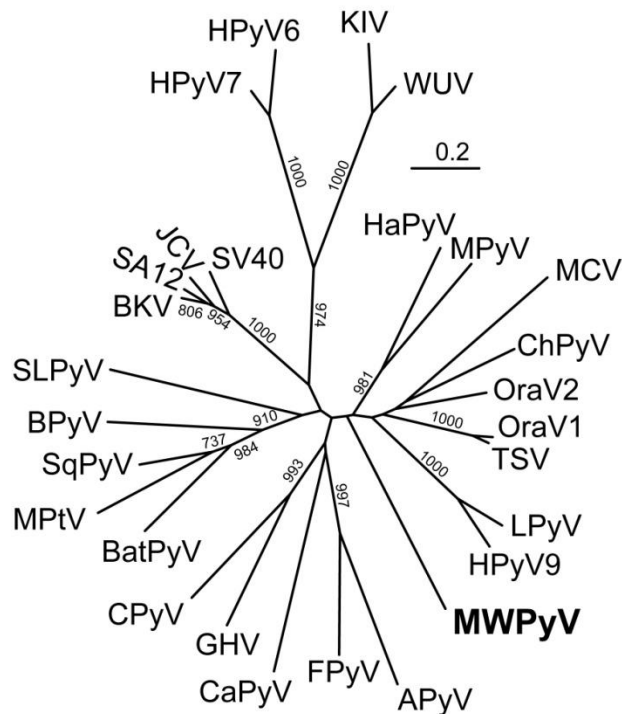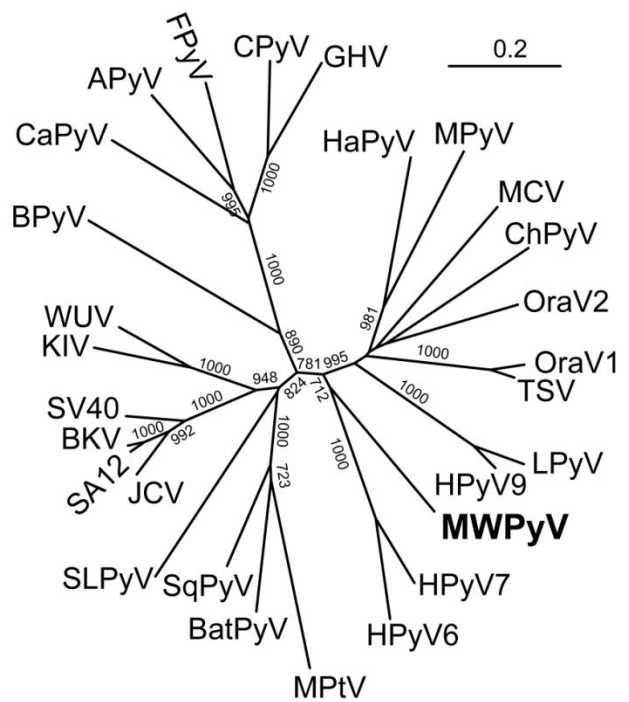
Prevalence of MWPyV. A Taqman real-time PCR assay targeting the MWPyV LTAg was designed and validated using a positive control plasmid; based on the standard curve, the MWPyV assay demonstrated a reliable detection limit of approximately five copies per reaction, yielded a linear regression R^2 value of 0.99 and was 93% efficient. This real-time PCR assay was used to screen a cohort consisting of 514 stool samples from children at St. Louis Children's Hospital presenting with diarrhea. Twelve samples (2.3%) from the St. Louis cohort tested positive for MWPyV (Table 2.2).

Table 2.2. Specimens and patients testing positive for MWPyV

Sample	Patient	Age	Sex	Ct	Date	Tested positive	Tested negative
WD972	1	5y 0m	M	21.68	8/10/09	*E. coli* serotype O Rough	Enteric pathogen culture* (except *E. coli*), *Giardea*, *Cryptosporidium*, Ova & parasite screen (O&P)
WD976	1			21.85	8/11/09	*E. coli* serotype O Rough	Enteric pathogen culture* (except *E. coli*), *Giardea*, *Cryptosporidium*, *C. difficile*, O&P
WD1226	1			28.21	12/22/09		Enteric pathogen culture*, O&P
WD1239	2	1y 0m	M	31.76	12/29/09		Enteric pathogen culture*, *C. difficile*
WD1314	3	1y 5m	F	30.37	2/11/10		Enteric pathogen culture*, Rotavirus
WD1300	4	1y 8m	F	34.99	2/4/10		Enteric pathogen culture*, Rotavirus, Viral culture
WD1260	5	1y 4m	F	29.91	1/12/10		Enteric pathogen culture*, O&P
WD958	6	1y 8m	M	31.89	8/3/09		Enteric pathogen culture*, *C. difficile*, O&P
WD1039	7	4y 3m	F	31.42	9/14/09		Enteric pathogen culture*, *C. difficile*
WD1233	8	4y 9m	M	32.33	12/25/09		Enteric pathogen culture*, Rotavirus
WD1055	9	5y 5m	M	30.90	9/22/09		Enteric pathogen culture*
WD1442	10	3y 0m	M	32.41	5/24/10	*C. jejuni*	Enteric pathogen culture* (except *C. jejuni*).

*Includes *Salmonella, Shigella, E. coli* O157, *E. coli* shiga toxins not 0157, *Yersinia, Aeromonas, Plesiomonas* and *Campylobacter*.

Three of the MWPyV positive samples were obtained from a five-year-old lung transplant recipient over a period of four months from August to December 2009 (Patient 1, Table 2.2). This patient had received a lung transplant three years earlier and at the time of sampling presented with persistent, recurrent diarrhea. Two of the samples, WD972 and WD976, were obtained on consecutive days in August 2009, and both samples were positive for *Escherichia*

coli serotype O Rough. The patient again presented with diarrhea in December 2009 (sample WD1226), but this sample had no growth in the enteric pathogen culture (including *E. coli*) and was negative for ova and parasites (Table 2.2). The other nine samples came from nine individual patients ranging in age from one to five-years-old (Table 2.2). Eight of the nine patients were negative for all organisms tested except MWPyV. Only patient 10 (sample WD1442) was positive for *Campylobacter jejuni*.

Strain variation. To assess the extent of sequence variation between the St. Louis and Malawi isolates, we sequenced the complete genome of MWPyV from St. Louis sample WD976 to greater than 3x coverage. The two whole genome sequences diverged by 5.3% at the nucleotide level. Strain WD976 had two insertions (11 bp and one bp) in the NCCR, which resulted in a genome size of 4,939 bp. The vast majority of the polymorphisms in the coding regions resulted in synonymous mutations. One notable mutation changed the size of the STAg ORF. The predicted TAA stop codon identified in the MA095 strain was mutated to AAA in WD976 resulting in a protein prediction of 206 amino acids, seven amino acids longer than the index genome's STAg.

DISCUSSION

We used a pyrosequencing strategy to identify a novel polyomavirus present in human stool. The initial discovery was in a stool specimen collected from a healthy child in Malawi. Further screening by real-time PCR demonstrated the presence of the virus in 12 stool samples collected from a cohort of patients in St. Louis, USA. These data demonstrated that MWPyV is geographically widespread in human populations and can be found on two continents. As the ICTV polyomavirus subgroup currently has no systematic naming convention for novel

polyomaviruses, we chose to name this new virus using a two letter convention following the model of BKPyV, JCPyV, KIPyV and WUPyV; we made this decision for two reasons. First, we did not employ the numerical system used in the naming of HPyV6, HPyV7 and HPyV9 because we have not yet formally demonstrated that this virus infects humans and to avoid potential conflicts in temporal priority in describing novel polyomaviruses. Second, both MCPyV and TSPyV are named based on putative disease associations, but no disease association currently exists for our new virus. Therefore, we chose a two-letter abbreviation reflecting the geographic location of the index case.

The ICTV polyomavirus subgroup recently defined two mammalian genera, *Orthopolyomavirus* and *Wukipolyomavirus*, within the family *Polyomaviridae* based primarily on phylogenetic analysis of the late genes (combined VP1 and VP2) (42). Classification of MWPyV into one of these two genera is confounded by the distinct phylogenetic tree topologies that were generated for the VP1 and VP2 proteins (Figure 2.2). The different topologies suggest that MWPyV is derived from an ancestral recombination event. Such recombination among polyomaviruses has been previously suggested (4).

We sequenced two complete genomes of MWPyV, one from the index child in Malawi and one from a child in St. Louis. A high degree of strain variation (5.3%) was observed between these two MWPyV strains, which is comparable to the ~ 5% sequence divergence present in strains of BKPyV (45). It contrasts sharply with the very limited variation (<1.2%) seen with WUPyV worldwide (46). The primers and probe used in the aforementioned MWPyV real-time PCR assay were perfectly conserved in both strains and thus detect both stains with equal efficiency. However, it remains to be determined whether even greater variation in MWPyV can be discovered when broader consensus sequence-based assays are used. Others have speculated

that sequence variation in BKPyV and JCPyV plays a role in viral pathogenesis and disease severity (47, 48). If MWPyV is ultimately found to be a pathogen, it will be interesting to determine whether there are strain-dependent pathogenic phenotypes. Among the differences we observed were a seven amino acid extension of the STAg and an 11 bp insertion in the NCCR in the WD976 strain versus the index Malawi strain. The functional consequences of these alterations remain to be defined.

One critical question is whether MWPyV is a bona fide infectious agent of humans and if so, what disease(s), if any, might be associated with MWPyV infection. The detection of MWPyV in stools of children with diarrhea, many of which have no known etiology, raises the possibility that MWPyV might play a role in human diarrhea. Alternatively, it is possible that MWPyV does not cause infection in the gastrointestinal tract but has a tropism for other human organ systems and is shed in stool as a mode of transmission or simply as a byproduct. It is also possible that MWPyV is a dietary contaminant and does not actively infect humans. Approaches to determine whether MWPyV is an infectious agent include serological studies to determine whether the host mounts an antibody-based immune response to MWPyV and additional screening of specimens collected from sterile sites, such as serum or cerebrospinal fluid. Further studies will be needed to define whether MWPyV has additional tropisms in the human body and to assess potential associations with human disease.

ACKNOWLEDGEMENTS

REFERENCES

1.   **Allander T, Andreasson K, Gupta S, Bjerkner A, Bogdanovic G, Persson MA, Dalianis T, Ramqvist T, and Andersson B.** 2007. Identification of a third human polyomavirus. J Virol **81:**4130-4136.
2.   **Le BM, Demertzis LM, Wu G, Tibbets RJ, Buller R, Arens MQ, Gaynor AM, Storch GA, and Wang D.** 2007. Clinical and epidemiologic characterization of WU polyomavirus infection, St. Louis, Missouri. Emerg Infect Dis **13:**1936-1938.
3.   **Feng H, Shuda M, Chang Y, and Moore PS.** 2008. Clonal integration of a polyomavirus in human Merkel cell carcinoma. Science **319:**1096-1100.
4.   **Schowalter RM, Pastrana DV, Pumphrey KA, Moyer AL, and Buck CB.** 2010. Merkel cell polyomavirus and two previously unknown polyomaviruses are chronically shed from human skin. Cell Host Microbe **7:**509-515.
5.   **van der Meijden E, Janssens RW, Lauber C, Bouwes Bavinck JN, Gorbalenya AE, and Feltkamp MC.** 2010. Discovery of a new human polyomavirus associated with trichodysplasia spinulosa in an immunocompromized patient. PLoS Pathog **6:**e1001024.
6.   **Scuda N, Hofmann J, Calvignac-Spencer S, Ruprecht K, Liman P, Kuhn J, Hengel H, and Ehlers B.** 2011. A novel human polyomavirus closely related to the african green monkey-derived lymphotropic polyomavirus. J Virol **85:**4586-4590.
7.   **Misra V, Dumonceaux T, Dubois J, Willis C, Nadin-Davis S, Severini A, Wandeler A, Lindsay R, and Artsob H.** 2009. Detection of polyoma and corona viruses in bats of Canada. J Gen Virol **90:**2015-2022.
8.   **Colegrove KM, Wellehan JF, Jr., Rivera R, Moore PF, Gulland FM, Lowenstine LJ, Nordhausen RW, and Nollens HH.** 2010. Polyomavirus infection in a free-ranging California sea lion (Zalophus californianus) with intestinal T-cell lymphoma. J Vet Diagn Invest **22:**628-632.
9.   **Wellehan JF, Jr., Rivera R, Archer LL, Benham C, Muller JK, Colegrove KM, Gulland FM, St Leger JA, Venn-Watson SK, and Nollens HH.** 2011. Characterization of California sea lion polyomavirus 1: expansion of the known host range of the Polyomaviridae to Carnivora. Infect Genet Evol **11:**987-996.
10. **Orba Y, Kobayashi S, Nakamura I, Ishii A, Hang'ombe BM, Mweene AS, Thomas Y, Kimura T, and Sawa H.** 2011. Detection and characterization of a novel polyomavirus in wild rodents. J Gen Virol **92:**789-795.
11. **Halami MY, Dorrestein GM, Couteel P, Heckel G, Muller H, and Johne R.** 2010. Whole-genome characterization of a novel polyomavirus detected in fatally diseased canary birds. J Gen Virol **91:**3016-3022.
12. **Groenewoud MJ, Fagrouch Z, van Gessel S, Niphuis H, Bulavaite A, Warren KS, Heeney JL, and Verschoor EJ.** 2010. Characterization of novel polyomaviruses from Bornean and Sumatran orang-utans. J Gen Virol **91:**653-658.

13. **Verschoor EJ, Groenewoud MJ, Fagrouch Z, Kewalapat A, van Gessel S, Kik MJ, and Heeney JL.** 2008. Molecular characterization of the first polyomavirus from a New World primate: squirrel monkey polyomavirus. J Gen Virol **89:**130-137.

14. **Leendertz FH, Scuda N, Cameron KN, Kidega T, Zuberbuhler K, Leendertz SA, Couacy-Hymann E, Boesch C, Calvignac S, and Ehlers B.** 2011. African great apes are naturally infected with polyomaviruses closely related to Merkel cell polyomavirus. J Virol **85:**916-924.

15. **Imperiale MJ, Major, E.O.** 2007. Polyomaviruses. *In* Knipe, DM, Howley, P.M. (ed.), Fields Virology, 5th ed, vol. 2. Lippincott Williams & Wilkins, Philadelphia, PA.

16. **Knowles WA.** 2006. Discovery and epidemiology of the human polyomaviruses BK virus (BKV) and JC virus (JCV). Adv Exp Med Biol **577:**19-45.

17. **Randhawa P, Vats A, and Shapiro R.** 2006. The pathobiology of polyomavirus infection in man. Adv Exp Med Biol **577:**148-159.

18. **Gjoerup O, and Chang Y.** 2010. Update on human polyomaviruses and cancer. Adv Cancer Res **106:**1-51.

19. **Kazem S, van der Meijden E, Kooijman S, Rosenberg AS, Hughey LC, Browning JC, Sadler G, Busam K, Pope E, Benoit T, Fleckman P, de Vries E, Eekhof JA, and Feltkamp MC.** 2012. Trichodysplasia spinulosa is characterized by active polyomavirus infection. J Clin Virol **53:**225-230.

20. **Yatsunenko T, Rey FE, Manary MJ, Trehan I, Dominguez-Bello MG, Contreras M, Magris M, Hidalgo G, Baldassano RN, Anokhin AP, Heath AC, Warner B, Reeder J, Kuczynski J, Caporaso JG, Lozupone CA, Lauber C, Clemente JC, Knights D, Knight R, and Gordon JI.** 2012. Human gut microbiome viewed across age and geography. Nature **486:**222-227.

21. **Reyes A, Haynes M, Hanson N, Angly FE, Heath AC, Rohwer F, and Gordon JI.** 2010. Viruses in the faecal microbiota of monozygotic twins and their mothers. Nature **466:**334-338.

22. **Cantalupo PG, Calgua B, Zhao G, Hundesa A, Wier AD, Katz JP, Grabe M, Hendrix RW, Girones R, Wang D, and Pipas JM.** 2011. Raw sewage harbors diverse viral populations. MBio **2**.

23. **Marchler-Bauer A, Lu S, Anderson JB, Chitsaz F, Derbyshire MK, DeWeese-Scott C, Fong JH, Geer LY, Geer RC, Gonzales NR, Gwadz M, Hurwitz DI, Jackson JD, Ke Z, Lanczycki CJ, Lu F, Marchler GH, Mullokandov M, Omelchenko MV, Robertson CL, Song JS, Thanki N, Yamashita RA, Zhang D, Zhang N, Zheng C, and Bryant SH.** 2011. CDD: a Conserved Domain Database for the functional annotation of proteins. Nucleic Acids Res **39:**D225-229.

24. **Grabe N.** 2002. AliBaba2: context specific identification of transcription factor binding sites. In Silico Biol **2:**S1-15.

25. **Rice P, Longden I, and Bleasby A.** 2000. EMBOSS: the European Molecular Biology Open Software Suite. Trends Genet **16:**276-277.

26. **Cantalupo P, Doering A, Sullivan CS, Pal A, Peden KW, Lewis AM, and Pipas JM.** 2005. Complete nucleotide sequence of polyomavirus SA12. J Virol **79:**13094-13104.

27. **Pawlita M, Clad A, and zur Hausen H.** 1985. Complete DNA sequence of lymphotropic papovavirus: prototype of a new species of the polyomavirus genus. Virology **143:**196-211.

28. **Seif I, Khoury G, and Dhar R.** 1979. The genome of human papovavirus BKV. Cell **18:**963-977.

29. **Schuurman R, Sol C, and van der Noordaa J.** 1990. The complete nucleotide sequence of bovine polyomavirus. J Gen Virol **71 (Pt 8):**1723-1735.

30. **Delmas V, Bastien C, Scherneck S, and Feunteun J.** 1985. A new member of the polyomavirus family: the hamster papovavirus. Complete nucleotide sequence and transformation properties. EMBO J **4:**1279-1286.

31. **Frisque RJ, Bream GL, and Cannella MT.** 1984. Human polyomavirus JC virus genome. J Virol **51:**458-469.

32. **Mayer M, and Dorries K.** 1991. Nucleotide sequence and genome organization of the murine polyomavirus, Kilham strain. Virology **181:**469-480.

33. **Griffin BE, Fried M, and Cowie A.** 1974. Polyoma DNA: a physical map. Proc Natl Acad Sci U S A **71:**2077-2081.

34. **Lebowitz P, and Weissman SM.** 1979. Organization and transcription of the simian virus 40 genome. Curr Top Microbiol Immunol **87:**43-172.

35. **Rott O, Kroger M, Muller H, and Hobom G.** 1988. The genome of budgerigar fledgling disease virus, an avian polyomavirus. Virology **165:**74-86.

36. **Johne R, Wittig W, Fernandez-de-Luco D, Hofle U, and Muller H.** 2006. Characterization of two novel polyomaviruses of birds by using multiply primed rolling-circle amplification of their genomes. J Virol **80:**3523-3531.

37. **Johne R, and Muller H.** 2003. The genome of goose hemorrhagic polyomavirus, a new member of the proposed subgenus Avipolyomavirus. Virology **308:**291-302.

38. **Deuzing I, Fagrouch Z, Groenewoud MJ, Niphuis H, Kondova I, Bogers W, and Verschoor EJ.** 2010. Detection and characterization of two chimpanzee polyomavirus genotypes from different subspecies. Virol J **7:**347.

39. **Bradley RK, Roberts A, Smoot M, Juvekar S, Do J, Dewey C, Holmes I, and Pachter L.** 2009. Fast statistical alignment. PLoS Comput Biol **5:**e1000392.

40. **Guindon S, Dufayard JF, Lefort V, Anisimova M, Hordijk W, and Gascuel O.** 2010. New algorithms and methods to estimate maximum-likelihood phylogenies: assessing the performance of PhyML 3.0. Syst Biol **59:**307-321.

41. **Abascal F, Zardoya R, and Posada D.** 2005. ProtTest: selection of best-fit models of protein evolution. Bioinformatics **21:**2104-2105.

42. **Johne R, Buck CB, Allander T, Atwood WJ, Garcea RL, Imperiale MJ, Major EO, Ramqvist T, and Norkin LC.** 2011. Taxonomical developments in the family Polyomaviridae. Arch Virol **156:**1627-1634.

43. **Pipas JM.** 1992. Common and unique features of T antigens encoded by the polyomavirus group. J Virol **66:**3979-3985.

44. **Liang B, Tikhanovich I, Nasheuer HP, and Folk WR.** 2012. Stimulation of BK virus DNA replication by NFI family transcription factors. J Virol **86:**3264-3275.

45. **Krumbholz A, Bininda-Emonds OR, Wutzler P, and Zell R.** 2009. Phylogenetics, evolution, and medical importance of polyomaviruses. Infect Genet Evol **9:**784-799.

46. **Bialasiewicz S, Rockett R, Whiley DW, Abed Y, Allander T, Binks M, Boivin G, Cheng AC, Chung JY, Ferguson PE, Gilroy NM, Leach AJ, Lindau C, Rossen JW, Sorrell TC, Nissen MD, and Sloots TP.** 2010. Whole-genome characterization and genotyping of global WU polyomavirus strains. J Virol **84:**6229-6234.

47.   **Boldorini R, Allegrini S, Miglio U, Paganotti A, Veggiani C, Mischitelli M, Monga G, and Pietropaolo V.** 2009. Genomic mutations of viral protein 1 and BK virus nephropathy in kidney transplant recipients. J Med Virol **81:**1385-1393.
48.   **Sunyaev SR, Lugovskoy A, Simon K, and Gorelik L.** 2009. Adaptive mutations in the JC virus protein capsid are associated with progressive multifocal leukoencephalopathy (PML). PLoS Genet **5:**e1000368.

CHAPTER 3

Determination of the cell and tissue tropism of WU and KI polyomaviruses

This work will be published as the following:

1. Immunohistochemical detection of KI polyomavirus in alveolar macrophages, lung and spleen

Erica A. Siebrasse[1*], Nang L. Nguyen[1*†], Colin Smith[2], Peter Simmonds[3] and David Wang[1]

[*]E.A.S and N.L.N contributed equally to this work.

[1]Washington University School of Medicine, St. Louis, Missouri, USA; [2]Department of Pathology and [3]Roslin Institute, University of Edinburgh, Scotland, UK

2. Detection of WU polyomavirus in respiratory epithelial cells in lungs transplanted into a patient with Job's syndrome.

Erica A. Siebrasse[1], Diana V. Pastrana[2], Nang L. Nguyen[1], Annie Wang[1], Mark J. Roth[2], Steven M. Holland[3], Alexandra F. Freeman[3], John McDyer[4], Christopher B. Buck[2] and David Wang[1]

[1]Washington University School of Medicine, St. Louis, Missouri, [2]National Cancer Institute and [3]National Institute of Allergy and Infectious Disease, National Institutes of Health, Bethesda, Maryland, [4]University of Pittsburgh Medical Center, Pittsburgh, Pennsylvania

3. Multi-organ WU polyomavirus infection in a bone marrow transplant recipient detected by electron microscopy, PCR and immunohistochemistry

Erica A. Siebrasse[1], Nang L. Nguyen[2], Dean D. Erdman[3], David Wang[1] and Marilyn A. Menegus[2*]

[1]Washington University School of Medicine, St. Louis, Missouri, [2]Clinical Microbiology Laboratories, Strong Memorial Hospital, University of Rochester Medical Center, Rochester, New York, [3]Centers for Disease Control, Atlanta, Georgia

ABSTRACT

WU polyomavirus (WUPyV) and KI polyomavirus (KIPyV) were both discovered in 2007 in respiratory tract secretions from patients with respiratory illness. Serological analysis demonstrated that both infect a majority of the population, and their DNA can be detected in a variety of specimen types. Little is known about the tissue tropism of WUPyV and KIPyV, and there are no studies to date describing any specific cell types they infect. The limited knowledge of their tropism has hindered study of these viruses and an understanding of their potential pathogenesis in humans. We describe tissues from five immunocompromised patients that stained positive for WUPyV or KIPyV antigen using newly developed immunohistochemical assays targeting either the WUPyV VP1 (WU-VP1) or KIPyV VP1 (KI-VP1) capsid protein. WU-VP1 and KI-VP1 were both detected in lungs within alveolar macrophages. WU-VP1 was also detected in bronchial epithelial cells from a bronchoalveolar lavage specimen and in close association with MUC5AC (a mucin)-positive cells in tracheal tissue. In addition, KI-VP1 was detected in splenic tissue. Two of the patients died of respiratory-related issues. In one of these cases, subsequent studies revealed polyomavirus-like particles in the patient's lung. This is the first definitive identification of specific cell types in which WU-VP1 or KI-VP1 can be detected and the first demonstration of putative WUPyV viral particles in a human. Collectively, these findings further our understanding of WUPyV and KIPyV biology and tropism and raise the question of whether these viruses cause disease, particularly in the immunocompromised.

INTRODUCTION

WU polyomavirus (WUPyV) and KI polyomavirus (KIPyV) were discovered in 2007 in patients with respiratory tract infections (1, 2). Subsequent studies detected both viruses in respiratory tract secretions, blood, stool and tonsil tissue (3) and suggested a seroprevalence of 55-70% (4, 5) for KIPyV and 69-89% for WUPyV (4-6), with infection occurring most frequently in childhood. Neither is currently associated with any human disease(s). However, other polyomaviruses are known to be important human pathogens. JC polyomavirus (JCPyV) is the etiological agent of progressive multifocal leukoencephalopathy, and BK polyomavirus (BKPyV) can lead to renal allograft loss in kidney transplant recipients and hemorrhagic cystitis in bone marrow transplant recipients. Both viruses are ubiquitous worldwide (7). Despite their high prevalence rates, infection by both viruses is typically asymptomatic unless the host is immunocompromised (7). More recently, Merkel cell carcinoma polyomavirus (MCPyV) and Trichodysplasia spinulosa-associated polyomavirus (TSPyV) were implicated as human pathogens in the context of immunosuppression (8, 9). MCPyV causes Merkel cell carcinoma, a rare but aggressive skin cancer (9), and TSPyV is associated with Trichodysplasia spinulosa, a rare skin disease seen in transplant recipients (8). Given the pathogenicity of these family members, a significant question is whether WUPyV and KIPyV follow this paradigm and cause disease in immunocompromised patients.

A complete understanding of the types of cells and tissues in which WUPyV and KIPyV replicate is critical to identifying potential diseases with which they may be associated. The viruses have most commonly been detected in respiratory secretions, but there have been only minimal efforts to explore additional specimen types. In addition, prior studies relied exclusively on PCR approaches to detect viral genomes in bulk-extracted nucleic acid, making it impossible

46

to define the specific cell type(s) that harbor WUPyV or KIPyV. There are no published reports describing the detection of viral antigens in tissues. In order to define the tissue and cell tropism of WUPyV and KIPyV and as a step toward understanding the roles of the viruses in human disease, we developed immunohistochemical (IHC) assays targeting either WUPyV or KIPyV VP1 (WU-VP1 or KI-VP1), the viral capsid proteins.

We applied this assay to tissue specimens from patients positive for WUPyV or KIPyV by PCR. Tissues from five different patients were positive. KI-VP1 was detected in the lung tissue of a deceased pediatric bone marrow transplant recipient, and a portion of the positive cells was identified as alveolar macrophages using a double immunohistochemical stain. In addition, KI-VP1 was detected in the spleen and lung tissues of a deceased HIV-positive patient. WU-VP1 was detected in respiratory epithelial cells from a bronchoalveolar lavage sample from a bilateral lung transplant recipient with Job's syndrome. WU-VP1 was also detected within alveolar macrophages in the lung of a deceased patient with viral pneumonitis and in the lung of another patient. These results provide the first insights into a specific cell types in which WUPyV or KIPyV can be detected.

MATERIALS AND METHODS

Development of anti-WU-VP1 and anti-KI-VP1 monoclonal antibodies. The methods used to develop anti-WU-VP1 and anti-KI-VP1 monoclonal antibodies were identical and performed in parallel. The WU-VP1 and KI-VP1 Gateway pENTR/SD/D-TOPO constructs previously described (4) were transferred into Gateway pDEST17 plasmids (Life Technologies) and expressed in *E. coli*. The resulting recombinant His-tagged VP1 proteins were purified via affinity Ni-NTA columns (Pierce Biotechnology). BALB/c mice were immunized with three

consecutive doses of either purified WU-VP1 or KI-VP1. Their spleens were harvested for

hybridoma fusion with the murine myeloma line P3X63Ag8.653 (Sigma-Aldrich). We screened

for clones producing anti-KI-VP1 or anti-WU-VP1 antibody by ELISA and Western blot using

purified GST-tagged WU-VP1 or KI-VP1 as the target antigen. Positive clones were then

screened by ELISA using the reciprocal GST-tagged antigen (4), and those demonstrating cross

reactivity were excluded. For example, a clone producing anti-KI-VP1 antibody was screened

using GST-WU-VP1 to determine if it cross-reacted. Two rounds of limiting dilutions were

performed to achieve clonality. Both monoclonal antibodies used in the following experiments,

NN-Ab03 for KI-VP1 and NN-Ab06 for WU-VP1, were isotype IgG2b.

Generation of positive controls. We generated positive controls for the two

immunohistochemistry assays by transfecting 293T cells with a plasmid (pDEST26, Life

Technologies) encoding either WU-VP1 or KI-VP1. Cells were harvested three days after

transfection, and a portion was fixed in 10% neutral buffered formalin for 24 hours, embedded in

paraffin, and sections of the cell block were transferred to glass slides.

Immunohistochemistry (IHC). Two slightly different IHC assay were used. The primary assay

was as follows. Formalin-fixed paraffin-embedded tissue sections were deparaffinized in xylene

for 15 minutes and then rehydrated in a series of graded ethanol solutions. Endogenous

peroxidases were quenched in 3% hydrogen peroxide for 15 minutes. Antigen retrieval was

accomplished in citrate buffer pH 6.0 (10mM citric acid, 0.05% Tween 20) in a pre-warmed

pressure cooker (Nesco PC6-25) for three minutes on the high setting. After blocking in 1.5%

normal horse serum (Vector Labs #S-200), the tissues were incubated first in primary antibody

overnight and then in secondary antibody (biotinylated anti-mouse IgG, Vector BA-2000) for 30

minutes. Primary antibodies included monoclonal antibodies against WU-VP1 (designated NN-

Ab06), KI-VP1 (NN-Ab03) or an isotype matched control antibody (mouse IgG2b, BD

Biosciences #557351). The staining was developed using the Vectastain standard ABC kit

(Vector Labs #PK-6100) and DAB (Vector Labs #SK-4100), counterstained with hematoxylin

and dehydrated in a series of graded ethanol solutions and xylene.

For the HIV-positive cases (#3 and 5), a second IHC assay was used. Tissue sections

were deparaffinized in three changes of xylene and then rehydrated in a series of graded ethanol

solutions. Antigen retrieval was accomplished in citrate buffer at $95^{\circ}C$ in a water bath for 35

minutes. Slides were then stained using the Histostain®-*Plus* 3rd Generation IHC Detection kit

(Life Technologies) according to the manufacturer's instructions, with Superblock T20 (Thermo

#37516) used as the blocking agent. NN-Ab03 or the isotype control was used as the primary

antibody. After completion of the Histostain protocol, the slides were counterstained with

hematoxylin and dehydrated in a series of graded ethanol solutions and xylene.

Double immunohistochemistry (dIHC). The dIHC staining protocol was similar to the primary

IHC protocol with the addition of several steps. Following chromagen development of the first

antibody using either DAB or ImmPACT SG (Vector Labs #SK-4705), tissues were blocked

with avidin and biotin (Vector Labs #SP-2001) and a second time with 1.5% normal horse

serum. They were incubated with the second primary and secondary antibodies and developed

using the ABC kit and DAB or ImmPACT SG, followed by dehydration. Tissues stained with

the dIHC protocol were not counterstained. Other primary monoclonal antibodies used were

against MUC5AC (Thermo Fischer #MA1-38223), CD45 (BD Biosciences #555480), CD45

(Dako # M351529-2, only used for dIF), CD68 (Dako #M081401), CD31 (Dako #M0823) and

an isotype matched antibody to these (IgG1, BD Pharmingen #555746). Citrate buffer was used

for antigen retrieval in the dIHC assays for MUC5AC, CD45 and CD68, while Tris-EDTA

buffer pH 9.0 (10mM Tris, 1mM EDTA, 0.05% Tween 20) was used for the CD31 dIHC assay.

Immunofluorescence (IF) and double immunofluorescence (dIF). Formalin-fixed paraffin-

embedded tissue sections were deparaffinized in xylene for 15 minutes and then rehydrated in a

series of graded ethanol solutions. Antigen retrieval was accomplished in citrate buffer in a pre-

warmed pressure cooker for three minutes on the high setting. Sections were blocked in

Superblock T20. A polyclonal antibody against WU-VP1 (4), designated NN-Ab01, was used as

the primary antibody. Following incubation with the fluorescently labeled secondary antibody

(anti-mouse-488, Life Technologies #A11001), the nucleus was counterstained with Hoechst

(Life Technologies #H21491), and the slides were mounted.

The dIF assay was accomplished in the same way, except two primary antibodies, NN-

Ab01 and a monoclonal antibody against cytokeratins (Dako #M3515) were applied

simultaneously, followed by two secondary antibodies (anti-rabbit-568 and anti-mouse-488, Life

Technologies #A10042 and A11001, respectively).

Nucleic acid extraction and real-time PCR (case #1). DNA was extracted from formalin-fixed

paraffin-embedded samples using the Qiagen BioRobot M48 workstation and MagAttract DNA

mini kit (Qiagen, Valencia, CA). A real-time PCR assay designed to detect both WUPyV and

KIPyV was used to screen 5 uL of a 1:100 dilution of extracted DNA. Extracts were also tested

for bocavirus using a previously described assay (10).

Complete genome sequencing (case #1). Segments of the WUPyV genome were amplified

using a series of primers that are available upon request. Amplicons were cloned and sequenced

using the ABI Prism BigDye Terminator Cycle Sequencing Ready Reaction Kit version 1.1 or

3.1 on an ABI 3130 XL DNA Sequencer (Applied Biosystems).

Accession numbers. The complete genome sequence for WUPyV isolate Rochester-7029 is available through GenBank under Accession #FJ794068. The genome sequence for WUPyV isolate J1 is under Accession #KJ643309.

Electron microscopy (case #1). Tissues were fixed in formalin following autopsy. They were post-fixed in glutaraldehyde before processing into epoxy resin for sectioning.

Image manipulation. IHC images were cropped to squares. The resolution was changed to 500-600 dpi in Photoshop with constrained proportions and no resampling. No other image manipulation was conducted for IHC images. IF images were also cropped to squares, and the resolution was changed in Photoshop. The brightness and contrast was also changed, but these changes were applied equally to the entire image.

Human studies. Studies performed with tissues from all cases except #2 and 4 were performed after the patients were deceased, so no institutional review board approval was sought. Studies on tissue from case #2 were approved by institutional review boards at the National Institutes of Health and Washington University in St. Louis. Studies on tissue from case #4 were approved by the Human Research Protection Office of Washington University in St. Louis.

RESULTS

Establishment of WU-VP1 and KI-VP1 specific immunohistochemistry assays. To study the cell and tissue tropisms of WUPyV and KIPyV, we established IHC assays using newly developed monoclonal antibodies against WU-VP1 and KI-VP1. To validate the new IHC assays and evaluate their specificity, we developed positive control cell pellets. Figure 3.1a shows 293T cells transfected with the pDEST26-KI-VP1 construct and stained with the KI-VP1 antibody (NN-Ab03). Several cells showed prominent dark staining (Figure 3.1a, b), while cells

from both a sequentially cut slide stained with the isotype control (Figure 3.1c) or mock

transfected 293T cells stained with NN-Ab03 (Figure 3.1d) did not. To independently evaluate

the specificity of NN-Ab03, a subset of the transfected cells were lysed to extract proteins for

Western blot analysis (Figure 3.1e). As negative controls, lysates of 293T cells from a mock

transfection and from a transfection of an analogous plasmid expressing the VP1 protein of WU

polyomavirus (pDEST26-WU-VP1) were included. A single band corresponding to the predicted

size of KI-VP1 was detected in the KI-VP1 lysate, while no band is seen in mock transfected

cells or in the WU-VP1 lysate (Figure 3.1e). The blot was stripped and blotted for actin

(Millipore #MAB1501) as a loading control.

Similar control experiments were performed using the anti-WU-VP1 monoclonal

antibody (NN-Ab06). Cells with prominent dark staining were seen (Figure 3.2a). A serial

section of the same cell block stained with an IgG2b isotype matched antibody (Figure 3.2b) and

mock transfected cells stained with NN-Ab06 (Figure 3.2c) were negative. In the Western blot

using NN-Ab06 (Figure 3.2d), a single band of the size corresponding to WU-VP1 was seen,

while no band was seen in lysate from an analogous pDEST26-KI-VP1 transfection or in lysate

from a mock transfection (Figure 3.2d). Given these data, we concluded both antibodies are

specific for their respective virus, and the assays can detect viral antigen in formalin-fixed

paraffin-embedded cell pellets.

Figure 3.1. Validation of anti-KI-VP1 monoclonal antibody specificity. IHC of 293T cells

transfected with pDEST26-KI-VP1 and stained with (A, B) a KI-VP1 monoclonal antibody (NN-

Ab03) or with (C) an isotype control. (D) IHC of mock transfected 293T cells stained with NN-

Ab03. Panels A and C are at 400x; panel B is at 600x, and panel D is at 200x. (E) Western blot

using NN-Ab03 of protein lysates from mock transfected 293T cells (lane 1) or cells transfected

with pDEST26-KI-VP1 (lane 2) or pDEST26-WU-VP1 (lane 3).
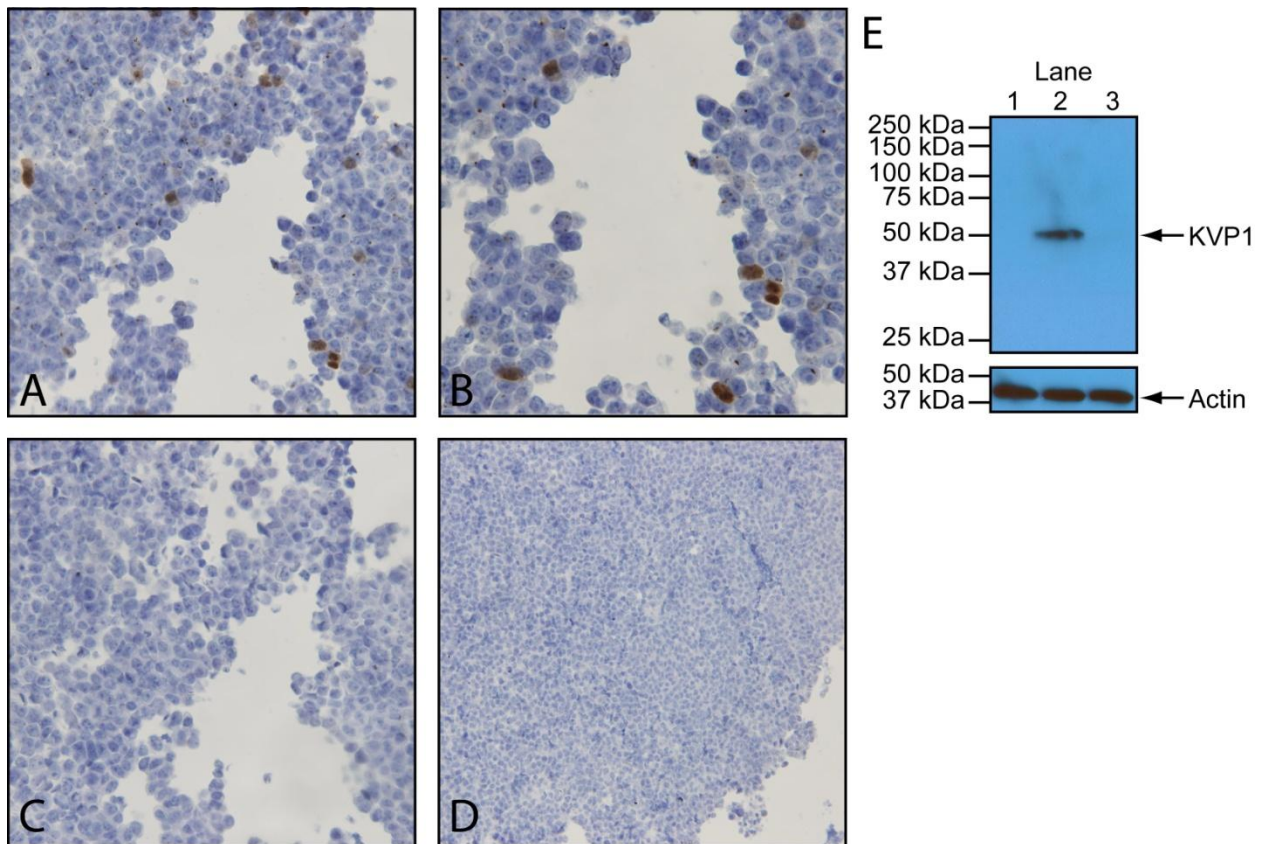
Figure 3.2. Validation of anti-WU-VP1 monoclonal antibody specificity. IHC of 293T cells transfected with pDEST26-WU-VP1 and stained with (A) a WU-VP1 monoclonal antibody (NN-Ab06) or (B) an isotype control. (C) IHC of mock transfected 293T cells stained with NN-Ab06. Figures A-C are at 400x. (D) Western blot using NN-Ab06 of protein lysates from mock transfected 293T cells (lane 1) or cells transfected with pDEST26-WU-VP1 (lane 2) or pDEST26-KI-VP1 (lane 3).
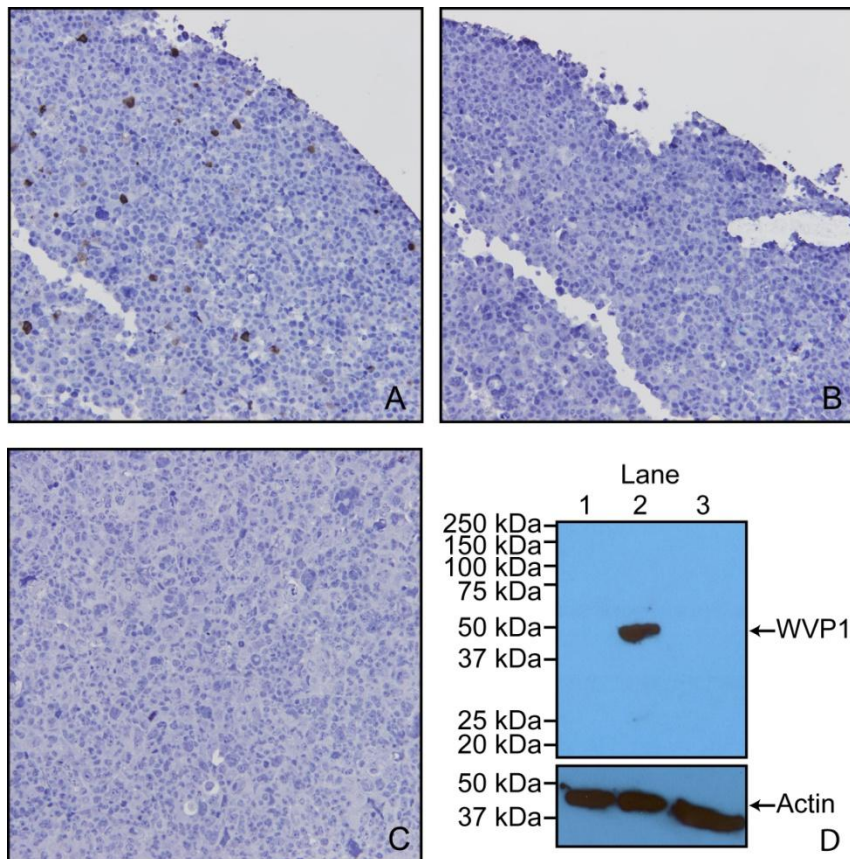
Case #1: Multi-organ WUPyV infection in a bone marrow transplant recipient detected by electron microscopy, PCR and immunohistochemistry. In January 2001, a 27 month-old child was admitted to the University of Rochester Medical Center for an unrelated 5/6 HLA-matched cord blood transplant. The patient was previously diagnosed with refractory

juvenile myelomonocytic leukemia at 16 month of age and underwent splenectomy in September 2000. The patient was born at 40 weeks gestation by normal vaginal delivery. Her medical history included leukocytosis at three months old and splenomegaly at six months old. She had multiple infections before two years of age, including otitis media, a central vein catheter infection and a urinary tract infection. She also demonstrated failure to thrive, was developmentally delayed and had mild pulmonic stenosis and gastroesophageal reflux.

Three weeks after transplant the patient developed fever, diarrhea, hepatomegaly and erythema on her face, palm and sole. Her hemodynamics was stable, and she weighed 10 kg. The patient was evaluated for graft versus host disease (GVHD), viral exanthema and drug eruption. Skin biopsies performed at four weeks post-transplant showed pathologic characteristics consistent with viral infection, not GVHD or drug eruption. A rectosigmoid biopsy done at the same time showed mild stromal edema but was negative for adenovirus and cytomegalovirus (CMV) by IHC stains. Throughout the course of hospitalization, adenovirus was intermittently isolated from the patient's stool and urine, while Influenza B was detected in her nose and throat. PCR testing of the blood for CMV was consistently negative. Despite aggressive therapy, the patient's condition continued to deteriorate. On March 1, 2001, the patient was transferred to the pediatric intensive care unit (PICU) secondary to respiratory failure. Her chest radiogram was remarkable for pulmonary edema. She was stabilized two days later. The patient again developed severe acute respiratory distress syndrome and distended abdomen on April 1. Her treatment was continued in the PICU and included mechanical ventilation. A radiogram on April 15 (about 11 weeks post-transplant) revealed free air in the abdominal cavity without identification of the source. The patient expired later that day. Viral pneumonitis was indicated as the probable cause of death.

The most important findings on gross examination at autopsy were bilateral pulmonary consolidation, acute tracheobronchitis, hepatomegaly with cholestasis, deep mucosal ulcerations throughout the small bowel and prominent generalized lymphadenopathy. The most notable pathologic finding was heavy hemorrhagic foci in the lungs. Microscopic examination of the lungs confirmed the presence of interstitial emphysema with profound hemorrhage of the right upper, right middle, left upper and left lower lobes. Multiple smudge cells and cells with Cowdry type A-nuclear inclusions were identified inside of reactive bronchial epithelium from both lungs. Similar inclusions were seen in the tracheal, bile duct, renal tubular and the urinary bladder epithelia. Small bowel mucosa revealed multifocal ulcerations and scattered inclusion bearing cells in the epithelium. Immunoperoxidase stains for CMV, adenovirus, influenza virus, human papillomavirus, respiratory syncytial virus (RSV), SV40 and *in situ* hybridization for Epstein barr virus were all negative. Attempts to culture virus from the lung, liver, gastrointestinal tract and lymph node tissues were unsuccessful. Gram stains from sections of lung, liver and lymph node showed greater than 25 neutrophils per low field with no organism seen. *Staphylococcus* species coagulase negative grew from a blood culture (at 10 CFU/mL) and from the gastrointestinal tract. No strict anaerobic growth was observed.

Interestingly, electron micrographs of the lungs showed spherical viral particles in the nuclei, many with para-crystalline arrays (Figure 3.3). The particles were 30.39-34.71 nm (mean 32.11 nm) in diameter. Although the diameter was less than the conventional diameter for polyomaviruses (45 nm), shrinkage due to formalin fixation is a well-established phenomenon, and the size of viral particles can vary based on the method of fixation and embedding (11). In addition, previously published electron microscopy on BKPyV particles yielded measurements ranging 30-50 nm (12). Despite the presence of viral particles indicative of polyomavirus, IHC

56

on lung tissue with a primary antibody against SV40 known to cross-react with BKPyV and JCPyV was negative. IHC for adenovirus and RSV was also negative. Although electron microscopy indicated a likely viral infection in the lungs, given the negative IHC, no further testing was performed at that time.

Figure 3.3. Electron micrographs of polyomavirus-like particles in a human lung. (A-C) Various fields of human lung demonstrating viral particles. Crystalline lattices seen in panel B are consistent with polyomavirus virions.
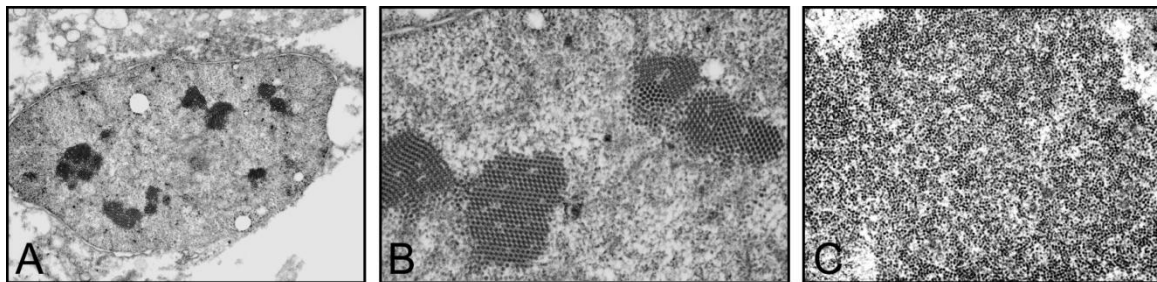
Detection of WUPyV in the lung. Two new polyomavirus, WUPyV and KIPyV, were discovered in 2007. Both were found in respiratory tract secretions from patients with respiratory illness. This discovery prompted us to investigate the possible involvement of WUPyV and KIPyV in this case. DNA extracted from formalin-fixed paraffin-embedded lung, liver, kidney and gastrointestinal tissues was tested by real-time PCR for WUPyV, KIPyV and bocavirus (Table 3.1). All four tissues were positive for WUPyV. KIPyV and bocavirus were not detected in any of the tissues. The entire WUPyV genome (designated Rochester-7029) was subsequently sequenced to 4x coverage using multiple primer sets (Accession #FJ794068) and found to be 5,306 base pairs. The genome contained a 77 base pair terminal duplication in *large T antigen* compared to the reference WUPyV genome (Figure 3.4). The duplication was not predicted to

have any effect on the size or sequence of the translated protein as the duplication was immediately 3' to the T antigen stop codon.

Table 3.1 Summary of findings. Numbers in parentheses are Ct values from real-time PCR.

Study	Lung	Liver	Kidney	Gastrointestinal
Intranuclear inclusions	Positive	Positive	Positive	Positive
Electron microscopy	Positive	Not done	Not done	Not done
WUPyV PCR	Positive (16.6)	Positive (30.8)	Positive (30.4)	Positive (30.2)
WUPyV IHC	Positive	Negative	Negative	Negative
KIPyV PCR	Negative	Negative	Negative	Negative
Bocavirus PCR	Negative	Negative	Negative	Negative

Figure 3.4. Nucleotide sequence of the 3' end of the *large T antigen* gene from WU polyomavirus strain Rochester-7029. The colored boxes show the duplicated sequence, with the stop codon underlined.

5'-ATATATAGGCCTTACTGAATTTGCTGACATGCAAATGAATGTAACAAATGGATG
CAACATACTTGAAAAACACAATGCTTAATAGGCCTTACTGAATTTGCTGACATGC
AAATGAATGTAACAAATGGATGCAACATACTTGAAAAACACAATGCTTAAAATTG-3'

Following detection of WUPyV in the patient's tissues by real-time PCR, WUPyV-specific IHC was performed on available tissue to determine whether WU-VP1 protein was also present. The liver, kidney and gastrointestinal tissues were all negative (Table 3.1). Strong staining was observed in both the lung (Figure 3.5a, c, d, f) and the trachea (Figure 3.5g, i), while no staining was seen in serial sections stained with the isotype control antibody (Figure 3.5b, e, h). Three staining patterns were seen. In some cells, WU-VP1 staining was primarily in the nucleus. In others, the perimeter of the nucleus was strongly positive. Finally, in some cases, the

58

staining was diffuse, making it difficult to discern its position within cells. Interestingly, the

tracheal staining appeared to be within a submucosal gland.

Figure 3.5. Detection of WU-VP1 in the human respiratory tract. Human lung tissue at 200x stained with (A, D) a monoclonal antibody against WU polyomavirus VP1 (NN-Ab06) or (B, E) an isotype control antibody. Human tracheal tissue at 200x stained with (G) NN-Ab06 or (H) an isotype control antibody. (C, F, I) Higher magnifications of panels A, D and G. Panels C and F are at 400x, and panel I is at 600x.
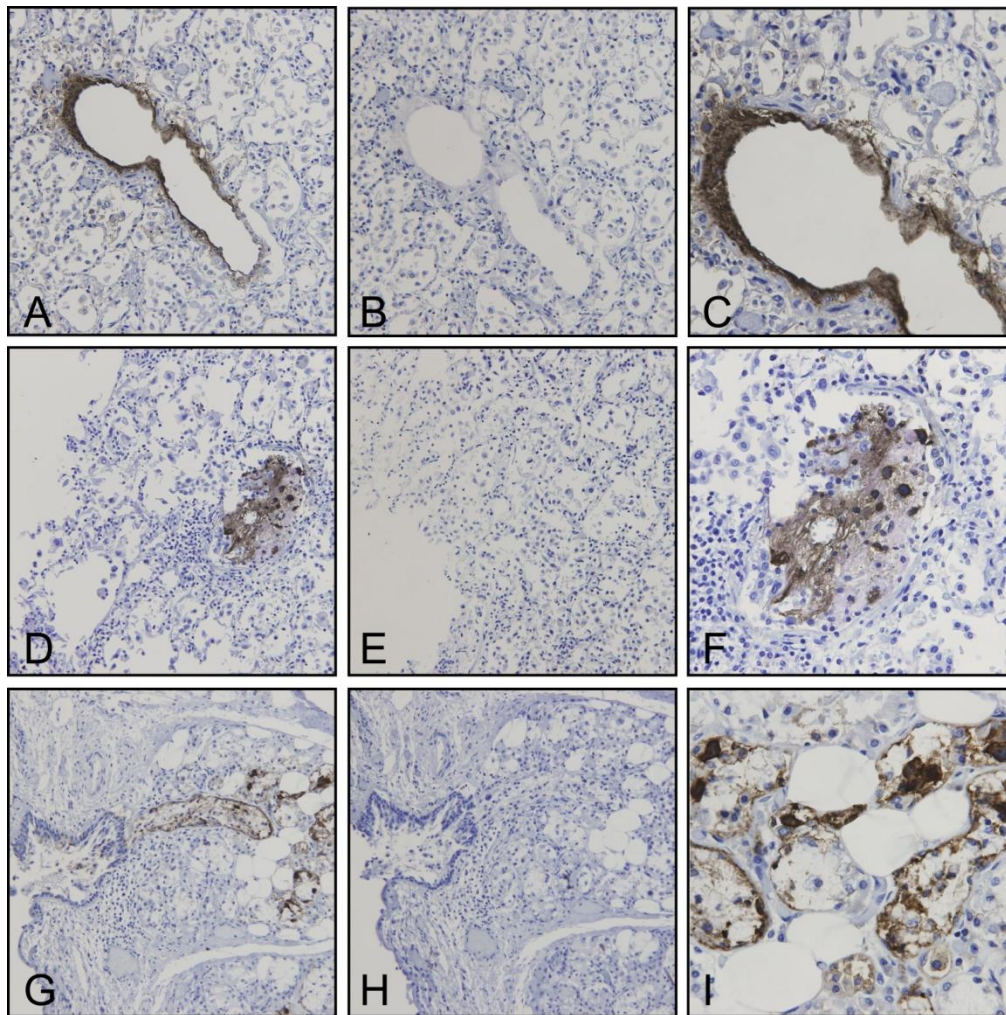
Detection of WU-VP1 antigen in alveolar macrophages. Case #2 described below detected WU-VP1 in respiratory epithelial cells. We hypothesized that some cells in this patient's lung tissues were also epithelial cells, but we did not explicitly confirm this due to the limited amount of lung tissue available. Instead we chose to explore additional hypotheses regarding potential tropism of WUPyV based on our recent detection of KIPyV in alveolar macrophages (case #4). We performed dIHC using NN-Ab06 and a monoclonal antibody against CD68, which primarily labels macrophages and monocytes. Cells double positive for WU-VP1 and CD68 were detected within the patient's lung tissue (Figure 3.6). In addition, the cell shown in Figure 3.6b was morphologically consistent with a foamy macrophage, a specific morphotype of macrophage that is laden with lipid droplets in the cytoplasm (13). KIPyV was also detected in a foamy macrophage in case #4 (14). A serial section stained with isotype matched antibodies (IgG2b for NN-Ab06 and IgG1 for the anti-CD68 antibody) was negative (not shown).

Figure 3.6. Detection of WU-VP1 in human alveolar macrophages. (A-C) Lung tissue stained with NN-Ab06 (blue) and a monoclonal antibody against CD68 (brown). The cell in panel B is consistent with a foamy macrophage. Panel A is at 400x; panels B and C are at 1000x. (D) A different field of the lung tissue section with another double positive cell at 1000x.
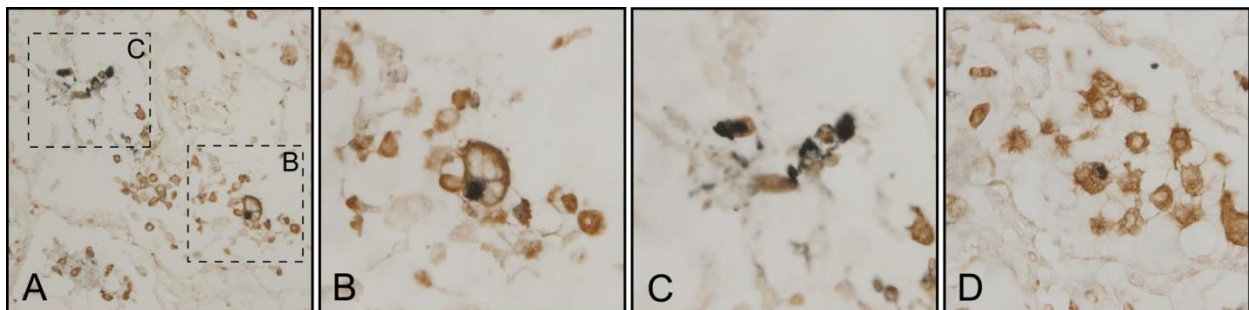
Detection of WU-VP1 antigen in association with mucin-producing cells. The initial

IHC staining of the tracheal tissue revealed positive cells within a submucosal gland. MUC5AC

is the principal mucin produced by goblet cells, while MUC5B is made by submucosal glands.

(15). We established two dIHC assays: (1) NN-Ab06 and a monoclonal antibody against

MUC5AC and (2) NN-Ab06 and a polyclonal antibody against MUC5B. Both assays were

performed on control cell pellets (not shown). The MUC5AC dIHC assay yielded clearer

staining, so we chose to apply this assay to the tracheal tissue. Figure 3.7 shows WU-VP1-

positive cells in association with clusters of cells showing MUC5-AC positivity. It is unclear

whether the two antigens colocalize to the same cell. WU-VP1-positive cells were also seen

separate from MUC5AC-positive cells, suggesting a subset of virus-positive cells do not produce

mucin. There were two such areas on the tracheal section.

Figure 3.7. Detection of WU-VP1 in close proximity to MUC5AC-positive cells in the trachea.

Tracheal tissue stained with an anti-WU-VP1 monoclonal antibody (blue) and a monoclonal

antibody against MUC5AC (brown). Panel A is at 200x, and panel B is at 600x.
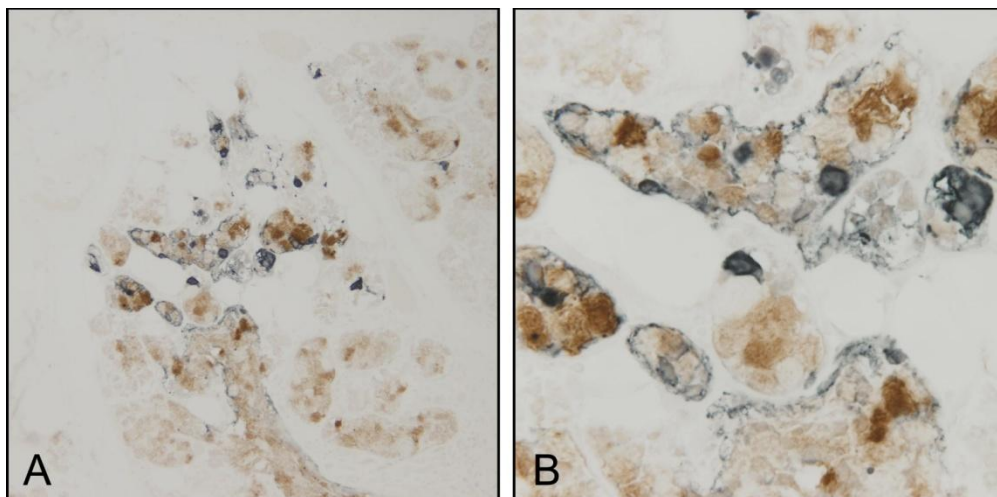
Case #2: Detection of WUPyV in respiratory epithelial cells in lungs transplanted into a patient with Job's syndrome. Job's syndrome is an immune disorder characterized by eczematoid dermatitis, recurrent skin and pulmonary infections, elevated IgE and impaired T and B cell memory (16). It is caused by dominant-negative mutations in *STAT3* (16). A 28-year-old woman with Job's syndrome was seen at the National Institutes of Health Clinical Center six months after bilateral lung transplantation. She had bronchoscopic evaluation to follow up on endobronchial aspergillosis. Pathological examination of the BAL sample revealed scattered cells, primarily columnar bronchial cells, with cytomorphologic changes reminiscent of BKPyV-infected "decoy cells." The cells stained positive with PAb419, a monoclonal antibody against the SV40 large T antigen. The patient had BKPyV viremia ($8.1x10^5$ copies/mL) and viruria ($6.9x10^9$ copies/mL). JCPyV was also detected in the urine but not in the blood. The BAL was very weakly positive for BKPyV by PCR (<250 copies/mL) and negative for JCPyV. Clinical or radiographic signs and symptoms of infection were not apparent. Given the positive staining but weak PCR results, further analysis of the BAL was performed.

Non-enveloped virions were purified from the BAL using ultracentrifugation with Optiprep (Sigma-Aldrich #D1556) (17). DNA extracted from the virion prep was subjected to random-primed rolling circle amplification (RCA) and restriction enzyme digestion, which yielded two strong bands. The bands were cloned and identified as WUPyV by Sanger sequencing. The complete genomic sequence of the isolate, designated J1 (accession #KJ643309), was confirmed by Illumina miSeq analysis of the RCA product. A second WUPyV variant with two nucleotide polymorphisms and a single base insertion was also detected in the RCA product. No other known viral species (including BKPyV) were observed in the deep sequencing.

We applied the WU-VP1 IHC assay to formalin-fixed, paraffin-embedded sections of the BAL sample. Figure 3.8a shows prominent, dark staining of cells with enlarged nuclei and a ground glass appearance characteristic of viral cytopathic changes (arrows). Staining was not seen in serial sections stained with the isotype antibody (Figure 3.8b) or with no antibodies (not shown).

Figure 3.8. WU-VP1 detected in a BAL from a lung transplant recipient with Job's syndrome. (A) The bronchoalveolar lavage stained with NN-Ab06 or (B) with an isotype control at 600x.
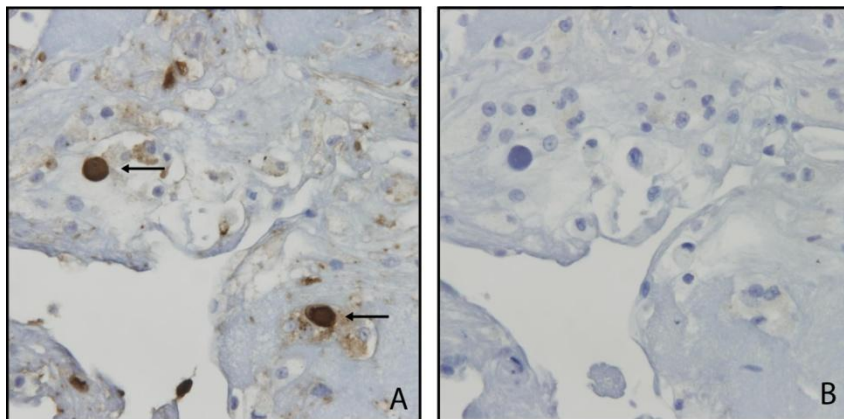
Many of the WUPyV-positive cells were cuboidal to columnar in shape with other morphologic features consistent with respiratory epithelial cells. To determine their etiology, we developed a dIF assay with a polyclonal antibody against WU-VP1 (4), designated NN-Ab01, and a monoclonal antibody against cytokeratins. To validate the assay, we first performed IF with NN-Ab01 on the positive control 293T cells expressing WU-VP1. Several WU-VP1-positive cells were observed (Figure 3.9a), while a serial section stained with pre-immune serum at the same dilution was negative (Figure 3.9b). In the dIF assay, we observed cells double positive for WU-VP1 and cytokeratin (Figure 3.9c-d), identifying these as epithelial cells. Of the

136 WU-VP1-positive cells, 77 (57%) were also cytokeratin-positive. A serial section of the BAL stained with an IgG1 isotype matched antibody to the cytokeratin antibody and pre-immune rabbit serum was negative (not shown).

Figure 3.9. WU-VP1 detected within respiratory epithelial cells. IF of 293T cells transfected with pDEST26-WU-VP1 and stained with (A) a WU-VP1 polyclonal antibody (NN-Ab01) or with (B) pre-immune serum. (C) dIF with NN-Ab01 (red) and a monoclonal antibody against cytokeratin (green) on the BAL specimen showing a double positive cell at 200x. (D) Field of the bronchoalveolar lavage with multiple WU-VP1/cytokeratin double positive cells.
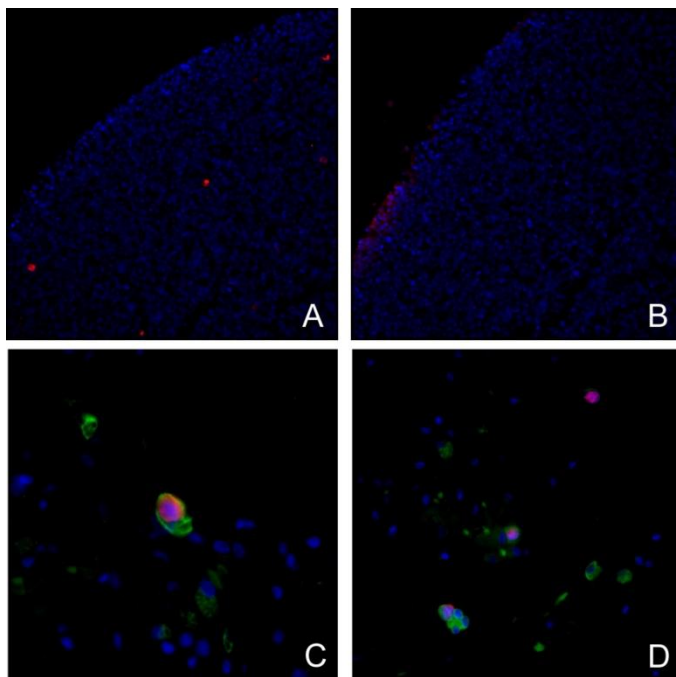
We hypothesized that the remaining 43% of WU-VP1-positive, cytokeratin-negative cells might be macrophages. However, a dIF assay using NN-Ab01 and the antibody against CD68 showed separate WU-VP1 and CD68 single-positive cells but no double positive cells (not

shown). In addition, a dIF stain using NN-Ab01 and an antibody against CD45, a marker for hematopoietic cells, was also negative (not shown).

Case #3: Detection of WUPyV in an HIV-positive patient. Sharp et al. previously screened 97 autopsy samples of lymphoid tissue by PCR and identified three samples positive for WUPyV, all from AIDS patients (18). We stained these specimens using the WU-VP1 IHC assay. Only one was positive, which was actually a lung. This sample was obtained from a 32-year-old male, whose date of HIV diagnosis was unknown. He presented with anal lymphoma and received radiotherapy. He subsequently developed bronchopneumonia and septicemia and died three months after initial radiotherapy. He also had a previous history of anal herpes virus infection and esophageal *Candida*. Neuropathology showed no significant pathology and no evidence of HIV encephalitis.

There were a relatively low number of darkly staining positive cells scattered throughout the section, similar to those seen in Figure 3.10a and c. More diffuse, lighter staining was also seen throughout the section. This was not present in serial sections of tissue stained with an isotype control antibody (Figure 3.10b) or stained without a primary or without both antibodies (not shown). However, we decided to score tissue conservatively and did not count this weaker staining as WU-VP1-positive. We attempted to identify these cells using the CD68 dIHC assay, but as we moved farther down into the tissue block, WU-VP1-positive cells became fewer and fewer, and we were ultimately not able to identify the specific cell types within this lung.

We were also able to obtain formalin-fixed, paraffin-embedded sections from the following: heart, thyroid, tongue, adrenal gland, kidney, liver, pancreas, pituitary gland, prostate, anus and various brain sections. All were negative for WU-VP1 by IHC.

Figure 3.10. WU-VP1 detected in a lung from an HIV-positive patient. (A) Lung tissue stained with NN-Ab06 or (B) with an isotype control at 400x. (C) Panel A at 600x.
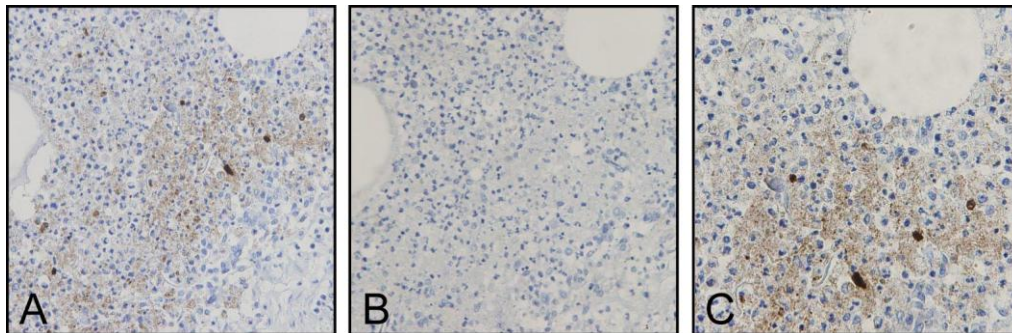
Case #4: **Immunohistochemical detection of KIPyV in alveolar macrophages in a pediatric transplant recipient.** During the course of a recent study to evaluate the prevalence of human polyomaviruses in a prospective pediatric transplant cohort (19), we identified one patient (#3001) whose nasopharyngeal aspirate sample (NPA) was strongly positive for KIPyV by real-time PCR. The patient's clinical parameters have been described in detail (19). In brief, the patient was a 17-month-old child who received a bone marrow transplant as treatment for Fanconi anemia in April 2009. The patient's disease course was complicated by recurrent pulmonary hemorrhage, severe GVHD, and renal failure. The patient ultimately died of acute respiratory failure and extensive pulmonary hemorrhage several months later. The autopsy of the lung revealed evidence of chronic pulmonary hemorrhage with numerous hemosiderin-laden macrophages in the alveolar spaces. Diffuse alveolar hemorrhage leading to respiratory failure was the listed likely cause of death. Infection was considered less likely due to the negative results of routine microbiology testing (via culture and/or PCR). There was no significant inflammation or airway fibrosis to suggest GVHD in the lungs. A NPA sample collected 24 days

prior to the death of the patient was strongly positive for KIPyV (1.3 x 10^9 genome copies per

mL of transport media) (19).

Tissue blocks obtained at autopsy from 17 different body sites were available for KI-VP1

IHC testing. These included skin, liver, lung, esophagus, stomach, small intestine, large intestine,

pancreas, spleen, right kidney, left kidney, bladder, left ventricle, right ventricle and pituitary,

right adrenal and left adrenal glands. Of these, only the lung was positive by IHC (Figure 3.11).

Two patterns of cellular staining were seen—strong, dark nuclear staining and weaker, granular

staining exclusively in the cytoplasm. Several controls were performed on serial sections to

analyze this staining pattern, including a corresponding IgG2b isotype control (Figure 3.11a) and

staining performed without the primary antibody or without both the primary and secondary

antibodies (not shown). The weaker cytoplasmic staining was occasionally seen in controls, but

the strong nuclear staining was exclusively seen in the KI-VP1 stained tissue. There were

positive cells scattered throughout the section (similar to Figure 3.11b and c) with a few

localized regions containing a high density of positive staining cells.

Figure 3.11. IHC of human lung with a KI-VP1 monoclonal antibody. Tissue stained with (A)

an isotype control or (B) the KI-VP1 antibody (both at 200x). (C) Higher magnification (600x)

of KI-VP1 staining in panel B.
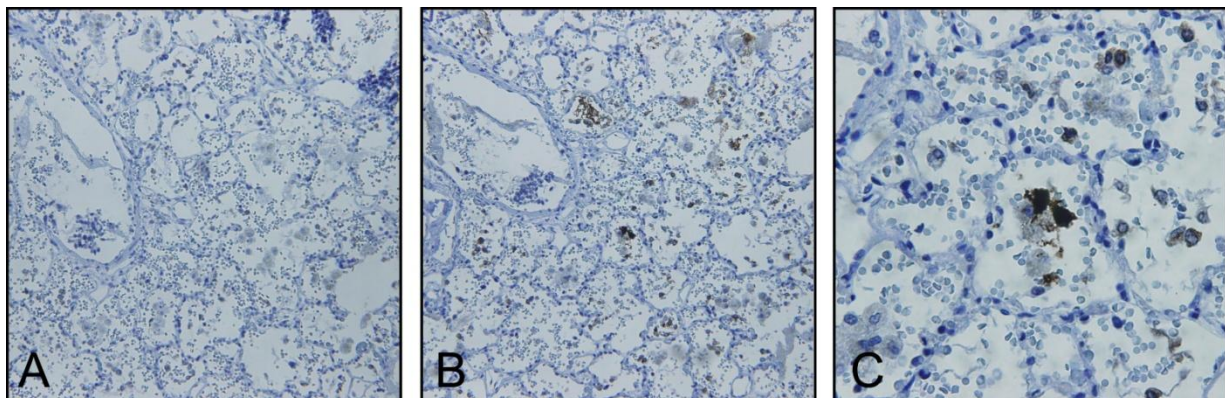
Detection of KI-VP1 in alveolar macrophages. We used a dIHC staining approach to identify the cell type(s) that were KI-VP1-positive. Many of the positive cells were found within the alveolar spaces and were morphologically consistent with immune cells, so we began our analysis by establishing a dIHC assay using the KI-VP1 monoclonal antibody and an antibody against human CD45, which marks all cells of hematopoietic origin. Double IHC using the CD45/KI-VP1 assay showed clearly staining double positive cells throughout the tissue (Figure 3.12b, c, e). Of the 105 KI-VP1-positive cells counted in one tissue section, 51 (49%) were also CD45-positive. An isotype control (IgG2b for the KI-VP1 antibody) performed on a serial section (Figure 3.12a, d) was negative. A hematoxylin and eosin stain showed dark staining "grape-like" clusters, morphologically consistent with phagocytic cells (Figure 3.12f). Based on these data, we hypothesized that the CD45/KI-VP1-positive cells may be alveolar macrophages

To test this hypothesis, we established a second dIHC assay using the KI-VP1 monoclonal antibody and an antibody against human CD68, which primarily marks macrophages and monocytes, and applied it to the lung tissue from patient 3001. Clear double staining was seen in ~48% of KI-VP1-positive cells (Figure 3.13a-c), while no staining was seen in the isotype control (not shown). This demonstrated a subset of the KI-VP1-positive cells were alveolar macrophages. In addition, the morphology of the alveolar macrophage presented in Figure 3.13c resembles that of a foamy macrophage, a specific morphotype of macrophage loaded with lipid droplets (13).

Figure 3.12. Detection of KI-VP1 in cells of hematopoietic origin in the lung. Lung tissue stained with a dIHC assay using antibodies against (A,D) CD45 (brown) and IgG2b (blue) as an isotype control or (B,C,E) CD45 (brown) and KI-VP1 (blue). (F) Hematoxylin and eosin-stained lung tissue. Panels A and B are at 400x; panel C is at 1000x; panels D and E are at 600x, and panel F is at 200x.
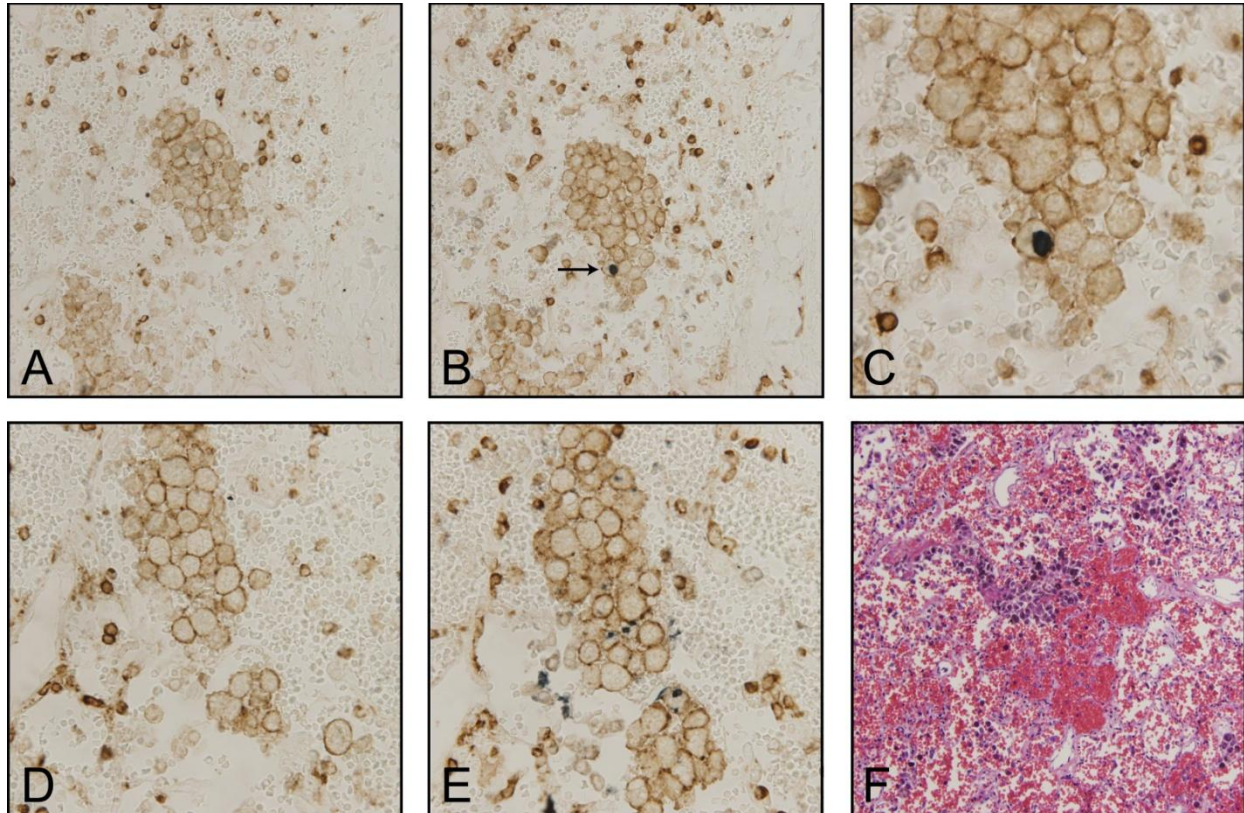
We next attempted to identify the remaining subset of KI-VP1-positive cells that were CD45-negative. Based on the observation that KI-VP1-positive cells lined the alveoli in case #5 described below, we established a dIHC assay using antibodies against KI-VP1 and cytokeratin, which labels epithelial cells. While cells staining single positive for either KI-VP1 or cytokeratin were evident, no double positive cells were seen (Figure 3.14), suggesting KIPyV was not present in epithelial cells in this lung specimen. One caveat to this interpretation is the absence of

a gold standard positive control (i.e. epithelial cells known to express KI-VP1 in lung tissue) to validate the cytokeratin/KI-VP1 double stain in the context of lung tissue.

Figure 3.13. Detection of KI-VP1 in alveolar macrophages. Double IHC staining with antibodies against CD68 (brown) and KI-VP1 (blue) at (A) 400x and (B) 1000x. (C) A second double positive cell from another field of the tissue at 1000x.
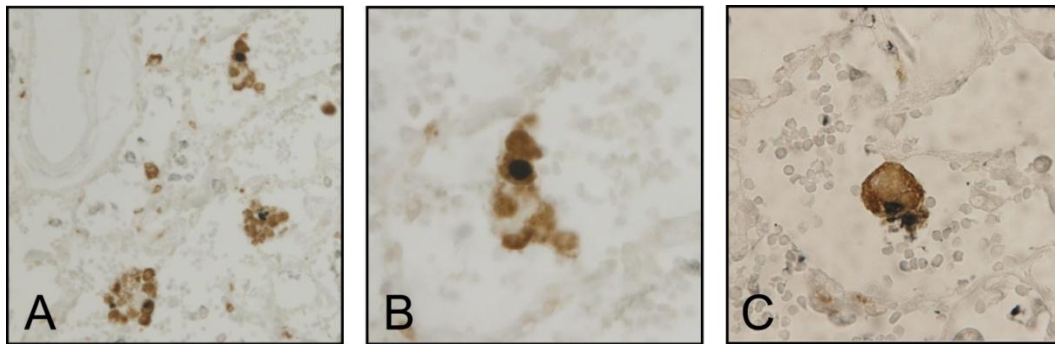
Figure 3.14. Double IHC of the lung with monoclonal antibodies against KI-VP1 (blue) and cytokeratin (brown) at 600x.
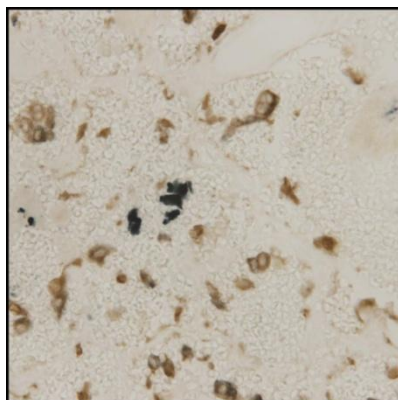
Case #5: Immunohistochemical detection of KIPyV in lung and spleen. Sharp, et al. (see case #3 above) also identified four samples positive by PCR for KIPyV, three from AIDS

patients and one from an HIV-negative patient (18). All four were tested using the KI-VP1 IHC

assay. One spleen sample had KI-VP1-positive cells scattered throughout the section with a few

localized regions containing a high density of positive staining cells (Figure 3.15a-c). This

sample was derived from a 42-year-old HIV-positive male who had initially presented with

peripheral neuropathy and atypical mycobacterial infection. He was re-admitted four months

later for CMV retinitis, and his condition continued to deteriorate until death. Autopsy showed

disseminated mycobacterial infection, CMV esophagitis, low grade CMV encephalitis and

vacuolar myelopathy.

Most of the KI-VP1 positive cells were in areas of white pulp, which also showed poorly

formed granulomas attributed to a mycobacterial infection, according to the autopsy report. One

such example with positive cells surrounding a blood vessel consistent with splenic white pulp is

shown in Figure 3.15b-c. The isotype matched control antibody (J6.36) targeting the E2

glycoprotein of Hepatitis C virus (20) yielded no staining, consistent with specific anti-KI-VP1

staining (Figure 3.15a). Based on morphology and the detection of KI-VP1 in alveolar

macrophages in the previously described case (case #4), we suspected hematopoietic cells may

harbor KIPyV. Double staining of KI-VP1 with CD45 or CD68, however, yielded only single

positive cells (Figure 3.16a, b). Given these negative results, we hypothesized that the KI-VP1-

positive cells may be endothelial cells, so we established a dIHC assay with the anti-KI-VP1

antibody and an antibody against CD31, which primarily marks endothelial cells. However, only

single positive cells were seen (Figure 3.16c). Therefore, the identity of the positive staining

cells in the spleen is currently unknown.

We obtained sections of all other available tissues from this patient from the tissue bank

for further analysis. These included the adrenal gland, carotid artery, colon, heart, ileum, kidney,

71

liver, lung, pancreas, pituitary gland, prostate, testis, thyroid gland, tongue and a lymph node. Besides the spleen, only the lung specimen was positive by IHC for KI-VP1 with strong staining throughout the tissue as represented in Figure 3.15d-f. Closer inspection of the lung showed KI-VP1 staining of some alveolar surfaces, raising the possibility that the infected cells might be pneumocytes. In addition, other cells (Figure 3.15f, arrows) of unknown identity that did not border the alveolar spaces were also positive, suggesting that KIPyV infects multiple cell types present in the lung. Definitive identification of the specific cell types staining positive in this tissue was not possible due to the lack of available tissue. According to the autopsy report, the lungs showed bronchopneumonia, but no granulomas or acid fast bacilli were identified. The lung weights and pathological findings did not suggest an acute interstitial pneumonia.

Figure 3.15. IHC of human spleen and lung with a KI-VP1 monoclonal antibody. Tissue surrounding a splenic blood vessel consistent with splenic white pulp stained with (A) the isotype control or (B) the KI-VP1 antibody (both at 400x). (C) Hematoxylin and eosin staining of the same splenic area at 200x. Gas exchange tissue near a bronchiole stained with (D) the isotype control at 200x or with (E) the KI-VP1 antibody at 200x and (F) 600x.
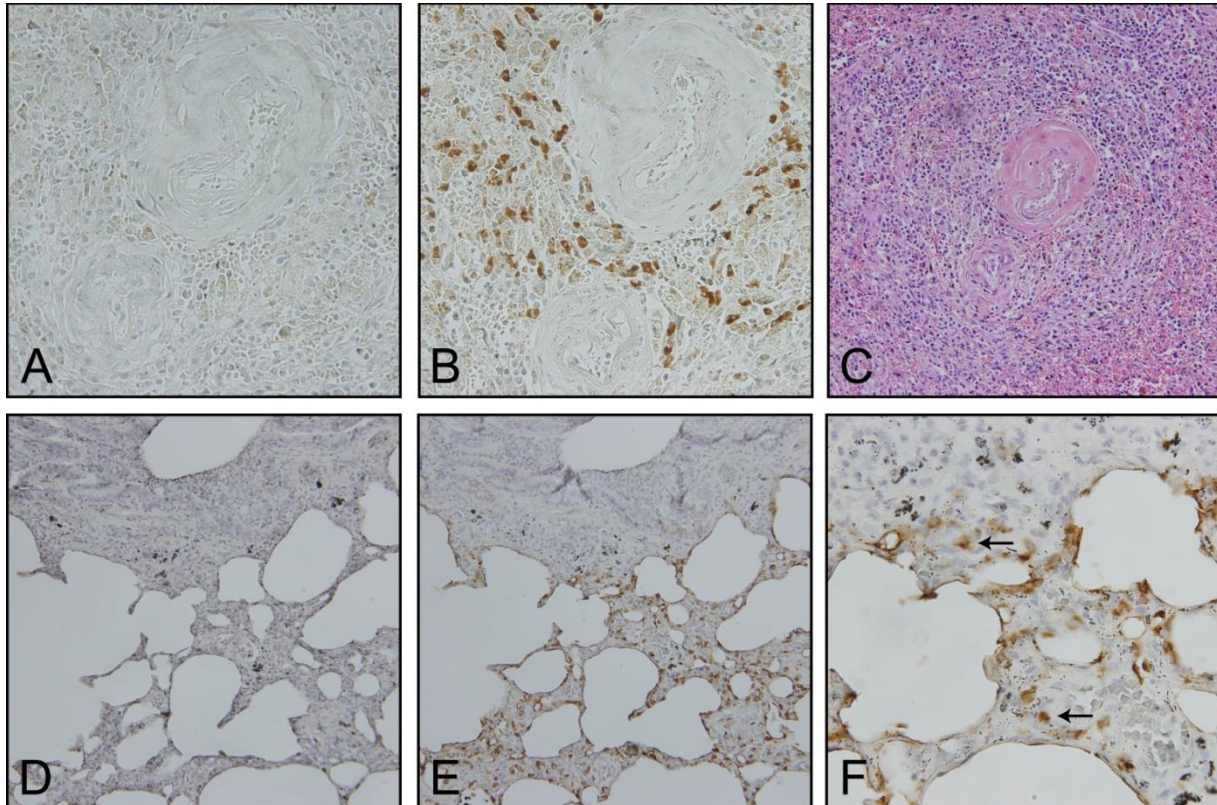
Figure 3.16. Additional dIHC stains of human spleen. Double IHC of spleen with monoclonal antibodies against (A) KI-VP1 (blue) and CD45 (brown) or (B) KI-VP1 (blue) and CD68 (brown) both at 600x. (C) Double IHC of the spleen with monoclonal antibodies against KI-VP1 (blue) and CD31 (brown) at 400x.
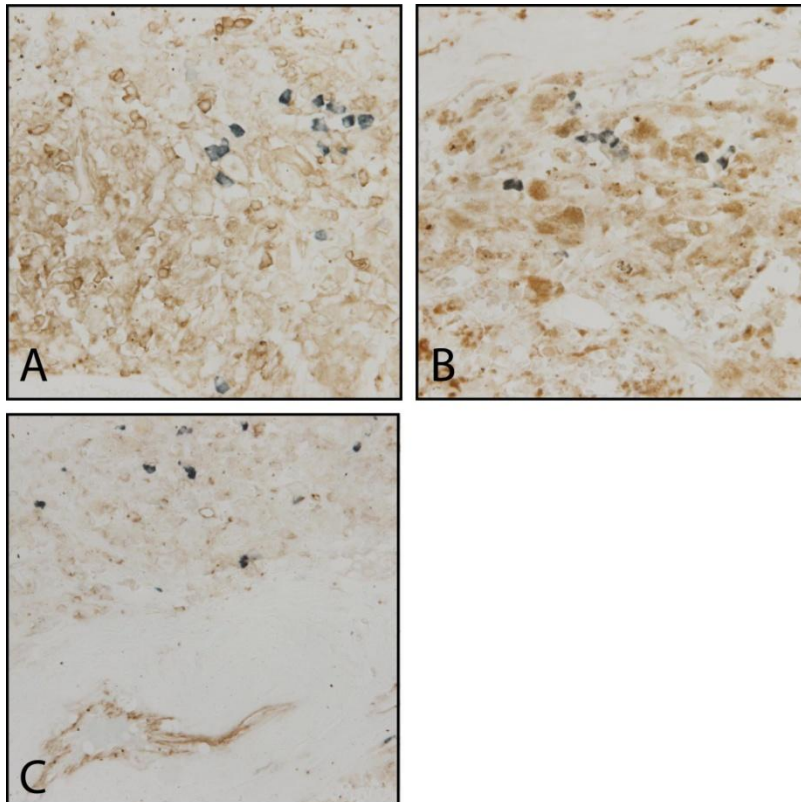
DISCUSSION

Detection of viral antigen in multiple tissues. We detected WU-VP1 in lung and tracheal tissues and in a BAL and KI-VP1 in lung and splenic tissues for the first time using newly developed IHC assays (Table 3.2). Putative WUPyV virions were also observed in the lung tissue of case #1 by electron microscopy. We identified a subset of both the WU-VP1-positive and KI-VP1-positive lung cells as alveolar macrophages, providing the first example of

a specific cell type in which these viruses are detected. In addition, WU-VP1 was detected in respiratory epithelial cells and in cells associated with MUC5AC (a mucin)-positive cells.

Table 3.2. Summary of results.

Virus	Case	Tissue	Cell type
WUV	1	Lung	1. **Macrophages** 2. CD68-negative population
		Trachea	1. Positive cells in **close proximity to Muc5AC-positive cells** 2. Muc5AC-negative population

	2	BAL	1. **Epithelial cells**
			2. Non-epithelial population
			   -CD68 dIF & dIHC negative
			   -CD45 dIF negative

	3	Lung	CD68 dIHC negative Remaining tissue is mostly negative
KIV	4	Lung	1. **Macrophages** 2. CD45-negative population -Cytokeratin dIHC negative
	5	Spleen	CD45,CD68 & CD31 dIHC negative
		Lung	Unknown – no tissue left

Detection of WU-VP1 and KI-VP1 in alveolar macrophages. The detection of viral antigen in alveolar macrophages in cases #1 and #4 was unexpected. The majority of prior WUPyV and KIPyV studies focused on respiratory secretions and relied on PCR of bulk-extracted DNA, making it impossible to determine specific cell types. Nonetheless, the simplest hypotheses regarding WUPyV and KIPyV tropism have focused on respiratory epithelial cells, the cell types infected by common respiratory viruses such as RSV (21) and influenza (22). While the IHC results alone do not prove that WUPyV and KIPyV can productively infect macrophages, they do demonstrate expression of capsid protein from the late region of the genome, a step in the polyomavirus life cycle that is generally thought to occur concomitantly with DNA replication (23). These results also suggest that efforts to develop *in vitro* culture

systems for WUPyV and KIPyV should explore the possibility that macrophage and monocyte cell lines may be permissive for productive infection.

Alveolar macrophages are long-lived, terminally-differentiated cells that permanently reside in the lung. They are thought to be one of the first cell types to respond to pathogens (24). The identification of alveolar macrophages as a potential site of WUPyV and KIPyV infection greatly expands our understanding of viral tropism and provides new insights into the biology of these viruses. The infection of macrophages and monocytes by BKPyV (25), early hematopoietic progenitor cells by JCPyV (26) and detection of MCPyV (27) in monocytes have been reported. Alveolar macrophages display α-2,3- and α-2,6-linked sialic acid (28), both of which are known receptors for other polyomaviruses. BKPyV and murine polyomavirus both bind to α-2,3-linked sialic acid, and JCPyV binds to α-2,6-linked sialic acid (29). It is currently unknown what receptors are utilized by WUPyV and KIPyV, but it is possible that they might use similar receptors to BKPyV and JCPyV.

The detection of WU-VP1 and KI-VP1 in alveolar macrophages could arise from one or more possible scenarios. First, alveolar macrophages may be susceptible to productive infection. Alternatively, it is also conceivable that circulating monocytes become infected in the bloodstream and remained infected after differentiation into alveolar macrophages in the lung. Third, other respiratory viruses, such as type A influenza virus, are known to abortively infect alveolar macrophages (30), where infection and subsequent steps of the viral life cycle occur but no virions are produced. Finally, we cannot rule out the formal possibility that the presence of WU-VP1 and KI-VP1 merely reflects phagocytosis of other virus infected cells. However, given the observation that viral staining is nuclear, this seems like an unlikely option. Bona fide infection versus abortive infection of macrophages by WUPyV or KIPyV would likely lead to

76

different outcomes, as is seen during influenza A infection (30). For example, an abortive infection would make the macrophage a dead end host and might allow the human host to mount a more effective immune response and delay viral spread. Conversely, a productive infection, whether initiated in the blood or lung, could incite a pro-inflammatory response from the infected macrophages, leading to greater immunopathology and increased viral spread.

Detection of WU-VP1 in association with mucin-positive cells. In addition to detection in alveolar macrophages, WU-VP1 protein was also detected in close proximity to MUC5AC-positive cells in tracheal tissue from case #1. The detection of WUPyV in tracheal tissue was unexpected and further expands the known tissue tropism of the virus. As previously mentioned, MUC5AC is a mucin primarily produced by goblet cells in the airway. Several viruses have been described in glandular tissue. Adenovirus was grown in primary cultured peribronchial submucosal gland cells (31), while rhinovirus was grown in human respiratory submucosal gland cells (32). Severe acute respiratory syndrome (SARS) associated virus antigen and RNA were detected in tracheal/bronchial serous gland epithelium (33). In addition, BKPyV has been shown to replicate in salivary gland cells (34, 35). The role of WUPyV in the trachea is currently unknown. However, viral shedding from the trachea or respiratory tissue could contribute to transmission of the virus via the respiratory route.

Detection of WU-VP1 in respiratory epithelial cells. WU-VP1 was also detected in bronchial epithelial cells in the BAL from case #2, a finding which was not unexpected. The presence of nuclease-resistant viral DNA from the Optiprep gradient and the detection of WU-VP1, which is thought to be expressed concomitantly with DNA replication (23), suggests a fully productive infection occurred. Although we attempted to identify a second population of WU-VP1-positive, cytokeratin-negative cells, the etiology of these cells remains uncertain.

Summary of cases. In all of the cases presented here, the patients were immunocompromised, either through a transplant or through infection with HIV. Other human polyomaviruses are thought to exclusively cause disease in immunocompromised hosts, and these cases suggest that immunosuppression may also play a role in WUPyV and KIPyV infection. All five cases had respiratory samples with detectable virus, supporting the hypothesis that the lung is an important site for both WUPyV and KIPyV infection. While it is impossible to prove causation or establish WUPyV and KIPyV as human pathogens from these cases, it does raise interesting questions about the pathogenicity of the viruses, especially in the respiratory tract, and their role in human infection, particularly in patients who are immunosuppressed. However, the five cases presented with unique clinical features and disease pathologies:

WUPyV cases. The likely cause of death for this pediatric bone marrow transplant recipient (case #1) was viral pneumonitis, and the patient suffered from severe acute respiratory distress syndrome shortly before death. IHC for several viruses were negative, as were attempts to grow virus from patient samples. Later testing by real-time PCR was also negative for KIPyV and bocavirus. WUPyV was the only virus detected in the patient's samples using PCR, IHC and electron microscopy. In addition to the lung, the liver, kidney and gastrointestinal tissues were also positive for WUPyV by real-time PCR and had similar intranuclear inclusions, although the viral loads were significantly lower. Electron microscopy was not attempted on these three tissues, and IHC was negative. However, it is possible the amount of virus present in these samples was below the limit of detection of our IHC assay.

In case #2, the patient suffered from Job's syndrome, a primary immunodeficiency, and received a bilateral lung transplant six months before demonstrating WUPyV-positivity. Job's syndrome has not previously been associated with polyomavirus susceptibility. However, to our

knowledge, lung transplants have not been performed in Job's syndrome patients before now, and it is possible that the addition of immunosuppressant medications could have altered susceptibility to viral infection. Following the bronchoscopic evaluation, the patient received immunoglobulin replacement therapy, which could have affected the viral infection; immunosuppressant medications were also decreased. A repeat evaluation three months later did not show any viral cytopathic changes, and SV40 staining was negative.

In contrast to the first two cases, the final WUPyV case (case #3) was an HIV-positive adult male, with several HIV-related illnesses at the time of death. Previous PCR results were positive for WUPyV. Lung tissue stained by IHC was only weakly positive for the virus, and we were unable to identify the specific cell types staining positive. Collectively, these results demonstrate WUPyV can be detected in lung samples from multiple immunocompromised patients. While the pathogenicity of WUPyV is still unclear, there is strong evidence for a WUPyV infection in case #1. In addition, respiratory-related issues contributed to death in cases 1 and 2, raising intriguing questions about the role of WUPyV in these cases.

KIPyV cases. Case #4 (patient 3001) was a pediatric patient who underwent a bone marrow transplant with multiple complications, including severe GVHD, and died from acute respiratory failure and extensive pulmonary hemorrhage. In contrast, the other patient (case #5) was an HIV-positive adult with multiple AIDS-defining illnesses at the time of death. The detection of KI-VP1 in the spleen of the adult HIV case and its absence in patient 3001 may reflect a distinct modality of KIPyV infection or possibly a dependence on HIV-mediated immunosuppression. Regardless, the IHC detection of KI-VP1 in the spleen of this patient corroborates the published PCR results (18), and provides evidence that additional specific cell types harbor KIPyV. Collectively, these results demonstrate that KI-VP1 can be detected in

multiple distinct cell types in more than one tissue type in the human body and suggest the possibility that additional parameters, such as host immune status or age, may be important factors affecting viral tropism. While the role of KIPyV in human disease remains to be determined, it is interesting to speculate about a potential role in respiratory illness given the high titers of KIPyV in patient 3001.

Final summary. In conclusion, we established immunohistochemical assays to detect WUPyV and KIPyV antigen in human tissue. We also demonstrated KI-VP1-positive staining in two lungs and one spleen from two separate patient cases and WU-VP1-positive staining in two lungs, a BAL and one trachea. Further analysis revealed a subset of the WUPyV and KIPyV-positive cells was alveolar macrophages, and subsets of the WUPyV-positive cells were respiratory epithelial cells or near mucin-positive cells in the trachea. Finally, putative WUPyV virions were seen in the lung tissue of one patient. These discoveries further our understanding of WUPyV and KIPyV biology and tropism. Moreover, the knowledge that WUPyV and KIPyV can both be detected in macrophages will benefit future efforts to develop cell culture systems for propagation of these viruses. The role of WUPyV and KIPyV as human pathogens remains unclear, although the evidence for their infection of the respiratory tract is building.

ACKNOWLEDGEMENTS

REFERENCES

1. **Allander T, Andreasson K, Gupta S, Bjerkner A, Bogdanovic G, Persson MA, Dalianis T, Ramqvist T, and Andersson B.** 2007. Identification of a third human polyomavirus. J Virol **81:**4130-4136.
2. **Gaynor AM, Nissen MD, Whiley DM, Mackay IM, Lambert SB, Wu G, Brennan DC, Storch GA, Sloots TP, and Wang D.** 2007. Identification of a novel polyomavirus from patients with acute respiratory tract infections. PLoS Pathog **3:**e64.
3. **Babakir-Mina M, Ciccozzi M, Perno CF, and Ciotti M.** 2011. The novel KI, WU, MC polyomaviruses: possible human pathogens? New Microbiol **34:**1-8.
4. **Nguyen NL, Le BM, and Wang D.** 2009. Serologic evidence of frequent human infection with WU and KI polyomaviruses. Emerg Infect Dis **15:**1199-1205.
5. **Kean JM, Rao S, Wang M, and Garcea RL.** 2009. Seroepidemiology of human polyomaviruses. PLoS Pathog **5:**e1000363.
6. **Neske F, Prifert C, Scheiner B, Ewald M, Schubert J, Opitz A, and Weissbrich B.** 2010. High prevalence of antibodies against polyomavirus WU, polyomavirus KI, and human bocavirus in German blood donors. BMC Infect Dis **10:**215.
7. **Knowles WA.** 2006. Discovery and epidemiology of the human polyomaviruses BK virus (BKV) and JC virus (JCV). Adv Exp Med Biol **577:**19-45.
8. **Kazem S, van der Meijden E, Kooijman S, Rosenberg AS, Hughey LC, Browning JC, Sadler G, Busam K, Pope E, Benoit T, Fleckman P, de Vries E, Eekhof JA, and**

Feltkamp MC. 2012. Trichodysplasia spinulosa is characterized by active polyomavirus infection. J Clin Virol **53:**225-230.

9. **Gjoerup O, and Chang Y.** 2010. Update on human polyomaviruses and cancer. Adv Cancer Res **106:**1-51.

10. **Lu X, Chittaganpitch M, Olsen SJ, Mackay IM, Sloots TP, Fry AM, and Erdman DD.** 2006. Real-time PCR assays for detection of bocavirus in human specimens. J Clin Microbiol **44:**3231-3235.

11. **Epstein MA.** 1962. Observations on the fine structure of mature herpes simplex virus and on the composition of its nucleoid. J Exp Med **115:**1-12.

12. **Herrera GA, Veeramachaneni R, and Turbat-Herrera EA.** 2005. Electron microscopy in the diagnosis of BK-polyoma virus infection in the transplanted kidney. Ultrastruct Pathol **29:**469-474.

13. **Russell DG, Cardona PJ, Kim MJ, Allain S, and Altare F.** 2009. Foamy macrophages and the progression of the human tuberculosis granuloma. Nat Immunol **10:**943-948.

14. **Siebrasse EA, Nguyen NL, Smith C, Simmonds P, and Wang D.** 2014. Immunohistochemical detection of KI polyomavirus in alveolar macrophages, lung and spleen. Virology **Submitted**.

15. **Proud D, and Leigh R.** 2011. Epithelial cells and airway diseases. Immunol Rev **242:**186-204.

16. **Sowerwine KJ, Holland SM, and Freeman AF.** 2012. Hyper-IgE syndrome update. Ann N Y Acad Sci **1250:**25-32.

17. **Schowalter RM, Pastrana DV, Pumphrey KA, Moyer AL, and Buck CB.** 2010. Merkel cell polyomavirus and two previously unknown polyomaviruses are chronically shed from human skin. Cell Host Microbe **7:**509-515.

18. **Sharp CP, Norja P, Anthony I, Bell JE, and Simmonds P.** 2009. Reactivation and mutation of newly discovered WU, KI, and Merkel cell carcinoma polyomaviruses in immunosuppressed individuals. J Infect Dis **199:**398-404.

19. **Siebrasse EA, Bauer I, Holtz LR, Le BM, Lassa-Claxton S, Canter C, Hmiel P, Shenoy S, Sweet S, Turmelle Y, Shepherd R, and Wang D.** 2012. Human polyomaviruses in children undergoing transplantation, United States, 2008-2010. Emerg Infect Dis **18:**1676-1679.

20. **Sabo MC, Luca VC, Prentoe J, Hopcraft SE, Blight KJ, Yi M, Lemon SM, Ball JK, Bukh J, Evans MJ, Fremont DH, and Diamond MS.** 2011. Neutralizing monoclonal antibodies against hepatitis C virus E2 protein bind discontinuous epitopes and inhibit infection at a postattachment step. J Virol **85:**7005-7019.

21. **Hacking D, and Hull J.** 2002. Respiratory syncytial virus--viral biology and the host response. J Infect **45:**18-24.

22. **Kuiken T, and Taubenberger JK.** 2008. Pathology of human influenza revisited. Vaccine **26 Suppl 4:**D59-66.

23. **White MK, Safak M, and Khalili K.** 2009. Regulation of gene expression in primate polyomaviruses. J Virol **83:**10846-10856.

24. **Schneberger D, Aharonson-Raz K, and Singh B.** 2011. Monocyte and macrophage heterogeneity and Toll-like receptors in the lung. Cell Tissue Res **343:**97-106.

25. **Traavik T, Uhlin-Hansen L, Flaegstad T, and Christie KE.** 1988. Antibody-mediated enhancement of BK virus infection in human monocytes and a human macrophage-like cell line. J Med Virol **24:**283-297.

26. **Monaco MC, Atwood WJ, Gravell M, Tornatore CS, and Major EO.** 1996. JC virus infection of hematopoietic progenitor cells, primary B lymphocytes, and tonsillar stromal cells: implications for viral latency. J Virol **70:**7004-7012.

27. **Mertz KD, Junt T, Schmid M, Pfaltz M, and Kempf W.** 2010. Inflammatory monocytes are a reservoir for Merkel cell polyomavirus. J Invest Dermatol **130:**1146-1151.

28. **Yu WC, Chan RW, Wang J, Travanty EA, Nicholls JM, Peiris JS, Mason RJ, and Chan MC.** 2011. Viral replication and innate host responses in primary human alveolar epithelial cells and alveolar macrophages infected with influenza H5N1 and H1N1 viruses. J Virol **85:**6844-6855.

29. **Neu U, Stehle T, and Atwood WJ.** 2009. The Polyomaviridae: Contributions of virus structure to our understanding of virus receptors and infectious entry. Virology **384:**389-399.

30. **Short KR, Brooks AG, Reading PC, and Londrigan SL.** 2012. The fate of influenza A virus after infection of human macrophages and dendritic cells. J Gen Virol **93:**2315-2325.

31. **Ebsen M, Anhenn O, Roder C, and Morgenroth K.** 2002. Morphology of adenovirus type-3 infection of human respiratory epithelial cells in vitro. Virchows Arch **440:**512-518.

32. **Yamaya M, Sekizawa K, Suzuki T, Yamada N, Furukawa M, Ishizuka S, Nakayama K, Terajima M, Numazaki Y, and Sasaki H.** 1999. Infection of human respiratory submucosal glands with rhinovirus: effects on cytokine and ICAM-1 production. Am J Physiol **277:**L362-371.

33. **Ding Y, He L, Zhang Q, Huang Z, Che X, Hou J, Wang H, Shen H, Qiu L, Li Z, Geng J, Cai J, Han H, Li X, Kang W, Weng D, Liang P, and Jiang S.** 2004. Organ distribution of severe acute respiratory syndrome (SARS) associated coronavirus (SARS-CoV) in SARS patients: implications for pathogenesis and virus transmission pathways. J Pathol **203:**622-630.

34. **Jeffers LK, Madden V, and Webster-Cyriaque J.** 2009. BK virus has tropism for human salivary gland cells in vitro: implications for transmission. Virology **394:**183-193.

35. **Burger-Calderon R, Madden V, Hallett RA, Gingerich AD, Nickeleit V, and Webster-Cyriaque J.** 2014. Replication of oral BK virus in human salivary gland cells. J Virol **88:**559-573.

CHAPTER 4

Development of a cell culture system for WU polyomavirus

ABSTRACT

WU polyomavirus (WUPyV) was discovered in 2007 in a respiratory sample from a child with pneumonia. While the virus infects the majority of the population, it is unclear whether it is causes disease in humans. Study of WUPyV has been limited by the lack of a cell culture system in which to grow the virus, a tool which is also critical to establishing disease causality. Although a replication system using a genomic clone is established, only one round of replication is achieved. This system does not represent a natural infection, and the virus cannot complete its life cycle by re-infecting neighboring cells. We attempted to establish a cell culture system for WUPyV. We used virus generated via the replication system to infect two primary human cell types and 12 immortal human cell lines. No viral replication was detected in most of these cell lines. However, increases in viral DNA over the course of the infection were detected in the monocytic cell lines KG-1, THP-1, U-937 and HL-60. Further studies with THP-1 cells showed this effect was reproducible and also seen following passage of infected cell lysates. Despite this promising data, no virions were seen by electron microscopy; no viral protein was detected by Western blot; and analysis of RNA transcripts was inconclusive. While we were not able to establish a robust cell culture system for WUPyV, these studies provide a framework on which to base future efforts.

INTRODUCTION

WU polyomavirus (WUPyV) was discovered in 2007 in a nasopharyngeal aspirate (NPA) from a three-year-old Australian child suffering from pneumonia (1). Subsequent studies, including those described in Chapter 3, described the viral epidemiology and tropism and began exploring potential disease associations. However, the gold standard for establishing disease causality is to fulfill Koch's postulates, which necessarily requires the virus to be grown in cell culture. As no such system currently exists for WUPyV, it is a fundamental barrier to both establishing disease causality and exploring the basic biology of this virus.

The two well-established human pathogens BK and JC polyomaviruses (BKPyV, JCPyV, respectively) can be cultured in mammalian cells. JCPyV grows in a very limited number of cell types in culture, including human glial cells and tonsillar stromal cells (2). BKPyV infects a greater variety of cells, including African green monkey kidney cells, human embryonic kidney (HEK), human diploid lung fibroblasts, infant urothelial cells, human fetal brain cells, monkey kidney cells and human embryonic lung cells (3, 4). The other human polyomaviruses have been found in a variety of sample types (Table 4.1), but none has yet been grown in cell culture. However, a replication system similar to that described below for WUPyV was established for Merkel cell polyomavirus (MCPyV) (5).

Prior to the studies noted in Chapter 3, WUPyV DNA was detected in a variety of sample types, but no specific cell tropisms were identified. The detection of WUPyV protein in alveolar macrophages and respiratory epithelial cells heavily influenced subsequent work. It is important to note, however, that while this tropism data was useful in the selection of different mammalian cells in which to attempt culture of WUPyV, BKPyV and JCPyV protein can be detected in cell types within the human body that do not support viral infection when grown in culture.

Table 4.1. Human polyomaviruses are detected in a variety of specimen types (6-16). Respiratory sample is abbreviated "RS" and includes NPAs and other respiratory tract samples.

Virus	Detected in:			
	RS	Blood	Urine	Stool
BKPyV	X	X	X	X
JCPyV	X	X	X	X
KIPyV	X	X		X
WUPyV	X	X		X
MCPyV	X	X	X	X
HPyV6	X			X
HPyV7	X		X	X
TSPyV	X			X
HPyV9		X	X	
MWPyV	X			X
STLPyV			X	X
HPyV12				X
NJPyV		X		

While no infectious cell culture system is currently available for WUPyV, a replication system using a WUPyV genomic clone was established in Vero cells (17). Genomic clones are widely used in the polyomavirus field and can be transfected into permissive cells to recapitulate one round of the post-entry viral life cycle. However, the newly formed virions (referred to as recombinant WUPyV, rWUPyV) cannot complete the cycle by infecting new cells. In the replication system, the viral genomic clone (cWUPyV) is transfected into Vero cells, and viral DNA and protein are detectable in the cells and supernatant by three days post-transfection (Figure 4.1). As no WUPyV culture system exists, we cannot assess the infectivity of these particles, although studies described in the results do address this issue. While this system is useful for studying some aspects of viral biology and can be used to produce virions, it is not a natural infection, which fundamentally limits the type of studies that can be performed using it.

Figure 4.1. Establishment of a WUPyV replication system (17). A) Supernatants from Vero cells show viral capsid protein expression starting at day 3 post-transfection when additional early region is also transfected (cWUPyV-wt + pER). A clone with a stop codon in the LT (cWUV-4981) was included as a negative control. B) Vero cell transfected with cWUPyV and pER at 4000x. C) Vero cell transfected with cWUPyV and pER at 40,000x. Scale bar is 200 nm. D) Supernatants from Vero cells show WUPyV DNA starting at day 3 post-transfection.
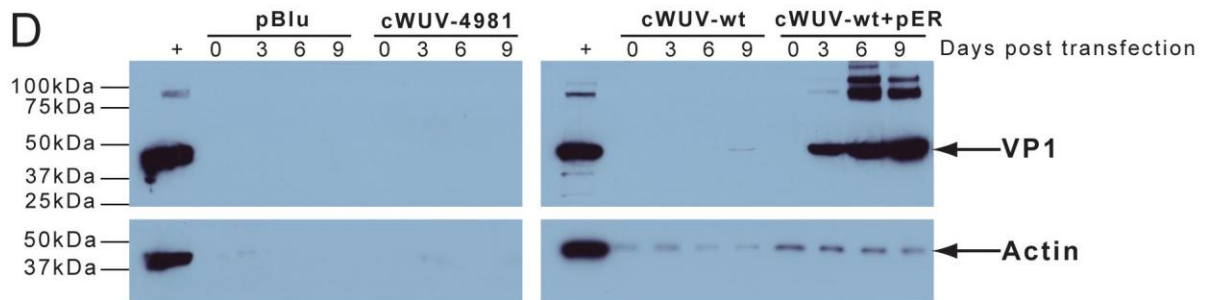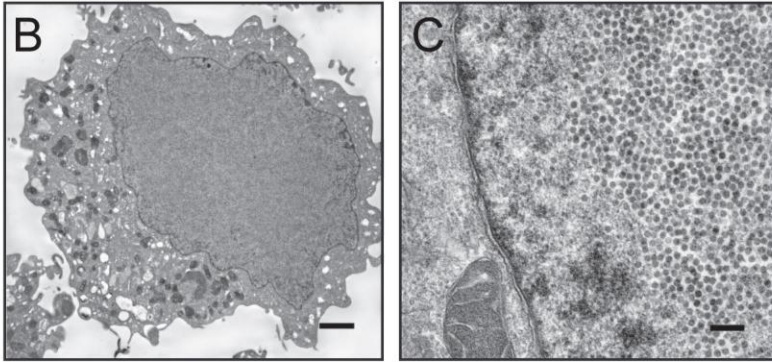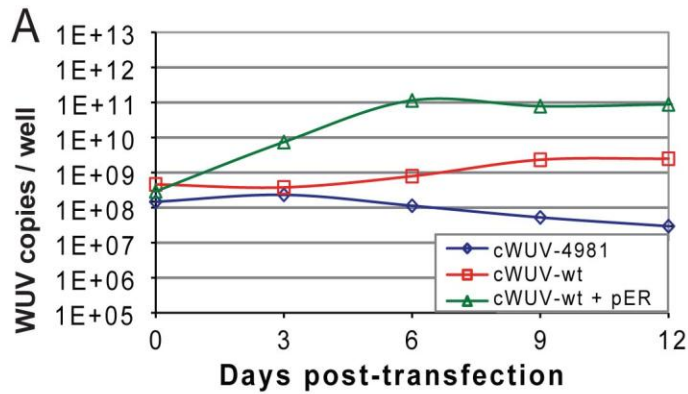
Despite the importance of a cell culture system for study of WUPyV, no such system currently exists and is a fundamental barrier to a better understanding of viral biology and pathogenesis. While numerous attempts to develop an infectious cell culture system for WUPyV are described here, they were ultimately unsuccessful. Data from rWUPyV infection of THP-1 cells was initially promising, although later experiments were more inconclusive. It is unclear whether the initial positive results were an artifact or a more complicated explanation is warranted. Establishing a fully functional culture system for WUPyV remains an important goal, and the experiments described here will provide a foundation on which to base future studies.

MATERIALS AND METHODS

Density gradient ultracentrifugation. Vero cells (1×10^6 cells/60mm dish) were transfected with 6.4 micrograms (ug) of the WUPyV genomic clone (cWUV-wt) and 6.4 ug of a plasmid (pcDNA3.1/Hygro+ from Invitrogen) containing the WUPyV early region (pER) using Lipofectamine 2000 (Invitrogen) in OptiMEM media (Gibco). At three days post-transfection, the cells were trypsinized, pelleted and resuspended in Buffer A (50mM NaCl, 10mM Tris-HCl pH 8, 0.01% TritonX-100, 0.01mM CaCl2). Lysates were freeze-thawed three times in DMEM (Gibco) containing 10% FBS and pelleted over a 20% sucrose cushion in a Beckman Optima L-100 XP ultracentrifuge using a SW41Ti rotor (Beckman Coulter) at 25,000 rotations per minute (rpm) for one hour. The pellet was resuspended in 1.0 mL TEN buffer (0.1M Tris-HCl pH 8, 0.01M EDTA, 1M NaCl), which was layered over a 13 mL 30-68% sucrose step gradient (5 mL 30% sucrose over 6 mL 68% sucrose) and spun in the SW41Ti rotor at 35,000 rpm for 23 hours. Six fractions, 2.0mL each, were collected using an Auto Densi-Flow fractionator (Labconco). A Western blot was performed using 20ul of each fraction. The fraction containing the most VP1

89

protein as determined by immunoblot was buffer exchanged from 2.0 mL sucrose solution to 1.0 mL Buffer A using an Amicon Ultracel-100k centrifugal concentrator. The sample was then layered over a 13 mL 2M-3M cesium chloride gradient prepared using the Auto Densi-Flow fractionator and spun in the SW41Ti rotor at 35,000 rpm for 24 hours. Twenty fractions of approximately 0.6mL were collected using the Auto Densi-Flow fractionator. The density of each fraction was determined using a Thermo Spectronic refractometer (Thermo Scientific). Each fraction was buffer exchanged from 600 uL cesium chloride solution to 100 uL Buffer A, and 20 uL was used for Western blot. Fifty microliters of each sample was DNase treated with 100U of DNaseI (Fermentas) in 2x Fermentas DNase Buffer for one hour at 37°C. DNA was then extracted. The 25ul real-time PCR (qPCR) reactions included 12.5 uL of Universal TaqMan real-time PCR master mix (ABI), 5 uL of extracted sample, 12.5 pmol of each primer and 4 pmol of probe. Primers and probe were from the previously published WU-C assay, which targets the non-coding control region (NCCR) (18). Each sample was tested in triplicate. Reactions were run on a CFX96 thermocycler (BioRad) and analyzed according to recommended BioRad parameters. A standard curve was run on each plate to determine the copy number.

Infection of primary cells. All infections of primary cells were done by Andrew Pekosz at Johns Hopkins University. Similar data to that noted in Figure 4.1 was obtained from transfection of the WUPyV genomic clone into 293T cells. Cell lysate containing rWUPyV from the 293T replication system was freeze-thawed three times, diluted 1:50 in culture media and used to infect primary human nasal epithelial cells (hNEC) and primary human tracheal epithelial cells (hTEC) in quadruplicate for two hours at 33°C or 37°C, respectively. Mock infections were also performed in quadruplicate. Cells were infected from both the apical (100 uL inoculum) and basolateral (500 uL inoculum) sides simultaneously. Cells were cultured as

90

previously described (19). Each cell type (hNEC or hTEC) originated from a single donor. Cultures were washed and incubated with 1000 uL (hNEC) or 500 uL (hTEC) of the appropriate media on the basolateral side. At two, 48 and 96 hours post-infection (hpi), media was added to the apical chamber (200 uL for hNEC, 100 uL for hTEC) for 10 min before collection and storage at -80°C. The basolateral media was also harvested and stored. At the two and 48 hour time points, the basolateral media was replaced, and the cells continued incubation. At 96 hpi, the cells were scraped and pelleted, and the cell pellets were stored at -80°C. This experiment was later repeated (five replicates) in the same manner.

A portion of the cell pellet was passaged by resuspending the cells in media, freeze-thawing three times and using this lysate as inoculum to infect a fresh culture of hNECs in quadruplicate. The rest of the experiment was performed as noted above.

Infection of immortal cell lines. Adherent cell lines were plated at 25% confluence in media containing antibodies against interferon alpha (IFNα, pbl interferon source #21100) and tumor necrosis factor alpha (TNFα, R&D Systems #MAB610) (both at 10 ug/mL) in a 24-well plate 24 hours before infection. Suspension cell lines were plated in the same way but at a concentration of $2x10^5$ cells/mL in 0.5 mL media. All cells were cultured as recommended by ATCC and split at least once before infection. When media changes were performed or an aliquot collected from the suspension cells, they were centrifuged; the supernatant was removed; and they were resuspended in the appropriate media. For both cell types, immediately prior to infection, the media was changed to serum-free media without antibodies. Infections were performed in the minimum amount of media needed to cover the well. Cells were infected with rWUPyV from the Vero replication system in duplicate for one and one-half hours at an approximate multiplicity of infection (MOI) of one or 100. MOI was based on the number of viral genome copies calculated

by qPCR analysis of DNase-treated inoculum. Following infection, the media was changed back to regular media containing the two antibodies. Aliquots of the supernatant were taken at two, 24, 72, 120 and 144 hpi and replaced with fresh media. At two and 24 hpi, this media contained the two antibodies, while no antibodies were included in media added at the later time points. Cells were checked daily for cytopathic effects (CPE). After the final time point was taken, the cells were scraped, and the cell pellet was frozen at -80°C. Half of the cell pellet was later resuspended in media, freeze-thawed three times and used as the inoculum for a new infection of fresh cells. This was repeated twice more, for a total of three passages. No antibodies were included in the media during the passages. Supernatant aliquots were collected at two, 96 and 144 hpi. Slight modifications of this protocol were utilized for the A549, MRC-5, WI-38, Calu-3 and hs198.ton cell lines. These cell lines were infected for two hours in media containing serum and the two antibodies. The media was not changed post-infection.

For the next infection (Figure 4.9), THP-1 cells were plated in a T75 flask at $2x10^5$ cell/mL in 10 mL media containing the two antibodies. Cells were infected with rWUPyV at an MOI of 100 in 5.0 mL serum-free media without antibodies for two hours. Following infections, the cells were centrifuged, and the media was replaced with normal media plus antibodies. At zero, 24, 72 and 120 hpi, a 2.0 mL aliquot was removed. Media was not replaced. The cells and supernatant were separated by centrifugation, and both were analyzed as noted below.

For the final infection (Figures 4.10-11), cells were plated at $1x10^5$ cell/mL in a 6-well plate with 2.5 mL media containing the anti-IFNα and anti-TNFα antibodies plus an antibody against interferon beta (IFNβ, R&D Systems #AF814). Cells were infected for two hours in duplicate with rWUPyV diluted in 1.25 mL serum-free media without antibodies. Three concentrations of diluted rWUPyV were used (1:10, 1:100 and 1:1000). Following the two hour

92

infection, the media was replaced with regular media containing the three antibodies. Aliquots were collected at zero, 12, 24, 48, 72 and 96 hpi. The media was not replaced. At the final time point, a portion of the cells were passaged into a new 6-well dish at $1x10^5$ cell/mL. The remaining cells and supernatant were processed as noted below.

DNA extraction. DNA was extracted from the primary cell supernatants using an Ampliprep Cobas extractor (Roche). We used the Qiagen Blood and Tissue kit to extract DNA from the immortal cells and their supernatants.

Analysis of viral DNA by real-time PCR. Two qPCR assays were used for these studies. Analysis of primary human cell infections was accomplished using the WU-C assay noted above. We used the WU-B assay (18), which targets the LTAg, with the same conditions for analysis of the immortal cell line infections. Reactions were cycled using either an ABI 7500 real-time thermocycler (Applied Biosystems) or the aforementioned CFX96. A standard curve of serial dilutions (5 to 5 x 10^6 copies per reaction) of a plasmid containing the cognate target sequence was run on each plate, from which actual DNA copy numbers of each sample were extrapolated.

Extraction of RNA and analysis by RT-PCR. RNA was extracted from cells using the Qiagen RNeasy kit. RT-PCR was performed using primers flanking the splice junction, AG86 (5'-TGCAAGAGTGTGTTAGTACAGTG-3') and AG108 (5'-CCAGGAGATTTAGGCATTTCC-3'), and the Qiagen one-step RT-PCR kit. Primers were annealed at 52°C with 40 cycles total.

RESULTS

  Analysis of virions produced by a WUPyV replication system. A replication system using a WUPyV genomic clone was previously established in our lab (Figure 4.1) (17), although it was impossible to determine whether virions produced by this system were infectious.

However, the densities of empty (1.29 g/mL) and mature (1.33 g/mL) polyomavirus particles resulting from a productive infection were well characterized. To determine the densities of viral particles produced in the WUPyV replication system, we performed cesium chloride density gradient ultracentrifugation as detailed in Figure 4.2a. The presence of WUPyV DNA was assayed by qPCR, and VP1 protein expression was assayed by Western blot (Figure 4.2b, c). Extrapolation of the qPCR data indicated 1.2×10^8 copies of WUPyV DNA were produced per 60mm plate (2.1×10^6 cells) of transfected Vero cells. A protein peak at 1.28 g/mL corresponded to the density of putative empty capsids. A second protein peak at 1.33 g/mL matched the single DNA peak and corresponded to putative mature virions. These values matched well with established virion densities for the polyomavirus family.

Infection of primary respiratory cells with rWUPyV. Polyomaviruses typically display marked species specificity (20). Previous studies detected WUPyV in various respiratory tract secretions and in lung and tonsillar tissue. Based on this data, we first focused on respiratory cells. Primary respiratory cell types have been shown to support infection by a number of respiratory viruses, including rhinovirus (21, 22), respiratory syncytial virus (23, 24) and Andes virus (19). In collaboration with Andy Pekosz at Johns Hopkins University, we infected hNECs and hTECs, both primary cell types, with rWUPyV. We infected from both the basolateral and apical sides of these polarized cells, as different viruses have been shown to selectively infect from one or the other side. For example, influenza preferentially infects the apical membrane (25), while adenovirus prefers the basolateral (26).

Figure 4.2. Determination of the density of rWUPyV viral particles. A) Schematic of WUPyV cesium chloride density gradient protocol. B) Viral genome copies in each density gradient fraction. C) Western blot of WUPyV VP1 protein in each density gradient fraction.

Human nasal epithelial cells and hTECs were infected or mock infected in quadruplicate with rWUPyV. DNA extracted from the supernatant (supe) was assayed at two, 48 and 96 hpi using a qPCR assay targeting the WUPyV NCCR (18). At 96 hpi, the cells were collected for analysis by Western blot. If viral replication was occurring, we would expect to see increasing amounts of viral DNA in the supernatant over the course of the infection. A reproducible increase in viral DNA in the apical supernatant was detected in three of the four replicates (Figure 4.3a). The fourth replicate, well A, showed a decrease in viral DNA over time. As this

trend was opposite from the other three replicates, we re-extracted nucleic acid from the well A supernatant. The qPCR results were contradictory to those from the first extraction (Figure 4.3b).

Results from qPCR of the basolateral supernatants were inconclusive but not promising (Figure 4.3c). The basolateral supernatant from well A was again extracted twice, yielding somewhat different results. Well B showed an initial increase, followed by a plateau. Well C showed a sharp increase, but no viral DNA was detectable by 96 hpi. Finally, Well D showed an initial decrease, followed by a sharp increase. No meaningful amount of viral DNA was detected in the mock infections (wells E-H). Protein was extracted from the cell pellets collected at 96 hpi for Western blot, but no WUPyV protein was detected. Overall, viral DNA consistently increased on the apical side of the hNECs, but no reproducible increase was seen on the basolateral side.

We did not detect any replication occurring following rWUPyV infection of the hTECs. (Figure 4.4). Only one well had detectable viral DNA in all three time points (well B-apical). This well showed an initial increase from two to 48 hpi, but viral DNA decreased sharply by 96 hpi. Wells A and B had detectable viral DNA at 48 and 96 hours post-infection on the basolateral side, but both showed slight decreases over time. Well A only had viral DNA detectable at 48 hpi. Well C had no detectable viral DNA at any time points on either side. Well D also had no detectable viral DNA on the basolateral side, and viral DNA decreased over time on the apical side, although there was no detectable DNA at 48 hpi. Given these results, no further experiments were conducted with the hTECs.

Figure 4.3. Viral DNA detected in supernatants from hNECs infected with rWUPyV. Each well is an independent replicate. (A) Apical supernatants, wells B-D; (B) Apical supernatant, well A, which was extracted twice; (C) Basolateral supernatants. Well A was again extracted twice.

Figure 4.4. Viral DNA detected in supernatants from hTECs infected with rWUPyV. Each well is an independent replicate. a, apical; b, basolateral.
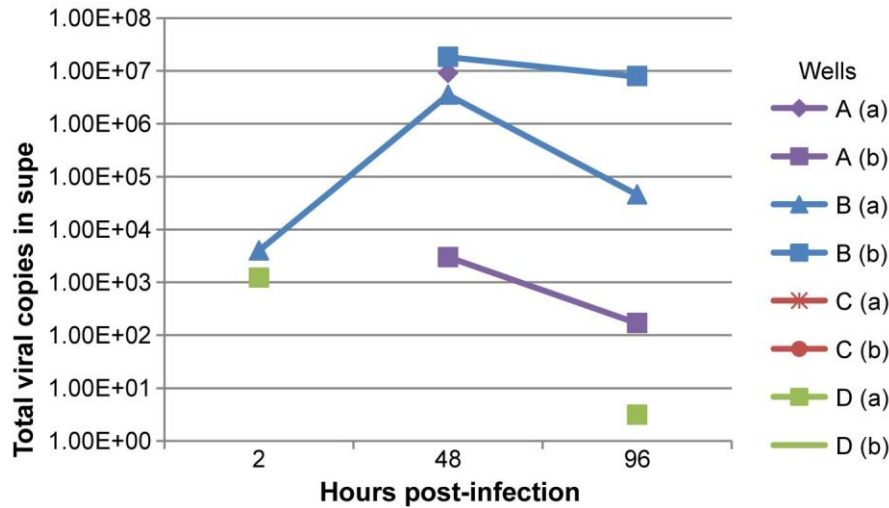
We repeated the hNEC infection with similar infection parameters and collected supernatants from the apical and basolateral sides at two, 48 and 96 hpi (Figure 4.5). Basolateral supernatants from all five replicates showed a slight initial increase (~ 0.5 log) in viral DNA from two to 48 hpi, followed by a plateau or very slight decrease from 48 to 96 hpi. Four of the five replicates showed mostly decreasing viral DNA in the apical supernatant. However, one replicate, well C, showed a steady increase of over one log. No viral protein was seen by Western blot of protein extracted form cell pellets harvested at 96 hpi.

We also used lysate collected from the first hNEC infection to infect fresh hNEC cells. If an infection was occurring, we would expect production of virions, which would infect new hNEC cells upon inoculation. As shown in Figure 4.6, a very slight increase in viral DNA was seen in basolateral supernatant from two of the four replicates, but no other sample showed any evidence of viral replication. No evidence of viral protein was detected by Western blot.
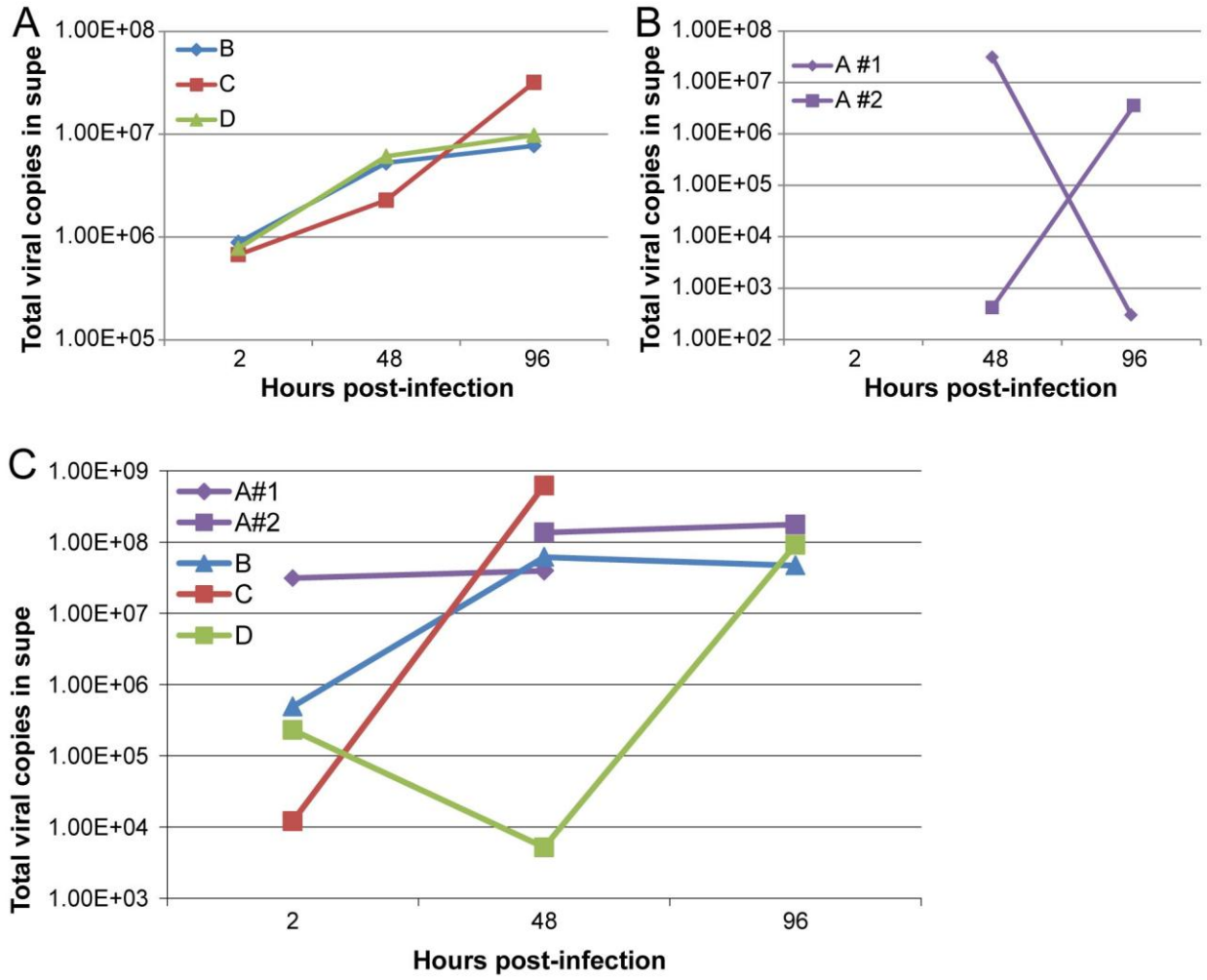
Figure 4.5. Viral DNA detected in supernatants from hNECs infected with rWUPyV. Each well

represents an independent replicate. a, apical (blue); b, basolateral (red).
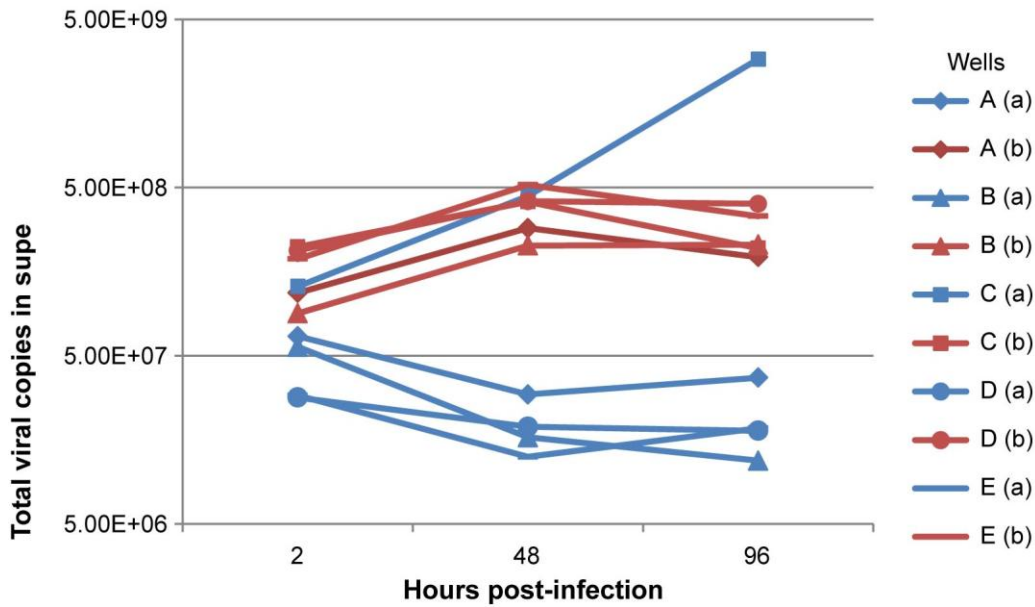
Figure 4.6. DNA detected in supes from hNECs infected with lysate passaged from a rWUPyV

hNEC infection. Each well is an independent replicate. a, apical (blue); b, basolateral (red).
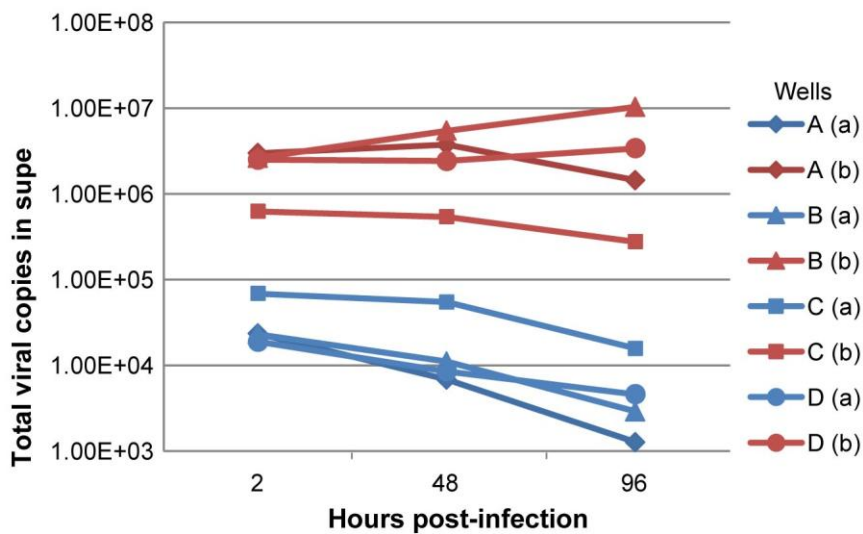
While the initial infection showed increases in viral DNA of one log in the apical supernatant (Figure 4.3), when we repeated the same infection (Figure 4.5) or passaged lysate to fresh hNECs (Figure 4.6), most wells showed a decrease in viral DNA. When an increase was seen, it was very slight, with the exception of one well (well A, apical side, Figure 4.5). Given this unconvincing data, no further infections were attempted in the hNECs.

Infection of immortal cell lines with rWUPyV. Only infections of immortal cell lines derived from human cells were attempted due to the species specificity of polyomaviruses (20). Based on the detection of WUPyV in alveolar macrophages and respiratory epithelial cells, we chose cell lines of either respiratory origin or of the myeloid lineage. We also included antibodies against TNFα and IFNα in the culture media pre- and post-infection, which has been shown to promote viral infection in cell culture by countering the host cell's innate immune response (27). Results from rWUPyV infections are shown in Table 4.2. No evidence of viral replication was observed in eight of the 12 cell lines (not shown). However, in four lines, KG-1, THP-1, U-937 and HL-60, an increase in viral DNA in the first 24 hpi was observed (Figure 4.7). As results from these four cell lines were similar, we chose to further characterize the infection in one cell line, THP-1. We repeated the THP-1 infection at an MOI of 100 with similar experimental parameters, which yielded similar results in three of four replicates (not shown).

Lysate from the initial infection of THP-1 cells with rWUPyV was passaged three times. In the first passage, an increase in viral DNA of approximately one log was detected between two and 96 hpi (Figure 4.8). Figure 4.8 shows data from both the initial infection (also seen in Figure 4.7) and the first passage for comparison. By passage two, only trace amounts of viral DNA remained, and none was detectable by passage three (not shown).

Table 4.2. Results of infections of immortal cell lines with rWUPyV.

Cell line	Cell type	Results
A549	Adenocarcinomic alveolar basal epithelials	No replication
MRC-5	Normal lung fibroblasts	No replication
WI-38	Normal lung fibroblasts	No replication
Calu-3	Adenocarcinomic bronchial epithelials	No replication
Hs 198.Ton	Normal tonsil fibroblasts	No replication
BEAS-2B	Normal lung/bronchial epithelials	No replication
H820	Adenocarcinomic lung/lymph node epithelials	No replication
KG-1a	Myeloid lineage (promyeloblast)*	No replication
KG-1	Myeloid lineage (myeloblast)*	Inconclusive
THP-1	Myeloid lineage (monocyte)*	Inconclusive
U-937	Myeloid lineage (monocyte)*	Inconclusive
HL-60	Myeloid lineage (myeloblast)*	Inconclusive

*All myeloid lineage cell lines were derived from cells from leukemias or lymphomas.

Figure 4.7. Viral DNA detected in supernatants from immortal cell lines following infection with rWUPyV at a MOI of ~100. Two replicates were performed for each cell type.
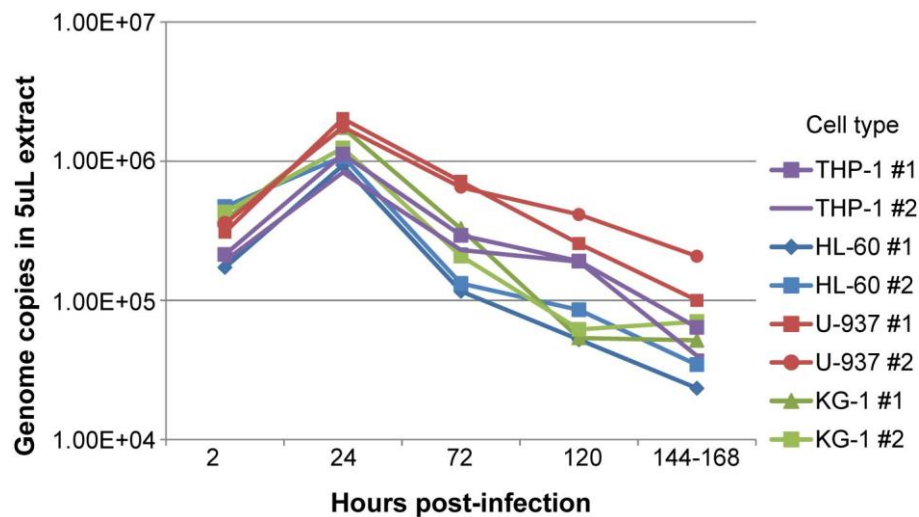
Figure 4.8. Passage of rWUPyV-infected THP-1 cell lysates into fresh THP-1 cells. An increase in viral DNA is seen during the initial infection (same data as Figure 4.7) and upon passage.
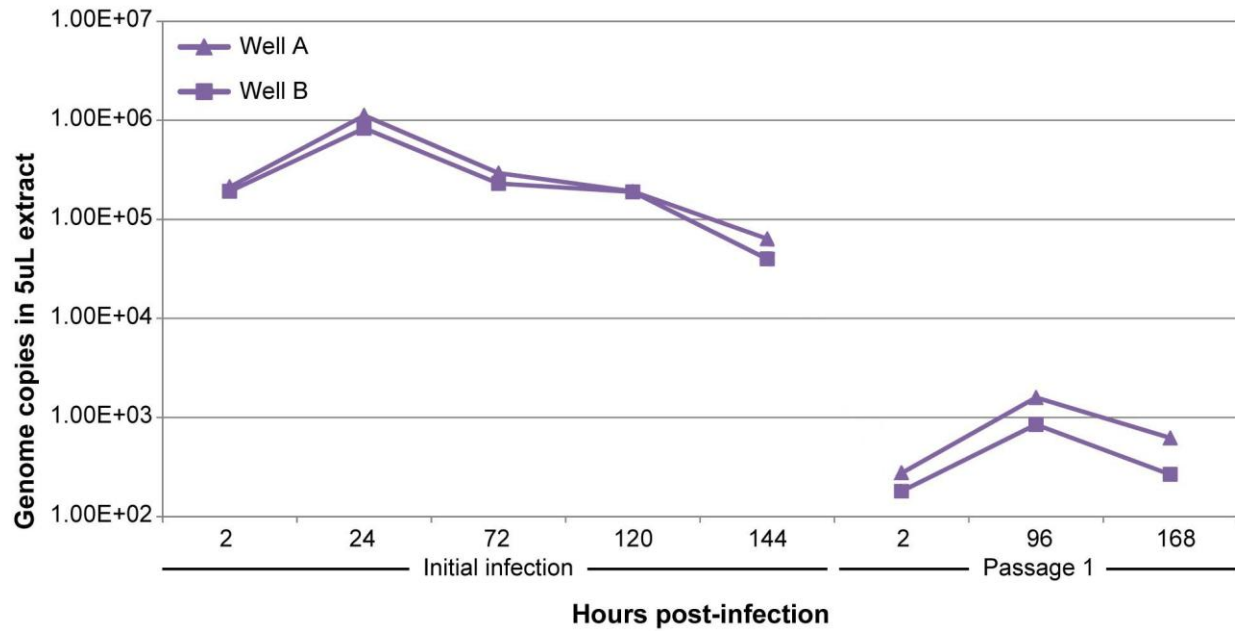
Having demonstrated that the increase in viral DNA in the supernatant following infection of THP-1 cells was reproducible and sustained through passage, we next sought to determine if viral DNA also increased inside the cells. THP-1 cells in a T75 flask were infected with rWUPyV. Aliquots of the suspension cells were taken at two, 24, 72 and 120 hpi, and the cells and supernatant were separated. DNA, RNA and protein were extracted from the cells. No WUPyV protein was seen by Western blot (not shown). While viral DNA increased in the supernatant, a steady decrease was seen in the cells (Figure 4.9a). RNA was used to assess whether splicing of viral transcripts was occurring. Both the WUPyV small T antigen (STAg) and large T antigen (LTAg) are spliced, and the splice products should only be detectable if an infection was initiated (Figure 4.9b).

Figure 4.9. Viral nucleic acid produced from a rWUPyV infection of THP-1 cells. (A) Viral DNA present in THP-1 cells and their supernatant following infection. (B) Schematic of RNA splicing in WUPyV. (C) RT-PCR of RNA from THP-1 cells. NTC, no template control.
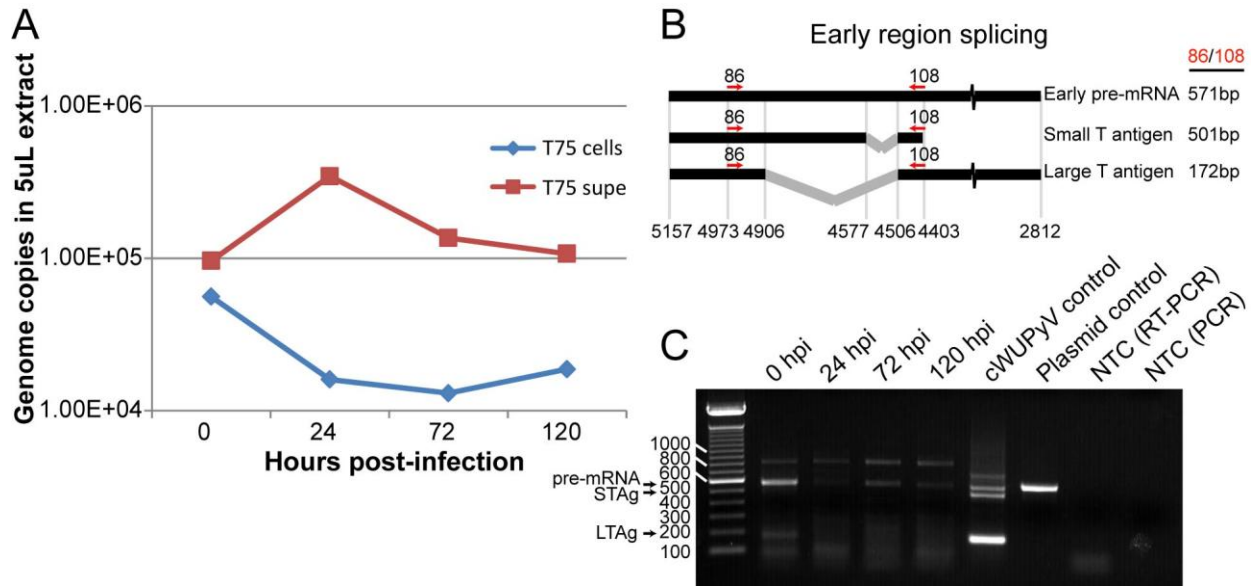
The early pre-mRNA was detected in all four time points (0, 24, 72 and 120 hpi). There was also a LTAg splice product at 0 hpi, but no band was seen in the later time points. No STAg splice product was seen. All three bands were detected in RNA extracted from a whole genome (cWUPyV) transfection of cells (lane six), as expected. The zero hpi time point was actually taken two hours after the infection was initiated, so it was possible RNA transcripts were generated. Alternatively, the band could be carry over from the input rWUPyV lysate, which is known to contain the splice products.

Although an increase in viral DNA was reproducibly seen by 24 hpi in THP-1 cells infected with rWUPyV, no spliced RNA transcripts were seen in the later time points. One hypothesis was that a very small number of cells were infected.; there was enough virus made during the initial infection to initiate a new infection in the first passage, but by the second

passage, the virus was too dilute. An approximate MOI of 100 was used for the aforementioned infections. However, this number is based on the genome copies calculated from qPCR analysis of DNase treated lysate, which cannot differentiate between infectious and defective particles. To test our hypothesis, we infected THP-1 cells in duplicate with increasing amounts of virus at dilutions of 1:1000 (MOI ~560), 1:100 (MOI ~5600) and 1:10 (MOI ~56,000). We also included a third antibody against IFNβ to further block the innate immune response, and all three antibodies were included in the media pre-infection and for the duration of the experiment. Supernatant was collected at zero, 24, 48, 72 and 96 hpi. Cells were collected at 96 hpi. RNA was extracted from half of the cells, while the remainder was prepared for electron microscopy.

No viral particles were seen in either the cells or the supernatant. However, viral DNA increased steadily from zero to 24 hpi in the two most concentrated dilutions (1:10, 1:100) before plateauing (1:10) or decreasing (1:100) (Figure 4.10a). In cells infected with the lowest concentration of rWUPyV (1:1000), an initial increase in viral DNA was seen in the first 24 hpi, but one replicate subsequently plateaued, while the other decreased at 48 hpi, increased again by 72 hpi and then plateaued. LTAg spliced transcripts were detected in all three samples (Figure 4.10b). No STAg spliced transcript was seen. While the RT-PCR of the DNA plasmid control yielded the expected band at 571 bp, it is unclear why we did not detect the pre-mRNA in RNA extracted from cells transfected with the WUPyV early region, although it was expected.

A portion of the cells from this THP-1 infection was passaged three times (every 3-5 days) into fresh media. DNA and RNA were extracted from cells immediately before passage for qPCR and RT-PCR analysis. Viral DNA decreased steadily over the three passages (Figure 4.11a). No STAg splice product was seen, but LTAg spliced transcripts were detected in both samples from the 1:10 dilution infection in passage one (wells A and D, lanes 2 and 5) (Figure

104

4.11b). The LTAg splice band was also present in the input, so it was possible the product in wells A and D is carry over from the inoculum. An early pre-mRNA band at 571 bp was visible in several lanes, but no specific pattern was evident. Again, the WUPyV early region control did not yield all three bands as was expected. It is unclear why this occurred.

Figure 4.10. Infection of THP-1 cells with varying concentration of rWUPyV. (A) Viral DNA detected in THP-1 cells post-infection. (B) RT-PCR of RNA from THP-1 cells at 96 hpi. NTC, no template control.
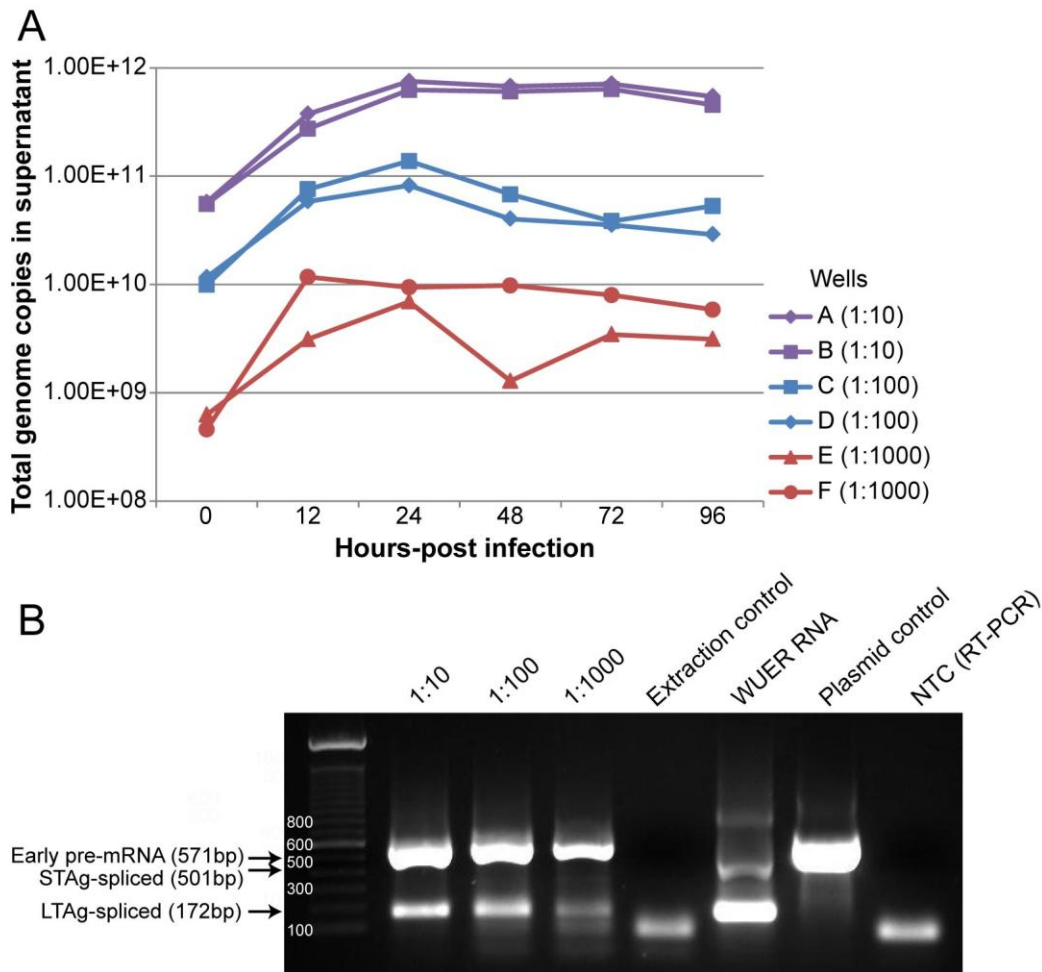
Figure 4.11. Passage of THP-1 cells infected with rWUPyV. (A) Viral DNA detected at the end of each passage. (B) RT-PCR of RNA from THP-1 cells at the end of each passage. NTC, no template control.
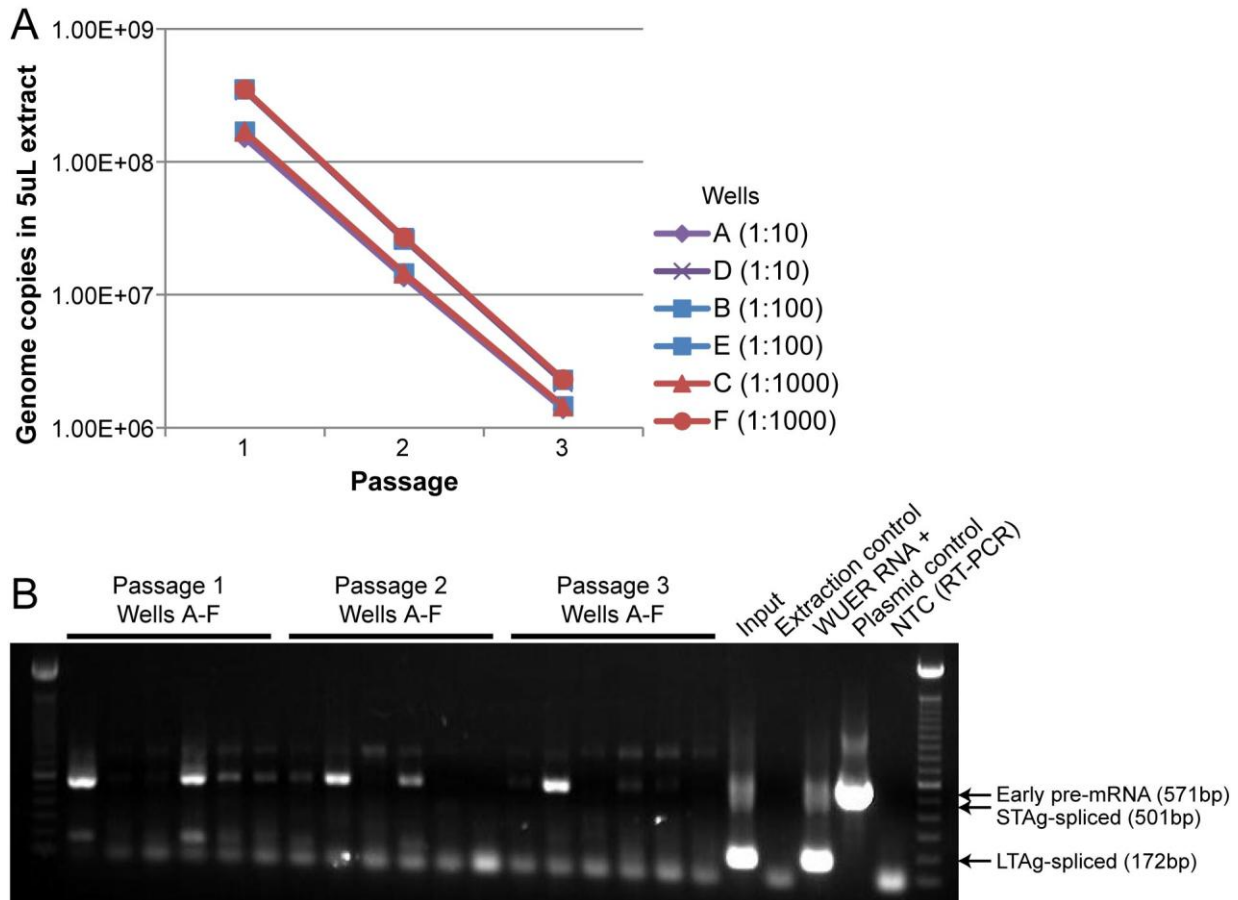
DISCUSSION

We attempted to establish a cell culture system for WUPyV in two primary human cell lines and in 12 immortal cell lines. While infection of four monocytic cell lines showed initial promising results, later experiments using THP-1 cells were inconclusive. Viral DNA increased over the first 24 hpi, after which levels either plateaued or decreased. This effect was also seen upon passage of lysate onto fresh cells. Despite these promising results, no viral protein was

detected by Western blot, and no virions were seen in the supernatants or in the cells by electron microscopy. Analysis of RNA splicing showed LTAg spliced transcripts at 96 hpi, although splicing was not seen in most samples from later passages. While we were not able to establish a system for robust culture of WUPyV, our work will serve as a solid foundation on which to base future attempts.

One explanation for these results is that infection is occurring in a very small portion of cells. Less sensitive means of measuring infection, such as electron microscopy or Western blot, likely would not have been able to detect virus produced at low levels. However, this would not explain why spliced viral transcripts were absent at later time points. We attempted to boost viral infection by adding an additional antibody against IFNβ and increasing the MOI of the inoculum. This did seem to have an effect on viral titers, as viral DNA plateaued instead of steadily decreasing, and spliced transcripts were seen at 96 hpi. Despite these effects, spliced transcripts were not consistently detected in the cells upon passage. If cells were infected at a higher but still relatively low rate, dilution of the cells by passaging may have negated the initial gains.

Future attempts to culture WUPyV should build on the results presented here. It may be useful to attempt infections of other cell lines, including other types of primary respiratory epithelial cells. It is currently debated whether pneumocytes can be grown in cell culture, but this could be a better option in the future. It may be advisable to attempt other means of knocking down the immune system. However, it is important to note that polyomavirus infections typically require the cells to be dividing, and growth can often be impeded by impairing innate immunity.

In conclusion, we were not able to establish a cell culture system for WUPyV. However, our data suggests other respiratory or monocytic cell lines may support growth of WUPyV.

ACKNOWLEDGEMENTS

REFERENCES

1. **Gaynor AM, Nissen MD, Whiley DM, Mackay IM, Lambert SB, Wu G, Brennan DC, Storch GA, Sloots TP, and Wang D.** 2007. Identification of a novel polyomavirus from patients with acute respiratory tract infections. PLoS Pathog **3:**e64.
2. **Monaco MC, Atwood WJ, Gravell M, Tornatore CS, and Major EO.** 1996. JC virus infection of hematopoietic progenitor cells, primary B lymphocytes, and tonsillar stromal cells: implications for viral latency. J Virol **70:**7004-7012.
3. **Yoshiike K, and Takemoto KK.** 1986. Studies with BK virus and monkey lymphotropic papovavirus, p. 295-326. *In* Salzman, NP (ed.), The Papovaviridae. Plenum Press, New York, NY.
4. **Takemoto KK, and Mullarkey MF.** 1973. Human papovavirus, BK strain: biological studies including antigenic relationship to simian virus 40. J Virol **12:**625-631.
5. **Feng H, Kwun HJ, Liu X, Gjoerup O, Stolz DB, Chang Y, and Moore PS.** 2011. Cellular and viral factors regulating Merkel cell polyomavirus replication. PLoS One **6:**e22468.
6. **Babakir-Mina M, Ciccozzi M, Perno CF, and Ciotti M.** 2011. The novel KI, WU, MC polyomaviruses: possible human pathogens? New Microbiol **34:**1-8.
7. **Mertz KD, Junt T, Schmid M, Pfaltz M, and Kempf W.** 2010. Inflammatory monocytes are a reservoir for Merkel cell polyomavirus. J Invest Dermatol **130:**1146-1151.
8. **Bialasiewicz S, Whiley DM, Lambert SB, Nissen MD, and Sloots TP.** 2009. Detection of BK, JC, WU, or KI polyomaviruses in faecal, urine, blood, cerebrospinal fluid and respiratory samples. J Clin Virol **45:**249-254.
9. **Siebrasse EA, Bauer I, Holtz LR, Le BM, Lassa-Claxton S, Canter C, Hmiel P, Shenoy S, Sweet S, Turmelle Y, Shepherd R, and Wang D.** 2012. Human polyomaviruses in children undergoing transplantation, United States, 2008-2010. Emerg Infect Dis **18:**1676-1679.
10. **Siebrasse EA, Reyes A, Lim ES, Zhao G, Mkakosya RS, Manary MJ, Gordon JI, and Wang D.** 2012. Identification of MW polyomavirus, a novel polyomavirus in human stool. J Virol **86:**10321-10326.
11. **Scuda N, Hofmann J, Calvignac-Spencer S, Ruprecht K, Liman P, Kuhn J, Hengel H, and Ehlers B.** 2011. A novel human polyomavirus closely related to the african green monkey-derived lymphotropic polyomavirus. J Virol **85:**4586-4590.

12. **Yu G, Greninger AL, Isa P, Phan TG, Martinez MA, de la Luz Sanchez M, Contreras JF, Santos-Preciado JI, Parsonnet J, Miller S, DeRisi JL, Delwart E, Arias CF, and Chiu CY.** 2012. Discovery of a novel polyomavirus in acute diarrheal samples from children. PLoS One **7:**e49449.

13. **Rockett RJ, Sloots TP, Bowes S, O'Neill N, Ye S, Robson J, Whiley DM, Lambert SB, Wang D, Nissen MD, and Bialasiewicz S.** 2013. Detection of novel polyomaviruses, TSPyV, HPyV6, HPyV7, HPyV9 and MWPyV in feces, urine, blood, respiratory swabs and cerebrospinal fluid. PLoS One **8:**e62764.

14. **Korup S, Rietscher J, Calvignac-Spencer S, Trusch F, Hofmann J, Moens U, Sauer I, Voigt S, Schmuck R, and Ehlers B.** 2013. Identification of a novel human polyomavirus in organs of the gastrointestinal tract. PLoS One **8:**e58021.

15. **Lim ES, Reyes A, Antonio M, Saha D, Ikumapayi UN, Adeyemi M, Stine OC, Skelton R, Brennan DC, Mkakosya RS, Manary MJ, Gordon JI, and Wang D.** 2013. Discovery of STL polyomavirus, a polyomavirus of ancestral recombinant origin that encodes a unique T antigen by alternative splicing. Virology **436:**295-303.

16. **Husseiny MI, Anastasi B, Singer J, and Lacey SF.** 2010. A comparative study of Merkel cell, BK and JC polyomavirus infections in renal transplant recipients and healthy subjects. J Clin Virol **49:**137-140.

17. **Gaynor AM, Wu G, and Wang D.** 2009. Replication of WU polyomavirus from a full-length genomic clone. In preparation.

18. **Bialasiewicz S, Whiley DM, Lambert SB, Gould A, Nissen MD, and Sloots TP.** 2007. Development and evaluation of real-time PCR assays for the detection of the newly identified KI and WU polyomaviruses. J Clin Virol **40:**9-14.

19. **Rowe RK, and Pekosz A.** 2006. Bidirectional virus secretion and nonciliated cell tropism following Andes virus infection of primary airway epithelial cell cultures. J Virol **80:**1087-1097.

20. **Imperiale MJ, and Major EO.** 2007. Polyomaviruses, p. 2263-2289. *In* Knipe, DM, Howley, PM, Griffin, DE, Lamb, RA, Martin, MA, Roizman, B, and Straus, SE (ed.), Fields Virology. Lippincott Williams & Wilkins, Philadelphia.

21. **Ghildyal R, Dagher H, Donninger H, de Silva D, Li X, Freezer NJ, Wilson JW, and Bardin PG.** 2005. Rhinovirus infects primary human airway fibroblasts and induces a neutrophil chemokine and a permeability factor. J Med Virol **75:**608-615.

22. **Suzuki T, Yamaya M, Kamanaka M, Jia YX, Nakayama K, Hosoda M, Yamada N, Nishimura H, Sekizawa K, and Sasaki H.** 2001. Type 2 rhinovirus infection of cultured human tracheal epithelial cells: role of LDL receptor. Am J Physiol Lung Cell Mol Physiol **280:**L409-420.

23. **Fonceca AM, Flanagan BF, Trinick R, Smyth RL, and McNamara PS.** 2012. Primary airway epithelial cultures from children are highly permissive to respiratory syncytial virus infection. Thorax **67:**42-48.

24. **Becker S, Soukup J, and Yankaskas JR.** 1992. Respiratory syncytial virus infection of human primary nasal and bronchial epithelial cell cultures and bronchoalveolar macrophages. Am J Respir Cell Mol Biol **6:**369-374.

25. **Rowe RK, Brody SL, and Pekosz A.** 2004. Differentiated cultures of primary hamster tracheal airway epithelial cells. In Vitro Cell Dev Biol Anim **40:**303-311.

26. **Pickles RJ, McCarty D, Matsui H, Hart PJ, Randell SH, and Boucher RC.** 1998. Limited entry of adenovirus vectors into well-differentiated airway epithelium is responsible for inefficient gene transfer. J Virol **72:**6014-6023.
27. **Chiu CY, Greninger AL, Chen EC, Haggerty TD, Parsonnet J, Delwart E, Derisi JL, and Ganem D.** 2010. Cultivation and serological characterization of a human Theiler's-like cardiovirus associated with diarrheal disease. J Virol **84:**4407-4414.

CHAPTER 5

Discussion and Future Directions

OVERVIEW

Two broad questions guided the research described in this dissertation: "Are there additional novel polyomaviruses infecting humans?" and "Do these polyomaviruses cause disease in their human hosts?" In the Introduction, I argued why I believe these questions are important to address, and the research presented in Chapters 2-4 detailed some initial answers. Here, I summarize these and offer some suggestions for future directions.

SECTION I: Are there additional, novel polyomaviruses infecting humans?

The easy answer to this question today is yes, of course, there are novel polyomaviruses infecting humans. However, prior to 2007, the answer would have been vastly different. The first two human polyomaviruses, JC and BK polyomaviruses (JCPyV, BKPyV, respectively) were both discovered in the 1970s, and no new additional human polyomaviruses were discovered until 2007. In 2006, discovering new polyomaviruses was not likely a goal of any research group, and most human polyomavirus research focused on studying the biology and pathogenesis of JCPyV and BKPyV. The intervening years also saw phenomenal discoveries in basic biology using the polyomaviruses SV40 and murine polyomavirus (MPyV). However, the discoveries of WU and KI polyomaviruses (WUPyV, KIPyV, respectively) in 2007 (1, 2) reinvigorated the field, and several groups began looking for new polyomaviruses. With the subsequent discoveries of Merkel cell carcinoma polyomavirus (MCPyV) (3) and Trichodysplasia spinulosa-associated polyomavirus (TSPyV) (4) and their associations with Merkel cell carcinoma (MCC) and Trichodysplasia spinulosa, respectively, interest in polyomaviruses, particularly MCPyV, increased substantially. Previous research showed polyomaviruses were strongly associated with various animal cancers; JCPyV and BKPyV were weakly associated with human cancers; and

their proteins displayed oncogenic properties *in vitro*. However, MCPyV was the first human polyomavirus to be strongly associated with a human cancer and was found clonally integrated into a large proportion of MCCs (3). This finding greatly increased interest in the role of polyomaviruses in human cancer and in additional oncogenic polyomaviruses that may exist. Taken together, the discoveries of these viruses brought more researchers to the field and broadened interest in polyomavirus biology and discovery.

Prior to the work described here, nine human polyomaviruses had been discovered, including those previously mentioned and human polyomavirus 6 (HPyV6) (5), human polyomavirus 7 (HPyV7) (5) and human polyomavirus 9 (HPyV9) (6). Shortly after our report describing the discovery of MWPyV (Chapter 2), two others groups published very closely related novel polyomaviruses, which ultimately turned out to be strains of MWPyV (Table 5.1). The first group, Buck, et al., described human polyomavirus 10 (HPyV10) in an anal wart from a person with WHIM (warts, hypogammaglobulinemia, infections, and myelokathexis) syndrome, a rare genetic disorder (7). No other samples were tested for HPyV10. This virus was 95-99% identical to MWPyV, depending to which MWPyV stain it was compared. The authors argued that the discovery of abundant levels of HPyV10 within the wart indicated the virus was not a contaminant but was instead a bona fide human virus. The second group, Yu, et al., detailed the discovery of MX polyomavirus (MXPyV) in pediatric stool samples (8). MXPyV was subsequently detected in 28 of 834 (3.4%) stool samples from children in California, Mexico and Chile and in one respiratory sample (out of 136) from a child in Mexico. The virus was not found in urine and blood samples from immunocompromised patients from California. The authors also performed a case-control study to examine whether MXPyV was associated with diarrhea, although no association was found. As with MWPyV, one patient had multiple samples over a

113

span of several months (91 days) that were positive for MXPyV. The virus was 99.8% identical

to the MWPyV St. Louis strain.

Table 5.1. Summary of MWPyV studies to date.

Study (year)	Cohort	Samples	MWPyV-positive
Siebrasse, et al. (2012) (9)	Children with diarrhea	514 stools	12 (2.3%)
Buck, et al. (2012) (7)	Adult with WHIM	1 anal wart	1 (100.0%)
Yu, et al. (2012) (8)	Children with diarrhea	96 stools	12 (12.5%)
	Children with respiratory infection	136 nasal washes	1 (0.7%)
	Children with or without diarrhea	546 stools	18 (3.3%)
	Transplant recipients	193 plasmas	0 (0.0%)
		287 plasmas/urines	0 (0.0%)
	Children with diarrhea	96 stools	0 (0.0%)
	Healthy children	96 stools	4 (4.2%)
Lim, et al. (2012) (10)	Adult renal transplant recipients	237 stools	0 (0.0%)
		261 plasmas	0 (0.0%)
		261 NPAs	0 (0.0%)
		373 urines	0 (0.0%)
	Children with diarrhea	332 stools	5 (1.5%)
	Healthy children	390 stools	5 (1.3%)
Rockett, et al. (2013) (11)	Patients with respiratory symptoms	1232 respiratory*	18 (1.5%) †
	Healthy children	153 respiratory*	14 (9.2%)
	Symptomatic patients (undefined)	161 bloods	0 (0.0%)
	Symptomatic patients (undefined)	171 CSFs	0 (0.0%)
	Symptomatic patients (undefined)	189 urines	0 (0.0%)
	Symptomatic patients (undefined)	185 stools	9 (4.9%)
	Healthy children	78 stools	10 (12.8%)
Li, et al. (2013) (12)	Children with diarrhea	211 stools	3 (1.4%)
	Healthy children	208 stools	6 (2.9%)
Ramqvist, et al. (2014) (13)	Adults with mucosal melanoma	37 mucosal melanomas	0 (0.0%)
Wieland, et al. (2014) (14)	HIV-positive men	205 skin swabs	19 (9.3%)
	HIV-negative men	238 skin swabs	8 (3.4%)

* Respiratory samples included NPAs, BALs, nose and throat swabs, bronchial washes, sputum and lung tissues.
† All MWPyV-positive samples were from children.

In addition to these two discovery reports, at least five other MWPyV prevalence studies

have been published (Table 5.1). MWPyV was not found in any of the adult samples (stool,

plasma, urine and nasopharyngeal aspirates (NPA)) that Lim, et al. tested (10). While MWPyV

was found in pediatric stool specimens, there was no difference between the prevalence in cases

versus controls. Rockett, et al. found MWPyV in respiratory and stool samples (11). The respiratory samples were taken from healthy children (9.2% positive) and children with respiratory tract infections (1.5%). The stool samples also came from healthy children (12.8%) and children with gastrointestinal illness (4.9%). All MWPyV-positive samples were obtained from children less than 10-years-old; samples from adults were tested but were negative. Four of the positive samples came from immunocompromised patients diagnosed with acute lymphoblastic leukemia. A number of these samples were co-infected with other viruses. One patient had multiple positive samples over a period of five days. Finally, MWPyV was more likely to be found in healthy, younger children (less than five-years-old) than in older children or in children with respiratory or gastrointestinal symptoms. Ramqvist, et al. tested 37 mucosal melanoma samples for MWPyV, all of which were negative (13). Wieland, et al. tested 443 forehead skin swabs from HIV-positive or HIV-negative men and found the virus significantly more frequently in the HIV-positive patients (9.3% versus 3.4%) (14). Finally, Li, et. al. conducted a case-control study of fecal samples from children with diarrhea and found no difference in MWPyV prevalence between the cases and controls (12).

These other MWPyV reports both corroborate and expand work presented in Chapter 2. Multiple reports found the virus in samples from the respiratory and gastrointestinal tracts (7-12). One report also described detection of the virus on the skin (14). Despite collective testing of over 700 plasmas and 700 urines, MWPyV was not detected (8, 10, 11). The virus was also not detected in mucosal melanomas or cerebrospinal fluid (CSF) (11, 13). Consistent with the initial findings in Chapter 2, MWPyV was predominantly detected in children. Yu, et al. tested 480 plasma and urine samples from adult transplant recipients; Rockett, et al. tested hundreds of various specimen types from adults; and the Lim, et al. study tested 1,132 samples (plasma,

urine, stool and NPA) from adult kidney transplant recipients. All were negative. The only adult

samples that were positive for MWPyV were skin swabs from adult men in the Wieland study.

Many of the adult specimens were from immunocompromised transplant recipients, who would

be expected to have an increased risk of polyomavirus infection given their immune status. It is

unclear why children seem more susceptible to infection with these viruses. Other human

polyomaviruses are typically acquired in childhood, so our detection of the virus in this

population may represent shedding during its initial infection. Perhaps MWPyV does not often

reactivate in adults, even in those with compromised immune systems.

Figure 5.1. Global distribution of MWPyV. Blue (Gregory Storch, unpublished data), red (9),

green (8), purple (7), orange (10), light blue (14), yellow (11) and pink (12).
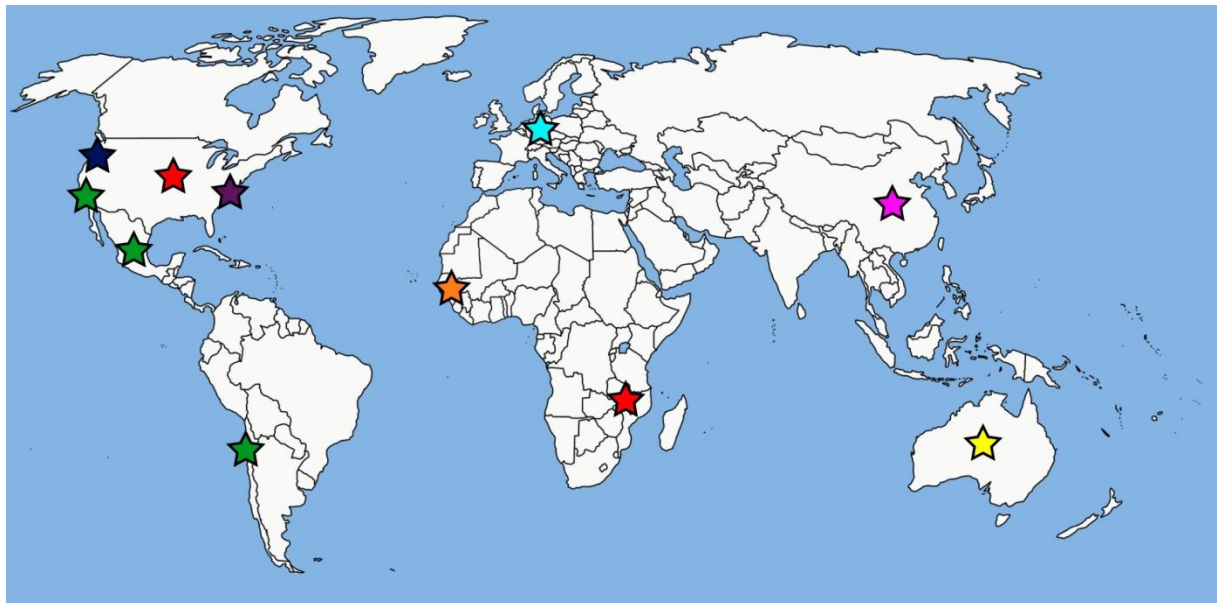
Since the initial discovery of MWPyV, strains of the virus have been detected globally

(Figure 5.1). Data described in Chapter 2 found the virus in Malawi and in the United States (St.

Louis). Subsequent work from our lab and others detected the virus in Washington, Maryland,

California, Mexico, Chile, The Gambia, China, Germany and Australia (see Figure 5.1 for references). Given the global distribution of the virus and its detection within a wart, it seems unlikely that the virus is a dietary contaminant. In addition, both our study (Chapter 2), the MXPyV study and Rockett, et al. found patients with multiple samples positive for the virus over several months. This likely represented chronic shedding of the virus rather than re-infection.

As with the discovery of any novel virus, there are many outstanding questions regarding MWPyV. First, does MWPyV infect humans? The data we already have, including the chronic shedding, global distribution and discovery of HPyV10 within a wart, suggests that it does. However, seroprevalence studies represent the best way to definitively demonstrate that MWPyV infects humans. This type of study can also determine the percentage and age distribution of the population that is infected, among other things. Other groups are currently pursuing this line of research. Second, what is the prevalence of MWPyV? While the seroprevalence of most polyomaviruses is quite high, the prevalence of viral DNA is typically quite low (<10%), so we would expect MWPyV to be similarly low. Studies have so far supported this hypothesis, with our study demonstrating a prevalence of 2.3% in stool samples and other studies having similarly low rates in stool and respiratory specimens. Additional studies with larger cohorts in different locals will be important to answering this question. Third, what is the tropism of MWPyV? As previously discussed, the virus has predominantly been detected in stool and respiratory samples. However, few samples from other body sites have been tested, and no specimens from other sites have been obtained from pediatric patients. Given the significantly higher prevalence of the virus in children, it will be important to test pediatric specimens in the future. If the virus is a resident of the gastrointestinal tract, it does not necessarily mean it causes disease there, although it could. It may be that the virus infects humans but is not pathogenic. Alternatively, the virus may

cause disease elsewhere in the body and be shed in the stool as a byproduct. For example, poliovirus is shed in and spread through feces but causes disease in the nervous system. In addition to detection of viral nucleic acids, as has been done in the past, future studies should also determine where in the body viral proteins can be detected (similar to experiments described in Chapter 3 for WUPyV and KIPyV).

While many more questions about MWPyV exist, perhaps the most important one is "Does MWPyV cause disease in humans?" While answering the earlier questions will provide useful information toward this end, answering this particular question directly is difficult. As mentioned in the introduction, the gold standard approach to determining disease causality is fulfillment of Koch's postulates. However, this either requires human volunteers, which is not ethical given the uncertain pathogenicity of this virus, or growth of the virus in culture. We have not yet attempted to grow MWPyV in culture, although we would expect to encounter similar difficulties as those noted for WUPyV. Despite this hurdle, growth of MWPyV in culture would represent a major advance and should be attempted in the future. As with WUPyV, defining the virus' tropism in the human body could inform selection of cell lines in which to attempt growing the virus. Another approach to addressing this question is the case-control study. Five such studies have been performed for MWPyV. None of the studies found an association between MWPyV and diarrhea (8, 10, 12) or between MWPyV and respiratory illness (11). However, MWPyV was found more frequently in skin samples from patients with HIV (14).

Following the discovery of MWPyV, three additional polyomaviruses were discovered in humans. STL polyomavirus (STLPyV) was also discovered in a stool sample from a child from Malawi and detected in the United States (St. Louis) and the Gambia (10). The virus was most closely related to MWPyV, and phylogenetic analysis demonstrated the viruses share an

ancestral recombinant origin. The STLPyV early region was alternatively spliced to yield a new form of T antigen designated 229T. Human polyomavirus 12 (HPyV12) was discovered in resected human liver tissue and subsequently detected in cecum and rectal tissues and a stool sample (15). It was not closely related to any known polyomavirus, and its seroprevalence rate was 17-23% depending on the cohort. Finally, New Jersey polyomavirus (NJPyV) was discovered in a muscle biopsy from a pancreatic transplant recipient who developed weakness, retinal blindness and necrotic plaques (16). Viral particles consistent with polyomavirus were visible by electron microscopy. *In situ* hybridization specific for NJPyV was also positive. Both viral particles and viral DNA were detected within vascular endothelial cells.

Collectively, these discoveries show the number of polyomaviruses is continuing to increase rapidly. It is likely that new polyomaviruses will continue to be discovered as molecular techniques, including high throughput sequencing, expand and are applied to more and more specimens. MWPyV and STLPyV were both discovered in specimens originally collected for a different study. As high throughput sequencing is now being applied to a myriad of specimens from all over the world, applying the viral discovery techniques mentioned in the Introduction to this existing data would likely yield numerous new viruses.

SECTION II: Do these polyomaviruses cause disease in their human hosts?

Again, the obvious answer to this question is yes, it is likely at least some of the new polyomaviruses cause disease in humans. However, this dissertation focuses on three of the new polyomaviruses, MWPyV, WUPyV and KIPyV. MWPyV has already been discussed in Section I, so the focus of this section will be the latter two viruses. We took two approaches to this question. The first approach was to establish a cell culture system for WUPyV. This system

119

would be used to study viral biology and as a step toward fulfilling Koch's postulates. As mentioned in the Introduction, the gold standard approach for establishing disease causality is the fulfillment of Koch's postulates, which require the virus to be grown in culture. Others have proposed alternatives to these criteria, including Stanley Falkow's Molecular Koch's postulates (17) and a similar revised version of Koch's from David Fredricks and David Relman (18). While neither of the two more recent criteria require the virus to be grown in culture, others have noted how establishment of a cell culture system for WUPyV is a chief requirement for studying the virus' molecular biology (19). We were ultimately unsuccessful at establishing a cell culture system for WUPyV, but our work should lay the groundwork for future attempts.

It is unclear why our attempts were unsuccessful. As noted in the discussion for Chapter 4, it is possible that very few cells were infected, and the infection was diluted further upon passage. Alternatively, host factors necessary for later stages of the viral life cycle may not be present. Monocytic cells produce a potent innate immune response, which could also have inhibited viral growth. It is also unclear why the WUPyV replication system only supports one round of replication. One hypothesis is that Vero cells do not express the WUPyV entry receptor. Alternatively, perhaps host factors necessary for release of intact, infectious particles into the supernatant are not present. While this is not an exhaustive list of potential hypotheses, they represent avenues for additional research. In addition, future attempts should expand the list of cell lines to infect to include other primary respiratory cells and additional monocytic cell lines.

The second approach we took was to determine the cell and tissue tropism of WUPyV and KIPyV *in vivo* in the human host. This is considered one of the most pressing research questions concerning the newer human polyomaviruses. Prior to our work, neither virus had been detected in specific cell types or tissues. Numerous studies, which are summarized in Table 4.1,

using nucleic acid-based methods detected both viruses in a variety of specimen types, but these methods did not allow detection of the viruses in single cells. In addition, most samples were body fluids, not tissues. Data presented in Chapter 3 is the first identification of specific WUPyV- and KIPyV-positive cell types. We also reported the first visualization of putative WUPyV viral particles in a human lung. A summary of these findings can be found in Table 3.2, but in brief, WUPyV and KIPyV VP1 proteins were both detected in alveolar macrophages within human lungs. WUPyV protein was also detected within respiratory epithelial cells and in close association with mucin-producing cells in the trachea. Finally, KIPyV protein was also detected within splenic cells. We tested a number of tissues that were negative for the viruses, which will help narrow future tropism studies. There were additional cell types positive for the viruses, which we were ultimately unable to identify. If patient cases positive by PCR for WUPyV or KIPyV are described in the future, applying the new immunohistochemical assays described in Chapter 3 will hopefully identify these additional cell types.

Future research should also focus on the potential pathogenesis of WUPyV and KIPyV in the lung. In two cases presented in Chapter 3, patients with acute respiratory illness that were positive for WUPyV or KIPyV later died. In both cases, viral or bacterial causes for the deaths were not identified, although both were thought to be of infectious etiology. The size and morphology of the viral particles found in the lungs of one of these patients was consistent with polyomavirus. While it is impossible to prove causality in either of these cases, they are the strongest evidence to date that WUPyV and KIPyV may be human pathogens.

KIPyV was also detected in a second case of an HIV-positive man. In this case, virus was found in a number of cells within both the lung and the spleen. One hypothesis for this is that the virus entered via the respiratory route and spread through the blood to the spleen. This

121

hypothesis is consistent with the second KIPyV case, where virus was only detected in the lung. Although both patients were immunocompromised, perhaps the HIV-positive patient's immune system was less capable of controlling the KIPyV infection. This case gives us insight into the potential pathogenesis and spread of KIPyV within the human host.

Finally, it is important to note that all the cases described in Chapter 3 were of immunocompromised patients. JCPyV and BKPyV both cause disease exclusively in immunocompromised patients, and MCPyV and TSPyV are also thought to follow this paradigm. Given our data, it seems reasonable to conclude that WUPyV and KIPyV may also cause disease only in immunosuppressed individuals. However, there is some amount of selection bias in our cases. Studies on WUPyV and KIPyV have tended to focus on immunosuppressed patients, and we did not test any immunocompetent cases. Immunocompetent patients are not routinely screened for the human polyomaviruses, so it is unlikely we would identify cases in this patient group unless they died of acute respiratory disease of unknown etiology.

To our knowledge, no additional studies of WUPyV or KIPyV tropism have been or are being performed. However, additional studies to establish a cell culture system, identify the remaining virus-positive cell types and further explore potential viral pathogenicity will be important toward answering the question of disease causality. In addition to the approaches we used here, other complementary approaches could be taken. While some case-control studies of WUPyV and KIPyV have already been performed, future studies should be narrowed to explore the role of these viruses in acute respiratory illness, particularly in immunocompromised individuals. We described the first electron microscopy of putative WUPyV particles. As it is difficult to perform electron microscopy on formalin-fixed, paraffin-embedded tissues, applying

this technique in combination with immunogold labelling to fresh tissue in cases of acute respiratory illness could provide more concrete evidence of the specific infecting virus.

Overall, the case for WUPyV and KIPyV being human pathogens is growing. Both have been detected in a variety of specimen types obtained from humans around the world. The majority of the population is infected with both viruses, with infection likely occurring in childhood. Both viruses can be detected in the lungs of immunocompromised patients with severe respiratory illness, and in at least one case, KIPyV appears to have spread outside the respiratory tract to the spleen. Finally, putative WUPyV particles were also detected within the lungs. All of this data is consistent with the viruses being pathogens, although none of it is conclusive. Future work as outlined above will be critical to answering the question of whether these viruses are human pathogens.

FINAL CONCLUSIONS

The work described in the preceding three chapters has expanded our understanding of the *Polyomaviridae* family. The addition of a tenth member to the family and the detection of WUPyV and KIPyV in specific cell and tissue types represent contributions to the field that will hopefully influence future work on these viruses.

REFERENCES

1. **Allander T, Andreasson K, Gupta S, Bjerkner A, Bogdanovic G, Persson MA, Dalianis T, Ramqvist T, and Andersson B.** 2007. Identification of a third human polyomavirus. J Virol **81:**4130-4136.
2. **Gaynor AM, Nissen MD, Whiley DM, Mackay IM, Lambert SB, Wu G, Brennan DC, Storch GA, Sloots TP, and Wang D.** 2007. Identification of a novel polyomavirus from patients with acute respiratory tract infections. PLoS Pathog **3:**e64.
3. **Feng H, Shuda M, Chang Y, and Moore PS.** 2008. Clonal integration of a polyomavirus in human Merkel cell carcinoma. Science **319:**1096-1100.

4. **van der Meijden E, Janssens RW, Lauber C, Bouwes Bavinck JN, Gorbalenya AE, and Feltkamp MC.** 2010. Discovery of a new human polyomavirus associated with trichodysplasia spinulosa in an immunocompromized patient. PLoS Pathog **6:**e1001024.

5. **Schowalter RM, Pastrana DV, Pumphrey KA, Moyer AL, and Buck CB.** 2010. Merkel cell polyomavirus and two previously unknown polyomaviruses are chronically shed from human skin. Cell Host Microbe **7:**509-515.

6. **Scuda N, Hofmann J, Calvignac-Spencer S, Ruprecht K, Liman P, Kuhn J, Hengel H, and Ehlers B.** 2011. A novel human polyomavirus closely related to the african green monkey-derived lymphotropic polyomavirus. J Virol **85:**4586-4590.

7. **Buck CB, Phan GQ, Raiji MT, Murphy PM, McDermott DH, and McBride AA.** 2012. Complete genome sequence of a tenth human polyomavirus. J Virol **86:**10887.

8. **Yu G, Greninger AL, Isa P, Phan TG, Martinez MA, de la Luz Sanchez M, Contreras JF, Santos-Preciado JI, Parsonnet J, Miller S, DeRisi JL, Delwart E, Arias CF, and Chiu CY.** 2012. Discovery of a novel polyomavirus in acute diarrheal samples from children. PLoS One **7:**e49449.

9. **Siebrasse EA, Reyes A, Lim ES, Zhao G, Mkakosya RS, Manary MJ, Gordon JI, and Wang D.** 2012. Identification of MW polyomavirus, a novel polyomavirus in human stool. J Virol **86:**10321-10326.

10. **Lim ES, Reyes A, Antonio M, Saha D, Ikumapayi UN, Adeyemi M, Stine OC, Skelton R, Brennan DC, Mkakosya RS, Manary MJ, Gordon JI, and Wang D.** 2013. Discovery of STL polyomavirus, a polyomavirus of ancestral recombinant origin that encodes a unique T antigen by alternative splicing. Virology **436:**295-303.

11. **Rockett RJ, Sloots TP, Bowes S, O'Neill N, Ye S, Robson J, Whiley DM, Lambert SB, Wang D, Nissen MD, and Bialasiewicz S.** 2013. Detection of novel polyomaviruses, TSPyV, HPyV6, HPyV7, HPyV9 and MWPyV in feces, urine, blood, respiratory swabs and cerebrospinal fluid. PLoS One **8:**e62764.

12. **Li K, Guo J, Zhao R, Xue Y, Chen L, Yang J, Peng J, and Jin Q.** 2013. Prevalence of 10 human polyomaviruses in fecal samples from children with acute gastroenteritis: a case-control study. J Clin Microbiol **51:**3107-3109.

13. **Ramqvist T, Nordfors C, Dalianis T, and Ragnarsson-Olding B.** 2014. DNA from human polyomaviruses, TSPyV, MWPyV, HPyV6, 7 and 9 was not detected in primary mucosal melanomas. Anticancer Res **34:**639-643.

14. **Wieland U, Silling S, Hellmich M, Potthoff A, Pfister H, and Kreuter A.** 2014. Human polyomaviruses 6, 7, 9, 10 and Trichodysplasia spinulosa-associated polyomavirus in HIV-infected men. J Gen Virol **95:**928-932.

15. **Korup S, Rietscher J, Calvignac-Spencer S, Trusch F, Hofmann J, Moens U, Sauer I, Voigt S, Schmuck R, and Ehlers B.** 2013. Identification of a novel human polyomavirus in organs of the gastrointestinal tract. PLoS One **8:**e58021.

16. **Mishra N, Pereira M, Rhodes RH, An P, Pipas JM, Jain K, Kapoor A, Briese T, Faust PL, and Lipkin WI.** 2014. Identification of a novel polyomavirus in a pancreatic transplant recipient with retinal blindness and vasculitic myopathy. J Infect Dis.

17. **Falkow S.** 1988. Molecular Koch's postulates applied to microbial pathogenicity. Rev Infect Dis **10 Suppl 2:**S274-276.

18. **Fredericks DN, and Relman DA.** 1996. Sequence-based identification of microbial pathogens: a reconsideration of Koch's postulates. Clin Microbiol Rev **9:**18-33.

19.   **White MK, Gordon J, and Khalili K.** 2013. The rapidly expanding family of human polyomaviruses: recent developments in understanding their life cycle and role in human pathology. PLoS Pathog **9:**e1003206.

Human Polyomaviruses in Children Undergoing Transplantation, United States, 2008–2010

Erica A. Siebrasse, Irma Bauer, Lori R. Holtz, Binh-minh Le, Sherry Lassa-Claxton, Charles Canter, Paul Hmiel, Shalini Shenoy, Stuart Sweet, Yumirle Turmelle, Ross Shepherd and David Wang

All are affiliated with Washington University School of Medicine, St. Louis, Missouri USA.

ABSTRACT

Immunocompromised patients are at risk for disease caused by infection by some polyomaviruses. To define the prevalence of polyomaviruses in children undergoing transplantation, we collected samples from a longitudinal cohort and tested for the nine known human polyomaviruses. All were detected; several were present in previously unreported specimen types.

INTRODUCTION

BK and JC polyomaviruses (BKPyV, JCPyV) cause disease in immunocompromised persons. Both are double-stranded DNA viruses in the family *Polyomaviridae*. Seven additional human polyomaviruses were discovered during 2007–2011: KI polyomavirus (KIPyV) (1), WU polyomavirus (WUPyV) (2), Merkel cell polyomavirus (MCPyV) (3), human polyomavirus 6 (HPyV6) (4), human polyomavirus 7 (HPyV7) (4), Trichodysplasia spinulosa-associated polyomavirus (TSPyV) (5), and human polyomavirus 9 (HPyV9) (6).

The seven novel polyomaviruses have been detected in various specimen types; detection has been extensively reviewed for KIPyV, WUPyV, and MCPyV (7). Polyomaviruses HPyV6, HPyV7, TSPyV, and HPyV9 have been detected in skin (4, 5, 8); TSPyV and HPyV9 have also been detected in urine, and HPyV9 was detected in serum (6). However, only two of these recently identified viruses have been specifically implicated in human diseases; MCPyV is associated with Merkel cell carcinoma (3), and TSPyV has been linked to Trichodysplasia spinulosa (5). Immunosuppression is a likely cofactor in both diseases. The potential pathogenicity of the other five novel polyomaviruses is unknown. As a first step toward exploring their disease potential, we sought to define their prevalence in immunocompromised

127

transplant recipients. To this end, we established a longitudinal cohort of children undergoing transplantation at St. Louis Children's Hospital, St. Louis, Missouri, USA.

THE STUDY

We recruited 32 patients who were scheduled to receive transplants (two lung, 11 liver, five heart, two kidney, one liver/lung, and 11 bone marrow transplants) during October 2008– April 2010. The Human Research Protection Office of Washington University in St. Louis approved this study. The mean age of enrolled patients was 5.8 years, and the median age was 3.1 years. Thirty patients received transplants and were studied for one year after transplantation. We collected 716 clinical specimens (160 nasopharyngeal swab, 169 urine, 122 fecal, 265 plasma) during 265 patient visits. We collected 298 specimens from patients during symptomatic episodes, which were defined as having more than one of the following: fever, respiratory symptoms, or gastrointestinal symptoms. We collected clinical data using a questionnaire and the medical records.

Fecal material was diluted 1:6 in phosphate-buffered saline and filtered through 0.45-μm membranes. For all specimens, we extracted total nucleic acids using an Ampliprep Cobas extractor (Roche). We used published real-time PCRs for WUPyV (9), KIPyV (9), TSPyV (5), MCPyV (10), BKPyV (11), and JCPyV (12) (Table 1). We developed assays for HPyV6, HPyV7, and HPyV9 using Primer Express software (Applied Biosystems) (Table 1). To assess the performance of each assay, we used serial dilutions (5 to 5×10^{6} copies/reaction) of a plasmid containing the target sequence. All three assays demonstrated a sensitivity of approximately five copies/reaction and yielded linear curves with R^2 values >0.99.

Table 1. Real-time PCR assays to detect human polyomaviruses in children undergoing transplants, United States, 2008–2010. NCCR, non-coding control region; LTAg, large T antigen.

Virus	Target	Primers	Probe
WUPyV	NCCR	WU-C-4824-F: GGCACGGCGCCAACT WU-C-4898-R: CCTGTTGTAGGCCTTACTTACCTGTA	WU-C-4861-TM: 5'-FAM-TGCCATACCAACACAGCTGCTGAGC-TAMRA-3'
KIPyV	LTAg	KI-B-4603-F: GAATGCATTGGCATTCGTGA KI-B-4668-R: GCTGCAATAAGTTTAGATTAGTTGGTGC	KI-B-4632-TM: 5'-FAM-TGTAGCCATGAATGCATACATCCCACTGC-TAMRA-3'
TSPyV	LTAg	LTF: TGTGTTTGGAAACCAGAATCATTTG LTR: TGCTACCTTGCTATTAAATGTGGAG	LTP: 5'-FAM-TTCTTCTTCCTCCTCATCCTCCACCTCAAT-TAMRA-3'
MCPyV	LTAg	LT.1F: CCACAGCCAGAGCTCTTCCT LT.1R: TGGTGGTCTCCTCTCTGCTACTG	LT probe: 5'-FAM-TCCTTCTCAGCGTCCCAGGCTTCA-TAMRA-3'
HPyV6	VP1	ES011F: GCCTGGAAGGGCCTAGTAAAG ES012R: ATTGGCAGCTGTAACTTGTTTTCTG	ES024: 5'-FAM-ACCAACCATCTGTTGCAGGCATTAAAGCTA-TAMRA-3'
HPyV7	VP1	ES017F: GGTCCAGGCAATACTGATGTAGCTA ES018R: TCTGCAACCCAGAGCTCTACTG	ES025: 5'-FAM-CCTGCAAGCCCTCAGAAAGCAAGTAAATG-TAMRA-3'
HPyV9	LTAg	ES026F: GAAGACCCTGATCCTGAGGAAGA ES027R: CTCTGGAGTATTAGGTTCAGGCTTCT	ES031: 5'-FAM-TGGATCATCCCAGAGTTCATTTACCTGCA-TAMRA-3'
BKPyV	LTAg	BK-Deg-F: AGCAGGCAAGRGTTCTATTACTAAAT BK-Deg-R: GARGCAACAGCAGATTCYCAACA	Bk-Deg-P: 5'-FAM-AAGACCCTAAAGACTTTCCYTCTGATCTACACCAGTTT-TAMRA-3'
JCPyV	VP2/3	JL1 (F): AAGGGAGGGAACCTATATTTCTTTTG JL1 (R): TCTAGCCTTTGGGTAACTTCTTGAA	JL1 (P): 5'-FAM-CTCATACACCCAAAGTATAGATGATGCAGACAGCA-TAMRA-3'

Each of the 25-µl quantitative PCRs included 5 µL of extracted sample, 12.5 pmol of each primer, and 4 pmol of probe. The MCPyV primers and probe were used as described (10). We tested samples in a 96-well plate format, with eight water negative controls and one positive control/plate. Reactions were cycled as recommended using either an ABI 7500 real-time thermocycler (Applied Biosystems) or a CFX96 real-time thermocycler (BioRad). The threshold of all plates was set at a standard value, and samples were counted as positive if their cycle threshold was <37.00.

All 716 specimens were tested for each virus (Table 2). The most frequently detected virus was BKPyV, which was found primarily in urine as expected. JCPyV was detected in one

plasma sample. HPyV6, HPyV7, MCPyV, and TSPyV were detected in specimen types not previously reported. HPyV6 and TSPyV were detected in fecal samples and nasopharyngeal swab samples, and HPyV7 was detected in a nasopharyngeal swab and urine. One fecal sample was positive for MCPyV. Because HPyV6, HPyV7, and MCPyV have been previously detected in skin, we cannot rule out the possibility that their presence in specimens could have been caused by shedding from skin.

Table 2. Polyomaviruses detected among specimens from children undergoing transplants, United States, 2008–2010. C_t, cycle threshold; ID, identification; BMT, bone marrow transplant; NP, nasopharyngeal;

Virus	Specimen type	Transplant	Ct	Patient ID	Additional information
HPyV6	Stool	BMT	32.19	3011	6/6/10, 1mo post-transplant
HPyV6	NP	Heart	36.13	4005	11/25/10, 7mo post-transplant
HPyV6	Stool	Lung	36.95	5001	8/17/10, 1mo post-transplant
HPyV7	NP	Liver	34.57	1002	6/16/09, 7mo post-transplant
HPyV7	Urine	Liver	36.54	1002	7/15/09, 8mo post-transplant
HPyV9	Urine	Liver	36.72	1009	2/09/10, 1wk post-transplant
KIPyV	NP	BMT	16.28	3001	7/7/09, 3mo post-transplant
KIPyV	NP	BMT	36.07	3001	5/19/09, 1mo post-transplant
KIPyV	NP	BMT	33.37	3008	11/12/09, pre-transplant
KIPyV	NP	BMT	31.04	3009	7/30/10, 6mo post-transplant
MCPyV	NP	BMT	36.29	3011	4/15/10, pre-transplant
MCPyV	Stool	BMT	34.56	3011	7/2/10, 2mo post-transplant
TSPyV	NP	Heart	32.98	4001	5/29/09, 1wk post-transplant
TSPyV	NP	Heart	30.74	4001	6/18/09, 1mo post-transplant
TSPyV	Stool	Heart	33.89	4001	5/29/09, 1wk post-transplant
WUPyV	NP	BMT	36.62	3005	7/15/09, pre-transplant
WUPyV	NP	BMT	28.81	3007	11/6/09, 2mo post-transplant
JCPyV	Plasma	BMT	36.12	3011	8/24/10, 3mo post-transplant
BKPyV	Urine	BMT	15.83	3010	4/15/10, 1mo post-transplant
BKPyV	Urine	Kidney	36.67	2022	7/1/10, 10mo post-transplant
BKPyV	Urine	BMT	30.80	3011	8/24/10, 3mo post-transplant
BKPyV	Urine	Heart	25.84	4001	8/14/09, 2mo post-transplant
BKPyV	Urine	Heart	35.89	4003	12/23/09, 2mo post-transplant

BKPyV	Urine	Heart	24.37	4001	9/23/09, 4mo post-transplant
BKPyV	Urine	Liver	28.56	1010	11/23/09, 1wk post-transplant
BKPyV	Urine	Lung	33.13	5002	5/3/11, 1 year post-transplant
BKPyV	Urine	Lung	25.25	5002	2/8/11, 10mo post-transplant
BKPyV	Urine	Kidney	9.97	2002	3/4/10, 6mo post-transplant
BKPyV	Urine	BMT	30.10	3009	3/5/10, 2mo post-transplant
BKPyV	Urine	Liver	22.89	1001	1/7/09, 3mo post-transplant
BKPyV	Urine	Kidney	34.41	2002	5/13/10, 8mo post-transplant
BKPyV	NP	Kidney	35.93	2002	3/4/10, 6mo post-transplant
BKPyV	Stool	Kidney	33.15	2002	3/4/10, 6mo post-transplant
BKPyV	Stool	Liver	33.33	1001	12/18/08, 2mo post-transplant
BKPyV	Stool	Liver	34.84	1001	1/7/09, 3mo post-transplant

We collected two serial nasopharyngeal samples that were positive for KIPyV from patient 3001 (Table 2), a one-year-old child who had received a bone marrow transplant as treatment for Fanconi anemia. The first sample, a nasopharyngeal swab obtained one month after transplant, had low levels of KIPyV. To determine the viral load of the second nasopharyngeal swab specimen collected two months later, we reanalyzed the sample in triplicate; on the basis of extrapolation of the standard curve run in parallel, we estimated the viral load to be 1.3×10^9 genome copies/mL of nasopharyngeal swab transport media. This patient's course was complicated by graft-versus-host disease of the gut and skin, renal failure requiring dialysis, and recurrent pulmonary hemorrhage. The patient was critically ill and had experienced multi organ failure at the time of the second sampling. Other microbiological test results were negative at that time, including PCR for Epstein-Barr virus, cytomegalovirus, human herpesvirus-6, and adenovirus in the blood; aspergillus antigen detection in blood; and bacterial cultures of blood, tracheal aspirate, urine, and peritoneal fluid. The fecal specimen collected at this time was negative for KIPyV; plasma and urine were not available for this study. The patient died of acute respiratory failure and extensive pulmonary hemorrhage 24 days after collection of this specimen. Despite the frequent detection of KIPyV in respiratory specimens, no studies have

definitively linked infection with respiratory disease. Titers of KIPyV were high in the nasopharyngeal swab sample from this patient three weeks before respiratory failure. Although this observation does not necessarily implicate KIPyV infection as a contributing factor in the death of the patient, it suggests a poorly controlled KIPyV infection in the respiratory tract.

Three specimens collected from patient 4001, a 13-year-old heart transplant recipient, were positive for TSPyV (Figure), but the patient did not have Trichodysplasia spinulosa. At one week after transplant, the nasopharyngeal swab and fecal samples were positive for TSPyV. At one month after transplant, the nasopharyngeal swab sample was again positive for TSPyV, with a viral load of approximately 2.3×10^4 genome copies/mL of transport media. There is currently only one TSPyV sequence in GenBank (accession no. GU989205). We used four primer pairs to amplify the complete genome of TSPyV from the nasopharyngeal swab taken one month after transplant. PCR products were cloned, and the complete genome was sequenced to 3x coverage (GenBank accession no. JQ723730) and compared with the other TSPyV sequence. There were five nucleotide substitutions: three in noncoding regions and two synonymous mutations.

Figure. Samples tested for TSPyV during May–June 2009 from patient 4001, a 13-year-old heart transplant recipient at St. Louis Children's Hospital, St. Louis, Missouri, USA. Samples tested at each time point are indicated by white squares. Black squares represent positive samples. NP, nasopharyngeal.

132
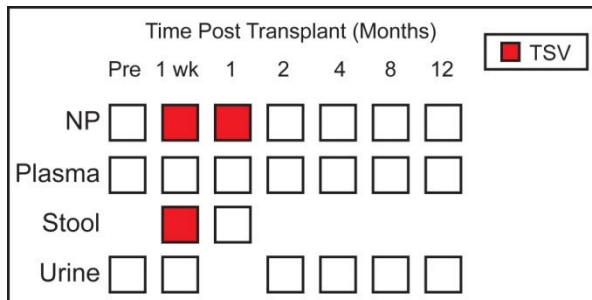
Although serologic studies have demonstrated that approximately 70% of adults in Europe have been infected by TSPyV (13), its mode of transmission is unknown. The detection of TSPyV in nasopharyngeal swab and fecal samples raises the possibility that it may be transmitted by a respiratory or fecal–oral route. Furthermore, in the current study, two sequential nasopharyngeal swab samples taken 20 days apart were positive for TSPyV, suggesting it may persist for extended periods in the respiratory tract, at least in immunosuppressed persons.

CONCLUSIONS

Our goals were to establish a longitudinal repository of different specimen types from transplant recipients and to define the prevalence of polyomaviruses in these patients. We detected all nine polyomaviruses in at least one specimen. Although the prevalence of each virus was generally low, TSPyV, HPyV6, HPyV7, and MCPyV were detected in specimen types not previously reported. These observations expand understanding of the recently identified polyomaviruses and the tissue and organ systems they may infect and suggest possible modes of transmission. Further studies to define their possible roles in human diseases are needed.

ACKNOWLEDGEMENTS

REFERENCES

1.   **Allander T, Andreasson K, Gupta S, Bjerkner A, Bogdanovic G, Persson MA.** 2007. Identification of a third human polyomavirus. J Virol. **81**:4130–6.
2.   **Gaynor AM, Nissen MD, Whiley DM, Mackay IM, Lambert SB, Wu G**. 2007 Identification of a novel polyomavirus from patients with acute respiratory tract infections. PLoS Pathog. **3**:e64.
3.   **Feng H, Shuda M, Chang Y, Moore PS.** 2008. Clonal integration of a polyomavirus in human Merkel cell carcinoma. Science. **319**:1096–100.
4.   **Schowalter RM, Pastrana DV, Pumphrey KA, Moyer AL, Buck CB.** 2010. Merkel cell polyomavirus and two previously unknown polyomaviruses are chronically shed from human skin. Cell Host Microbe. **7**:509–15.
5.   **van der Meijden E, Janssens RW, Lauber C, Bouwes Bavinck JN, Gorbalenya AE, Feltkamp MC.** 2010. Discovery of a new human polyomavirus associated with trichodysplasia spinulosa in an immunocompromized patient. PLoS Pathog. **6**:e1001024.
6.   **Scuda N, Hofmann J, Calvignac-Spencer S, Ruprecht K, Liman P, Kuhn J**. 2011. A novel human polyomavirus closely related to the African green monkey–derived lymphotropic polyomavirus (LPV). J Virol. **85**:4586–90.
7.   **Babakir-Mina M, Ciccozzi M, Perno CF, Ciotti M.** 2011. The novel KI, WU, MC polyomaviruses: possible human pathogens? New Microbiol. **34**:1–8.
8.   **Sauvage V, Foulongne V, Cheval J, Ar Gouilh M, Pariente K, Dereure O.** 2011. Human polyomavirus related to African green monkey lymphotropic polyomavirus. Emerg Infect Dis. **17**:1364–70.
9.   **Bialasiewicz S, Whiley DM, Lambert SB, Gould A, Nissen MD, Sloots TP.** 2007. Development and evaluation of real-time PCR assays for the detection of the newly identified KI and WU polyomaviruses. J Clin Virol. **40**:9–14.
10.   **Goh S, Lindau C, Tiveljung-Lindell A, Allander T.** 2009. Merkel cell polyomavirus in respiratory tract secretions. Emerg Infect Dis. **15**:489–91.
11.   **Dumoulin A, Hirsch HH.** 2011. Reevaluating and optimizing polyomavirus BK and JC real-time PCR assays to detect rare sequence polymorphisms. J Clin Microbiol. **49**:1382–8.
12.   **Pal A, Sirota L, Maudru T, Peden K, Lewis AM Jr.** 2006. Real-time, quantitative PCR assays for the detection of virus-specific DNA in samples with mixed populations of polyomaviruses. J Virol Methods. **135**:32–42.
13.   **van der Meijden E, Kazem S, Burgers MM, Janssens R, Bouwes Bavinck JN, de Melker H.** 2011. Seroprevalence of trichodysplasia spinulosa–associated polyomavirus. Emerg Infect Dis. **17**:1355–63.

Erica A. Siebrasse

esiebrasse@wustl.edu | (620) 820-3806

SUMMARY OF QUALIFICATIONS

Ph.D. candidate in the laboratory of David Wang, Ph.D., with a focus in molecular virology and discovery of novel viruses. Over seven years of experience in development and implementation of informal science education programs. Organized and managed a program of approximately 200 volunteers to reach over 1,000 students annually. Built and maintained relationships with school and community leaders to grow the program locally and nationally.

HIGHLIGHTS

• Discovered and characterized MW polyomavirus.
• Determined the tissue and cell tropisms of WU and KI polyomaviruses.
• Awarded a 2010 National Defense Science & Engineering Graduate Fellowship.
• Awarded a 2013 American Heart Association Pre-doctoral Fellowship.
• Created and directed several science education programs, which included organizing events, volunteers and financial support, and effectively communicating with diverse groups.

EDUCATION

• Ph.D., Molecular Microbiology and Microbial Pathogenesis, June 2014
     Thesis: "Discovery and characterization of novel polyomaviruses in humans"
     Washington University in St. Louis, St. Louis, Missouri
• B.A., Biochemistry Molecular Biology, *Magna cum laude* with distinction, May 2009
     Hendrix College, Conway, Arkansas

PROFESSIONAL EXPERIENCE

• Graduate research assistant, Washington University in St. Louis (August 2009-present)
     Thesis mentor: David Wang, Ph.D., Associate Professor of Microbiology
          • Determined the cell and tissue tropisms of WU and KI polyomaviruses.
          • Discovered and characterized the genomic organization, prevalence and phylogenetic relationship of MW polyomavirus, a novel virus.
          • Developed, tested and refined immunohistochemical and real-time PCR assays for detection of novel viruses.
          • Supervised research projects of other graduate and undergraduate students.
          • Managed discussion sections, developed review materials and assisted students as a Teaching Assistant for Biology 303A, Human Biology, a non-majors course.
          • Organized volunteers for Microbiology student recruitment activities (2010-present).
• Young Scientist Program at Washington University (2009-2013). YSP is a graduate student organization designed to attract students in grades 6-12 into scientific careers through activities emphasizing hands-on research and individualized contact between young people and scientists.
     • Assistant Director of the Young Scientist Program (January-December 2013). Managed approximately 200 volunteers and the eight programs that run under the YSP auspices.
          • Developed, implemented and evaluated programming; moderated planning discussions; developed and edited grant applications; budgeted; networked with companies to gain support; forged partnerships with other student, university and community leaders.

- • Led YSP in applying to and attending the 2013 Clinton Global Initiative University, which ultimately resulted in the University's commitment to sustainable funding for YSP.
  - • Planned and implemented in-services for the St. Louis Public Schools (2012, 2013).
- • Director of the Summer Focus program (summer 2012), which brings disadvantaged area high school students on campus for summer research internships. Directed selection of 50 volunteers and high school student participants and managed all aspects of this program.
- • Creator and Co-Director of the Family Science Experience (2011-2012), an interactive science outreach camp for St. Louis middle school students and their parents.
- • Creator and Co-Director of the Summer Focus college prep program (summer 2011-2013), which helps Summer Focus students explore their college options.
- • Creator and Co-Director of "Ridin' Dirty with Science" (June 2007), a summer science outreach program which is still running at Hendrix College. More information can be found at www.youtube.com/watch?v=miWrmzFEbRU.
- • Undergraduate research assistant, Hendrix College (2006-2007).
  - Mentor: Andrea Duina, Ph.D., Associate Professor of Biology

HONORS AND AWARDS

- • Selected for the 2014 ASBMB Hill Day.
  - Spoke with legislative staff to advocate for biomedical research and STEM education.
- • 2014 Academic Women's Network Student Leadership Award (Washington University)
- • 2013 American Heart Association Pre-doctoral Fellow
- • 2013 Schlesinger Fellow (Washington University Department of Molecular Microbiology)
- • 2010 National Defense Science & Engineering Graduate Fellow
- • Doctoral qualifying exam - passed with distinction
- • Phi Beta Kappa
- • 2007 Barry M. Goldwater Scholar
- • Tri-Beta Biological Honor Society member (served as President 2007-2008)

PUBLICATIONS

- • **Siebrasse, E.A.**, N.L. Nguyen, D.D. Erdman, D. Wang and M.A. Menegus. WU polyomavirus detected in alveolar macrophages in the lungs of a pediatric patient diagnosed with viral pneumonitis. *In preparation.*
- • **Siebrasse, E.A.**, D.V. Pastrana, N.L. Nguyen, A. Wang, M. Roth, S.M. Holland, A.F. Freeman, J. McDyer, C.B. Buck and D. Wang. Detection of WU polyomavirus in respiratory epithelial cells. EID, submitted.
- • **Siebrasse, E.A.**, N.L. Nguyen, C. Smith, P. Simmonds and D. Wang. Immunohistochemical detection of KI polyomavirus in alveolar macrophages, lung and spleen. Virology, submitted.
- • **Siebrasse, E.A.**, A. Reyes, E.S. Lim, G. Zhao, R.S. Mkakosya, M.J. Manary, J.I. Gordon and D. Wang. Identification of MW polyomavirus, a novel polyomavirus in human stool. J Virol. 2012 Oct;86(19):10321-6.
- • **Siebrasse, E.A.**, I. Bauer, L.R. Holtz, B.M. Le, S. Lassa-Claxton, C. Canter, P. Hmiel, S. Shenoy, S. Sweet, Y. Turmelle, R. Shepherd and D. Wang. Human polyomaviruses in children undergoing transplantation, United States, 2008-2010. Emerg Infect Dis. 2012 Oct;18(10):1676-9.
- • Lloyd, A., K. Pratt, **E. Siebrasse**, M. Moran and A.A. Duina. Uncoupling of the patterns of chromatin association of different transcription elongation factors by a histone H3 mutant in yeast. Eukaryot Cell. 2009 Feb;8(2):257-60.

ABSTRACTS
• **Siebrasse, E.A.**, N.L. Nguyen, P. Simmonds, C. Smith and D. Wang. Here WUKI, WUKI, WUKI! Hunting the cell tropism of the elusive WU & KI polyomaviruses (Presentation)
    2013 DNA Tumor Virus meeting, Birmingham, United Kingdom
• **Siebrasse, E.A.**, A. Reyes, E.S. Lim, G. Zhao, R.S. Mkakosya, M.J. Manary, J.I. Gordon and D. Wang. Viral discovery: sifting through the poop (Presentation)
    2013 Cell and Molecular Biology symposium, St. Louis, Missouri
• **Siebrasse, E.A.**, A. Reyes, E.S. Lim, G. Zhao, R.S. Mkakosya, M.J. Manary, J.I. Gordon and D. Wang. Viral discovery: sifting through the poop (Presentation)
    2013 American Society for Microbiology Missouri branch meeting, Columbia, Missouri
• Bradley, M.J., **E.A. Siebrasse**, S.N. Rodriguez, J. Mosher and T. Woolsey. Young Scientist Program: A model for science outreach at Washington University in St. Louis (Prepared poster)
    2013 American Society for Biochemistry and Molecular Biology, Boston, Massachusetts
• **Siebrasse, E.A.**, A. Reyes, E.S. Lim, G. Zhao, R.S. Mkakosya, M.J. Manary, J.I. Gordon and D. Wang. Identification of MW polyomavirus, a novel polyomavirus in human stool (Presentation)
    2012 DNA Tumor Virus meeting, Montreal, Quebec, Canada
• **Siebrasse, E.**, A. Lloyd, K. Pratt, M. Moran and A.A. Duina. Studies on the effects of a histone H3 mutant on transcription elongation in yeast (Presentation)
    2008 National Conference on Undergraduate Research (NCUR), Salisbury, Maryland
• **Siebrasse, E.**, A. Lloyd, K. Pratt, M. Moran and A.A. Duina. Uncoupling of the patterns of chromatin association of different transcription elongation factors by a histone H3 mutant in yeast (Poster)
    Fall 2007 Arkansas INBRE Fall Research Conference, Fayetteville, Arkansas

MEMBERSHIPS
• American Society for Biochemistry and Molecular Biology
• American Society for Microbiology
• American Association for the Advancement of Science